MATHEMATICAL MODELS OF EPSTEIN-BARR VIRUS INFECTION AND ASSOCIATED DISEASES

by

Giao T. Huynh

A dissertation submitted to the faculty of
The University of Utah
in partial fulfillment of the requirements for the degree of

Doctor of Philosophy

Department of Mathematics

The University of Utah

December 2010

The University of Utah Graduate School

STATEMENT OF DISSERTATION APPROVAL

The dissertation of **Giao T. Huynh**

has been approved by the following supervisory committee members:

Frederick R. Adler	, Chair	**July 22, 2010** Date Approved
James P. Keener	, Member	**July 22, 2010** Date Approved
Aaron Fogelson	, Member	**July 22, 2010** Date Approved
Jon Seger	, Member	**July 22, 2010** Date Approved
Vicente Planelles	, Member	**July 22, 2010** Date Approved

and by **Aaron Bertram** , Chair of the Department of **Mathematics**

and by Charles A. Wight, Dean of The Graduate School.

ABSTRACT

Epstein-Barr virus (EBV) infects more than 90% of human population worldwide and has the ability to persist for the lifetime of the infected person. Although EBV infection is most often asymptomatic, the virus causes infectious mononucleosis (IM) in teenagers and young adults. Within a host, EBV can alternate infection between B cells and epithelial cells. The presence of EBV DNA inside these infected cells has been associated with different types of cancers. Many aspects of EBV infection within a host including the switching infections between cell types, the effects of this switching, the factors involve in regulation of the persistent infection, and what parts of the regulation can go wrong that induce different types of disease, are not well understood. The aim of our work is studying these aspects using the tools of mathematical models. We first explore the role of EBV glycoprotein gp42 in the virus entry into target cells. Our models support the role of cooperation of multiple viral glycoproteins in virus entry and suggest that the intracellular interactions of gp42 with HLA class II in B cells may disrupt gp42 function. We then study the dynamics of EBV infection within a host and show that EBV switching host cell tropism shapes the persistence, evolution, and coexistence of the virus infection. Our model of the within host dynamics suggests that the age dependence of IM can be explained by the host antibodies that enhance infections of epithelial cells and the cross-reactive responses of aggressive but functionally ineffective T cells previously created by other infections. We also investigate the association of EBV infection with the development of nasopharyngeal carcinoma (NPC), a cancer of epithelial cells in the pharynx. Our model predicts a threshold of the number of effector T cells below which a bifurcation leads to a jump from a low to high level of latently infected epithelial cells that can greatly elevate the risk of NPC development. Our model also produces the patterns of age-incidence curves that have been observed in low risk and high risk populations.

For my family

CONTENTS

LIST OF FIGURES

LIST OF TABLES

ACKNOWLEDGEMENTS

This dissertation would not be possible without support from many people. I would like to express my deepest appreciation to my advisor, Professor Frederick Adler, for everything he has done for me throughout my graduate studies. I could not ever thank him enough for the countless hours that he has spent reading and editing my manuscripts. Needless to say, his humor helped me go through my graduate student life easier. Without his support, encouragement, and insight in both mathematics and biology, this work would not have been completed. I also would like to thank Professor Jim Keener for always welcoming questions and discussion, Professor Jon Seger for critiquing and providing valuable feedback on presentations, Professors Aaron Fogelson and Vicente Planelles for their care, support, and encouragement.

I also thank Dr. David Thorley-Lawson and other members at his lab for allowing me to visit and spend my summer at the lab studying the biology of Epstein-Barr virus (EBV) infection, sharing their knowledge and enthusiasm about this field of study. I am grateful to Dr. Lindsey Hutt-Fletcher for sharing with me her immense knowledge in EBV and allowing me to bombard her with questions.

I also would like to thank the members of the sLaM group meeting for listening and critiquing my presentations and providing constant support. I am especially indebted to Amber Smith, the best officemate I could ever have, for always being there for me and for our lively discussions in mathematics, biology, and graduate student life. A special thank you to Sean Laverty who has spent this year being my new and wonderful officemate. Last but not least, I would not have been able to complete my graduate studies without the love and support from my mom, sister, brother, and especially my husband who is always very supportive.

CHAPTER 1

INTRODUCTION

Epstein-Barr virus (EBV) was first isolated in 1964 from tumor samples taken from patients with Burkitt's lymphoma (BL) [22]. The virus belongs to the family of Herpesviridae, infects over 90% of humans worldwide and can persist for the lifetime of the person [74]. EBV is transmitted by intimate contact, through saliva and oropharyngeal secretion [3]. Most people infected with EBV are asymptomatic (i.e. healthy carriers), especially if infected in early childhood. However in the US and many other Western countries, primary infection with EBV is often delayed until young adult ages, where as many as 50% of cases develop into infectious mononucleosis (IM) [85].

Within a host, EBV infects two major cell types, B cells and epithelial cells [33]. The ability of virus to alternate tropism between cell types helps to both maintain a long-term infection within one host and to amplify its population for transmission to new hosts [4]. Persistent infection with EBV has been associated with different types of cancers including the B cell cancers Burkitt's lymphoma (BL) and Hodgkin's lymphoma (HL), and the epithelial cell cancer nasopharyngeal carcinoma (NPC). EBV infection in immunosuppressed people such as transplant recipients and HIV patients can lead to other types of lymphomas [15].

The abilities of EBV to establish a long-term infection within a host, to persist through the lifetime of the host, but also to escape regulation and trigger cancer development motivate and inspire the work in this thesis.

We begin with models of viral entry that control how the virus attacks different cell types. We then study how the use of these different cells affects viral shedding, persistence, and evolution. Next, we extend these models to study two common pathologies associated with EBV. Infection mononucleosis occurs during primary infection and involves inappropriate immune responses. Nasopharyngeal carcinoma occurs

only afters many decades of infection, triggered by a failure of viral regulation and an interaction with the immune system.

1.1 Virus entry: viral glycoprotein gp42, the switch of tropism

Within a host, EBV infects two major cell types, B cells and epithelial cells. Entry of the virus into B cells and epithelial cells occurs through different routes, determined by glycoproteins on the surface of the virus. The viral glycoprotein gp42 plays a key role in the switch of tropism. To enter a B cell, gp42, in the form of a three part complex with gH and gL, needs to bind to HLA class II molecules on B cell to trigger fusion. Epithelial cells do not express HLA class II; not only is gp42 unnecessary, it also has an inhibiting effect on EBV infection of epithelial cells [4, 36, 37].

Intracellular interaction with HLA class II molecules produced in B cells can lead to degradation of some gp42. Hence, EBV viruses derived from B cells, which we term "B cell viruses," express 2- to 5-fold lower levels of gp42 compared to virus derived from epithelial cells, or "epithelial cell virus." Intriguingly, this decrease in gp42 level leads to 30 to 100-fold decrease in the infectivity of B-cell virus to B cells, compared to epithelial-cell virus [4]. This nonlinear relationship suggests the possibility of cooperation among multiple viral gH/gL/gp42 complexes for fusion to B cells, or disrupted function of the remaining gp42 in viruses derived from B cells. In our study, we explore these two hypotheses using mathematical models of protein binding kinetics for surface interactions between viral glycoproteins and target cell receptors for virus entry, and models for intracellular interaction between gp42 and HLA class II in B cells.

The glycoprotein gp42 is related to certain types of natural killer cell receptors that can recognize HLA class II molecules, with 22% to 28% sequence identity. It is thought that gp42 may have been originally acquired by EBV from a host, and diverged through many generations of viral evolution and selection [59]. The structure of gp42 and its essential role in virus entry into B cells have been intensively studied [47, 48, 71, 79, 81]. However, the exact mechanisms of how EBV uses gp42 to trigger fusion still await further studies. The goal of our models is to give insights into these

further studies (Chapter 2).

1.2 Regulation of virus dynamics and the association with infectious mononucleosis

1.2.1 EBV latent and lytic infections

After a virus successfully enters a naive B cell (one that has not been exposed to antigen), it downregulates the expression of its own genes to only about 9 out of more than 100 genes that control progression through the different stages of latent infection. EBV uses combinations of these genes to drive infected cells through a similar pathway of a normal B cell activation process. A normal B cell, upon stimulation by antigen, will become activated and proliferate. These proliferating B cells need help from T cells in order to differentiate into memory cells. With antigen stimulation, memory B cells can differentiate into plasma cells that release antibodies [85].

When EBV infects a naive B cell, it uses the combination of genes called the"growth program" to activate and transform the cell into the first stage of latent infection. This transformed B cell can proliferate. Often, proliferating cells are recognized and eliminated by the immune response. Those that survive enter the memory stage as the virus switches to use another gene combination called the"default program." Once the cell reaches the memory stage, *in vitro* study has shown that EBV expresses none of its genes, the "latency program" [35]. EBV is thought to use this strategy to escape immune recognition and to help the virus survive inside an infected cell. The number of infected cells within a host is estimated to be in the range of $5-3,000$ per 10^7 memory B cells in the blood [49]. The same range is estimated for the number of infected memory B cells in the oropharynx. The total number of infected cells per person is estimated to be around 0.5×10^6 [85]. The infected cell has the same characteristics of a resting memory B cell except that EBV genomes exist inside its nucleus as a separate episome. As members of memory B cell population, infected cells circulate within the blood and can be found in the lymphoid tissues [33].

Infected memory B cells are under the same regulation as normal memory B cells. At any given time, 2-3% of infected memory B cells in the blood are undergoing cell division [85]. Memory B cells use this homeostatic mechanism to maintain the cell

population at a stable level. The virus EBNA1 gene is expressed at this stage so that the virus genome can replicate with the cell [35]. Normal memory B cells can differentiate into plasma cells to produce antibodies in response to secondary infection. Infected memory B cells can differentiate into lytically infected cells found in the lymphoid tissues of the oropharynx. These infected cells have similar characteristics to plasma B cells [49]. How EBV switches on its lytic replication within the latent infected cell is still not completely understood. *In vitro* studies on the Akata cell line show that the lytic cycle can be quickly (in order of minutes) switched on by cross linking of the antigen receptor on these cells [85]. *In vivo*, the differentiation of a memory B cell into a plasma cell requires days [85]. Lytic replication is a key step that helps spread the virus to new hosts and maintain EBV infection within one host.

Lytic EBV infection is divided into three phases: immediate early (IE), early, and late [41]. EBV expresses most of its genes during the stages of lytic infection. First, IE genes are expressed for viral proteins to be produced. Early genes are then turned on to encode viral proteins involved in replication. After lytic replication, late genes are expressed to encode proteins that are needed for the viral genome to be packaged into the free virions that burst out of the cell. Plasma-like B-cell derived virus may get amplified through lytic infection of epithelial cells before virus genomes are shed into the saliva. It remains unknown whether viruses produced from the lytic infection need to infect more B cells to keep the infection cycle going on or if homeostasis of memory B cells alone is enough to maintain the low level of latent infection within the host.

During the latent cycle, EBV expresses only a few of its genes, thus avoiding the immune recognition. Three of the genes expressed during different stages of the latent infection, LMP1, LMP2, and EBNA1, help the virus to manipulate the immune response. LMP1 and LMP2 provide necessary signals for differentiation into the memory stage [55]. EBNA1, on the other hand, interferes with the process of proteasomal degradation of proteins to limit the amount of viral antigens presented by HLA class I and reducing the $CD8^+$ T cell response. Throughout the lytic cycle, EBV expresses more than 60 proteins, many of which downregulate the immune response [60].

1.2.2 T cell response

The T cell response to most viral infections includes two cell types: $CD4^+$ helper T cells and $CD8^+$ cytotoxic T cells. An *in vitro* study demonstrated that $CD4^+$ T cells can inhibit the proliferation of newly infected B cells [63]. Most studies of T cell responses to EBV infection have focused on $CD8^+$ responses in IM patients. $CD8^+$ T cells that respond to EBV infection can kill infected cells and control the growth of EBV transformed B cells and epithelial cells through the secretion of interferon gamma (IFNγ) [60]. Different lineages of $CD8^+$ T cells respond to lytic and latent infection [33].

During acute IM infection, specific response to EBV lytic epitopes can make up 1%-40% of the total $CD8^+$ population [33]. These aggressive T cell responses are the main reasons causing IM symptoms. These activated $CD8^+$ T cells are antigen stimulated and have a high turnover rate. These highly aggressive lytic responses are quickly reduced during the resolution of acute IM. Specific responses to latent infection are smaller in magnitude. Latent-specific $CD8^+$ T cells also reduce their population after IM but at a lower rate than lytic-specific $CD8^+$ T cells. In the long term, both lytic and latent EBV specific $CD8^+$ T cells make up 1-5% [60] of the $CD8^+$ T cell population.

1.2.3 Mathematical modeling of virus dynamics and modified application to study persistent viral infection

The basic mathematical model of virus dynamics has been built and modified to study viral infections including HIV, HBV, and HCV [61, 65, 68]. This basic model describes the population dynamics of viral infection within an infected host [66, 68]. The model tracks three state variables: uninfected susceptible cells X, infected cells Y, and free virus particles V. Uninfected cells are produced or replenished with a constant rate π and die with rate δ. Free virus particles encounter and successfully infect cells at rate β. Infected cells produce virus at rate k and die at rate a. Virus particles are removed at rate μ to give the system

$$\frac{dX}{dt} = \pi - \delta X - \beta XV$$

$$\begin{aligned} \frac{dY}{dt} &= \beta XV - \alpha Y \\ \frac{dV}{dt} &= kY - \mu V. \end{aligned} \tag{1.1}$$

This nonlinear system has two possible steady states. At the virus-free equilibrium, clearance occurs and both infected cells and virus populations die out: $X^* = \pi/\delta$, $Y^* = 0$, and $V^* = 0$. At the second steady state, all three populations coexist. Stability analysis of these steady states gives the condition $\frac{\beta\pi k}{\alpha\delta\mu} < 1$ for clearance to be the only steady state and to be stable. When $\frac{\beta\pi k}{\alpha\delta\mu} > 1$, the second steady state exists and is stable. The quantity $\frac{\beta\pi k}{\alpha\delta\mu}$ is the number of newly infected cells that arise from one infected cell when introduced into a population of uninfected cells. It is called the basic reproduction number, R_0, a key quantity in epidemiology.

Extending this model to also track the number of latently infected cells, a mathematical model of the dynamics of EBV has been built to study the T cell response to a persistent virus infection [18],

$$\begin{aligned} \frac{dX}{dt} &= \pi - \delta X - \beta XV \\ \frac{dY}{dt} &= \beta XV + \epsilon L + rY - (\lambda + \alpha)Y \\ \frac{dV}{dt} &= kY - \mu V \\ \frac{dL}{dt} &= \lambda Y - (\epsilon + \gamma)L. \end{aligned} \tag{1.2}$$

This model assumes that infection of target cells (X) gives rise to lytically (i.e. productively) infected cells (Y). These lytically infected cells can proliferate with rate r, turn into latently infected cells (L) at rate λ, produce virus at rate k and die at rate α. Latently infected cells can be activated to turn into lytically infected cells at rate ϵ and die at rate γ.

In addition to including multiple stages of infection, the model can include a T cell response. In a simplified version, only lytically infected cells are recognized and killed by T cells. This effect can be included in the death rate α. In combination with a model of effector T cells activation from naive cells, the model can be used to study how

the T cell response develops during a persistent infection. This model, however, does not distinguish target cells as B cells or epithelial cells. The assumption that lytically infected cells can produce virus without going through latent stages of infection applies only to infection of epithelial cells. The assumption that these productively infected cells can proliferate and become latently infected cells does not reflect the biology of EBV infection of either cell type.

Besides this mathematical model, the dynamics of EBV infection of B cells and the T cell response have been explored using the agent-based models C-ImmSim and PathSim [9, 78]. PathSim includes the interactions of viruses, uninfected, latently infected and lytically infected B cells, and T cells. Infection of naive B cells gives rise to the population of latently infected B cells that can proliferate and be killed by T cells. These latently infected B cells can hide from T cell recognition by entering the blood compartment which represents the memory stage. Coming out of the blood compartment, these B cells can be activated to become lytically (or productively) infected cells which in which virus can replicate and exit the cell. Lytically infected cells can be recognized and killed by T cells. Simulations of PathSim have been used to investigated if clearance of EBV infection is possible and to identify the critical parameters that control the dynamics of infection. PathSim shows that maintenance of a latent infection within the memory B cell population is a key requirement for EBV to persist within a host. The dynamics of infection prove to be especially sensitive to variation in the reactivation rate of lytic infection from infected memory B cells. A small increase in this rate causes the number of infected cells to expand quickly and remain at a high level. However, this sensitivity may be due to the lack of T cell proliferation in PathSim. Although the interactions between agents in PathSim include a detailed description of the biology of B cell infection, infection of epithelial cells is not included. Furthermore, the model can be studied only via computer simulation without the aid of analytical methods that can provide better understanding of its behavior.

Our models build upon the interaction between viruses and B cells described in PathSim, but add T cell proliferation and infection of epithelial cells to develop a

mathematical model of EBV infection that extends the basic model of viral infection (Chapter 3). Our model can explore how the dynamics of EBV infection are shaped by the presence of two cell types, and the possible effects of switching infection between cell types on virus shedding, persistent infection, and evolution.

1.2.4 Infectious mononucleosis

Adolescents and young adults infected with EBV may develop infectious mononucleosis (IM) with symptoms including fever and fatigue that may last from a few weeks up to several months [3, 15]. Aggressive T cell responses with expansion in the number of $CD8^+$ T cells, especially against EBV lytic proteins, are the main cause for these symptoms. Three hypotheses have been proposed to explain the prevalence of IM in this age group and its absence in children. The first hypothesis is that a young adult may be initially infected by a high dose of virus [33]. In young adults, transmission often occurs through close oral contact, which may transmit large number of viruses. The second hypothesis concerns the complexity of the preexisting $CD8^+$ repertoire. In children, the memory T cell repertoire is simple and most of the $CD8^+$ responses to viral infection is from activation of naive cells. After the infection is controlled, these activated cells either die out or become memory cells. As people get older, the memory $CD8^+$ repertoire becomes more complex due to exposure to multiple pathogens. In older people, the $CD8^+$ response to the primary EBV infection may come primarily from cross-reactive memory $CD8^+$ T cells created in response to infections by other viruses. These cross-reactive responses may not be as efficient as the responses from the activation of naive cells [85]. The final hypothesis involves the role of host saliva and antibodies to EBV proteins that increase with age [21, 67]. Antibodies may actually promote infection of epithelial cells [4], altering the typical balance between cell types and inducing a high level of $CD8^+$ T cell response against lytic infection. To investigate these three hypotheses, we modify the basic model described in Chapter 3 to allow cross-reactive T cell responses and include the effects of host saliva and antibodies on the infection of the two cell types (Chapter 4).

1.3 EBV and cancer: nasopharyngeal carcinoma

Studies have linked EBV infection with several cancers, presumably because EBV has proteins, such as LMP1 and EBNA1, that can cause cell proliferation and inhibit apoptosis. In fact, EBV was first isolated from a Burkitt's lymphoma (BL) tumor, a cancer of B cells and that mostly occurs in children from Central Africa [24]. EBV infection together with malaria infection are thought to contribute to the pathogenesis of BL [24]. Hodgkin's lymphoma (HL), a malignant disease of Hodgkin/Reed Sternberg (HRS) cells that originate from B cells, is another cancer associated with EBV. Not all HL cases are EBV related. The link of EBV infection to HL is through the finding of the EBV genome in up to 40% of HL tumors. Post-IM patients have been shown to be at higher risk of getting EBV positive HL compared to healthy carriers [34]. The risk of EBV negative HL does not increase after IM. It is assumed that B cells infected by EBV can escape the cellular regulation process in favor of growth and survival which induces the development of lymphoma. In addition, an impaired immune response may fail to control the growth of the infected cell population, allowing the lymphoma to progress quickly to HL within a few years after getting IM [34].

EBV is strongly associated with nasopharyngeal carcinoma (NPC), with all tumor samples of undifferentiated type III containing EBV DNA. NPC is a cancer of epithelial cells in the nose and pharynx with highest incidence in Southern China and Southeast Asia [70]. Infection of epithelial cells normally results in lytic infection where viral particles are released and cells die. Genetic changes and diet may give rise to a pool of epithelial cells that are susceptible to EBV latent infection [11, 70]. Immunoglobulin A (IgA) to EBV viral capsid antigen and especially to viral glycoprotein 350 can enhance EBV infection of the predisposed epithelial cells [53, 83]. Expression of EBV latent genes, such as LMP1 and EBNA1, within the latently infected epithelial cells contributes to cell proliferation, survival, and accumulation of regulatory T cells [50, 86], which can accelerate tumor development. NPC tumors represent the clonal expansion of an EBV latently infected epithelial cell [70]. $CD8^+$ T cells can recognize and kill these latently infected tumor cells [51]. However, host genetics, accumulation of regulatory T cells, and EBV strains with certain base pair deletion in LMP1 genes

can affect the functionality of these $CD8^+$ T cells [70].

We focus our study on the regulation of EBV infection in the population of latently infected epithelial cells local to the pharynx, assuming that the risk of getting NPC is proportional to the number of these latently infected epithelial cells (Chapter 5). Our model, describing the dynamics of these latently infected cells, adapts a model built to describe the dynamics of tumors being attacked by effector $CD8^+$ T cells [30]. We use the model to study critical breakdown in regulation of the infection that can lead to a high level of latently infected epithelial cells, and hence an increased risk of NPC.

1.4 Concluding remarks

Since its discovery more than 40 years ago, EBV has attracted many empirical studies of its ability to persist within one host and its association with cancers. However, EBV infects only humans and a limited range of host cells, and lacks a good animal models to investigate EBV infection *in vivo* [72]. Most hypotheses and conclusions about EBV infection are based on studies of cell cultures in epithelial and B cell lines. Viral loads and infected cell data must be obtained from saliva and blood collected from infected people. Many aspects of EBV infection still remain open questions. This is why mathematical models can be helpful. Exploring the dynamics of EBV infection with mathematical models can help to formulate questions and provide insight for specific biological study of EBV infection in the laboratory. Our goals are to use mathematical models to investigate (1) the mechanism of EBV entry and switching infections between cell types, (2) how infections of the two cell types are regulated and the role of alternating tropism on virus shedding, persistent infection, and evolution, (3) factors affecting the dynamics of infection that may lead to IM, and (4) association of EBV infection with the development of NPC.

CHAPTER 2

MECHANISMS OF EPSTEIN-BARR VIRUS SWITCHING TROPISM: THE EFFECTS OF VIRAL GLYCOPROTEIN 42

2.1 Abstract

Epstein-Barr virus (EBV) persists in B cells, but sheds via epithelial cells. Viruses emerging from one cell type preferentially infect the other type, with a mechanism involving a set of glycoproteins on the viral envelope. The glycoprotein gp42 plays a key role in the switch by binding to HLA-II. HLA-II is expressed by B cells, but not epithelial cells. Due to intracellular association of gp42 with HLA-II molecules in B cells, virus derived from B cells expresses 2- to 5-fold decreased level of gp42 and is 30- to 100-fold less efficient in infecting B cells than virus derived from epithelial cells. In this study, we use mathematical models to investigate two different hypotheses explaining this nonlinear relationship between gp42 level and its effects on the infectivity of viruses to B cells. In the first hypothesis, we assume intracellular interactions of gp42 with HLA-II in B cells may modify and disrupt functions of gp42 in fusion. Our numerical result shows that only a small fraction of the three-part complexes gH/gL/gp42 produced in B cells has gp42 that has not interacted with HLA-II molecules. In the second hypothesis, cooperation of multiple gH/gL/gp42 complexes are required for virus fusion. Our model demonstrates that the more gH/gL/gp42 complexes are needed, the greater the decrease in infectivity of B-cell virus to B cells. These results suggest the value of further studies to investigate functional differences between gp42 expressed on B-cell and epithelial-cell viruses.

2.2 Introduction

Within a host, Epstein-Barr virus (EBV) infects two major cell types, B cells and epithelial cells. EBV uses different complexes of glycoproteins to enter and infect the two cell types. The virus uses gp350, the most abundant glycoprotein on its envelope, to bind CD21 on B cells [4]. The viral entry into a B cell then requires binding of the three-part glycoprotein gH/gL/gp42 complex to HLA-II, human genes that encode antigen presenting proteins on the surface of antigen presenting cells. Another glycoprotein gB is also invovled in a way that has not been fully understood [48]. Epithelial cells express CD21 at a low level and do not express HLA-II. Hence, EBV gp350 and gp42 are not needed for viral entry into epithelial cells. Fusion of virus with an epithelial cell requires only the complexes gH/gL and gB binding to integrins expressed on the cell [4, 12]. The presence of gp42 reduces the infectivity of EBV to epithelial cells [4].

As gH, gL, and gB are required for EBV fusion with both epithelial cells and B cells, the viral glycoprotein gp42 serves as the molecular switch that EBV uses to alternate infections between the two cell types. This glycoprotein has separate binding sites for gH and HLA-II molecule [48]. In a B cell, gp42 interacts with HLA-II, and can become a target for degradation. Viruses derived from B cells thus express low levels of gp42. Because epithelial cells do not express HLA-II, no such intracellular interactions occur and viruses derived from epithelial cells express 2- to 5-fold higher levels of gp42 than viruses derived from B cells [4, 25]. As a result, B-cell derived viruses are approximately 5 times more efficient at infecting epithelial cells than epithelial-cell derived viruses. More surprisingly, epithelial-cell viruses are 30-100 times more efficient in infecting B cells than viruses derived from B cells [4, 36]. The 2- to 5-fold increase in gp42 level is amplified to a 30- to 100-fold increase in the infectivity of epithelial-cell virus. Our aim is to use mathematical models to study this nonlinear relationship between the gp42 level and the infectivity of viruses. The structure and different mutational forms of gp42 have been intensively studied and the requirement of this protein for fusion of B cells has been confirmed [48, 79, 81]. However, the mechanism of how it triggers fusion and the number of gH/gL/gp42 complexes involved in fusion remain unknown

[4, 79].

We propose models to investigate two hypotheses on mechanisms causing the difference between the efficiency of B-cell and epithelial-cell viruses in infecting B cells. The first hypothesis concerns how the association of gp42 with HLA-II molecules inside B cells may affect the functions of gp42 in fusion. The glycoprotein gp42 is produced late in the lytic cycle when virus is replicated within an infected cell. After translation, gp42 is glycosylated and modified before being transported to cell membrane and incorporated into the viral envelope [71]. HLA-II molecules are also being produced in B cells and gp42 has been shown to interact with these molecules throughout different stages of their maturation [4, 71]. We hypothesize that intracellular association of gp42 with HLA-II molecules may not only degrade some gp42, but may also interfere with glycosylation and modification of this protein in B cells. Changing a few residues in certain parts of gp42 can disrupt its function in inducing fusion [81]. Virus derived from B cells may not only have a 2- to 5-fold decrease in the gp42 level, but also express gp42 with disrupted ability to trigger fusion.

The second hypothesis suggests that multiple viral gH/gL/gp42 complexes must bind to HLA-II for successful fusion with B cells [4]. A small increase in the level of gp42 could then lead to a multiplicative effect on the infectivity of the virus.

2.3 Intracellular association of gp42 with HLA-II molecules

2.3.1 Epithelial cells

There is no production of HLA-II molecules inside epithelial cells. Our model (Figure 2.1(a)) tracks the levels of gp42 (G), gH/gL (H), and the complex gH/gL/gp42 (C_H) resulting from the association of gp42 with gH/gL using the following equations

$$\begin{aligned}
\frac{dG}{dt} &= \alpha_G + k_1^- C_H - k_1 GH - d_G G \\
\frac{dH}{dt} &= \alpha_H + k_1^- C_H - k_1 GH - d_H H \\
\frac{dC_H}{dt} &= k_1 GH - k_1^- C_H - d_{CH} C_H.
\end{aligned} \tag{2.1}$$

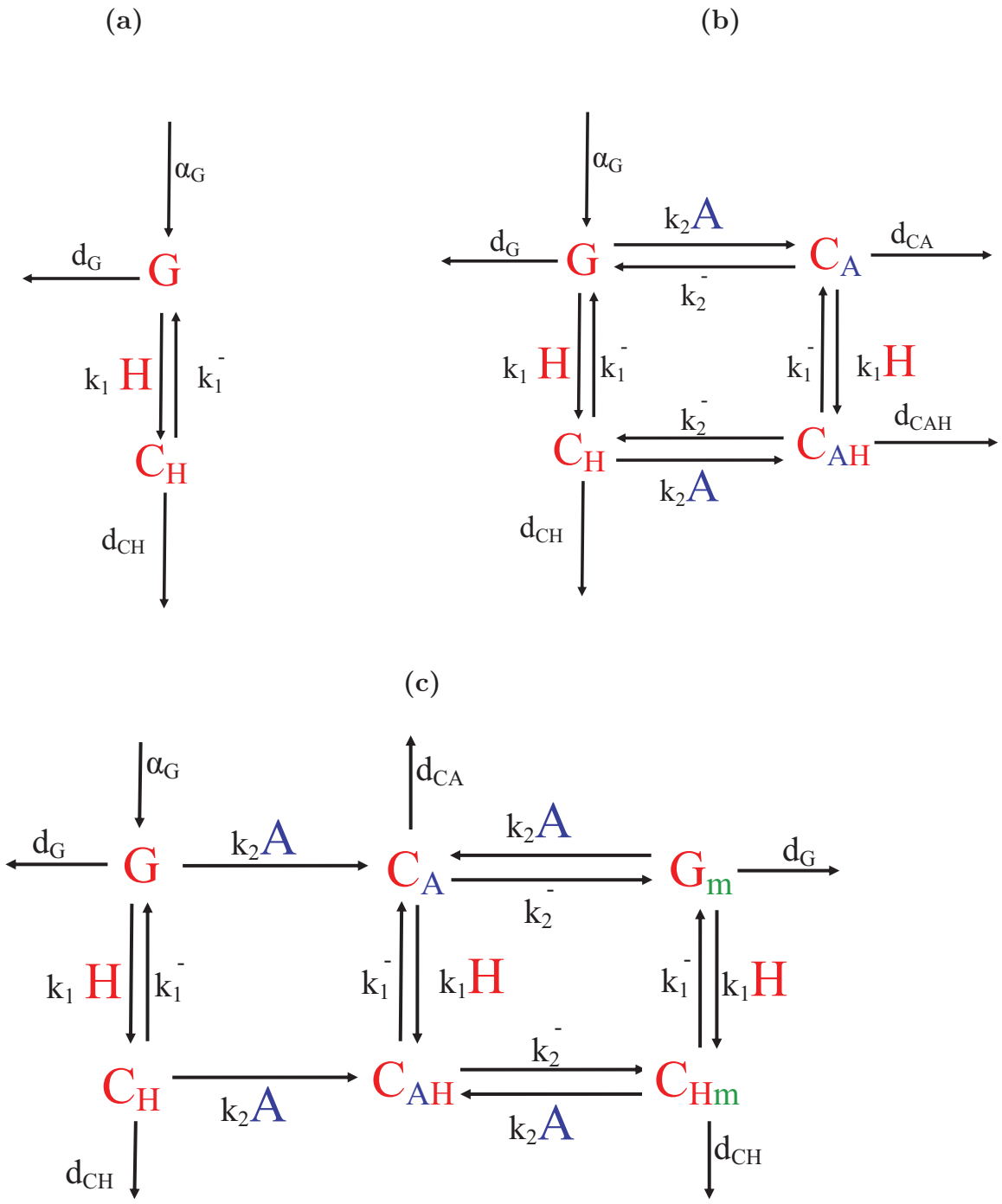

Figure 2.1. Production of gp42 (G) and the kinetics of its interaction with gH (H) and HLA-II (A). **(a)** In epithelial cells with no production of HLA-II. **(b)** In B cells assuming interaction with HLA-II has no effect on gp42 function. **(c)** In B cells assuming interaction with HLA-II can modify gp42 (G_m and C_{Hm}) and affect its function in fusion.

The model assumes gp42 and gH/gL are produced with constant rates α_G and α_H, respectively. They are removed or degraded at rates d_G and d_H respectively. The gp42 can bind gH with rate k_1 that gives rise to the complex gH/gL/gp42, which unbinding rate is k_1^-.

It has been shown that gp42 binds gH/gL with strong affinity ($K_d = 8.5$ nM) [47]. At a low 10 nM concentration of gp42 and gH/gL, the same study observed a binding rate (k_{ob}) between these two proteins of 0.908 min^{-1} and a half life of the gH/gL/gp42 complex of approximately 10 min. We then can use the formulas

$$k_1 = \frac{k_{ob} - k_1^-}{10 \text{ nM}} \text{ and } K_d = \frac{k_1^-}{k_1},$$

to calculate the values for $k_1 = 0.0491 \text{ min}^{-1} \cdot \text{nM}^{-1}$ and $k_1^- = 0.4172 \text{ min}^{-1}$. Using the half life information, the degradation rate of gH/gL/gp42 complex can also be calculated, $d_{C_H} = 0.07 \text{ min}^{-1}$. We assume the half life of gp42 is similar to gH/gL/gp42. The production rates of gp42 and gH/gL, (α_G and α_H), and the degradation rate of gH/gL (d_H) are estimated to give the observed ratio gp42:gH (C_H:H) in the literature [4]. A summary of parameter definition and values using for the model of gp42 interaction in epithelial cells can be found in Table 2.1.

Table 2.1. Parameter definitions and values for production and interaction of gp42 with gH/gL (Equation 2.1 and 2.2).

Parameter	**Value**	**Units**	**Definition**
α_G	1	nM/min	Production rate of gp42
k_1	0.0491 [47]	$1/(\text{nM} \cdot \text{min})$	Binding rate of gp42 to gH
k_1^-	0.4172 [47]	1/min	Unbinding rate of gp42 from the complex gH/gL/gp42
d_G	0.07	1/min	Death rate of gp42
α_H	2.5	nM/min	Production rate of gH/gL
d_H	0.035	1/min	Death rate of gH/gL
d_{C_H}	0.07 [47]	1/min	Death rate of gH/gL/gp42

2.3.2 B cells

HLA-II molecules are produced inside B cells and associate with gp42 throughout different stages of the glycoprotein maturation. In addition to gp42, gH/gL, and the complexes gH/gL/gp42, the model also tracks the levels of HLA-II molecules (A) and the complexes of gp42 and gH/gL/gp42 binding to HLA-II (C_A and C_{AH}) (Figure 2.1(b)). Assuming the intracellular association of gp42 with HLA-II in B cells may lead to modification of gp42 that can affect its function in fusion, the model tracks these modified gp42 (G_m) and its form in complex with gH/gL (C_{Hm}) separately from the ones that have not associated with HLA-II (Figure 2.1(c)). The model, thus, includes the eight equations

$$\begin{aligned}
\frac{dG}{dt} &= \eta\alpha_G + k_1^- C_H - k_1 GH - k_2 GA - d_G G \\
\frac{dG_m}{dt} &= k_2^- C_A + k_1^- C_{Hm} - k_1 G_m H - k_2 G_m A - d_G G_m \\
\frac{dH}{dt} &= \eta\alpha_H + k_1^-(C_H + C_{Hm} + C_{AH}) - k_1(G + G_m + C_A)H - d_H H \\
\frac{dA}{dt} &= \alpha_A + k_2^-(C_A + C_{AH}) - k_2(G + G_m + C_H + C_{Hm})A - d_A A \\
\frac{dC_H}{dt} &= k_1 GH - k_1^- C_H - k_2 C_H A - d_{C_H} C_H \\
\frac{dC_{Hm}}{dt} &= k_1 G_m H + k_2^- C_{AH} - k_1^- C_{Hm} - k_2 C_{Hm} A - d_{C_H} C_{Hm} \\
\frac{dC_A}{dt} &= k_2(G + G_m)A + k_1^- C_{AH} - k_1 C_A H - k_2^- C_A - d_{C_A} C_A \\
\frac{dC_{AH}}{dt} &= k_1 C_A H + k_2(C_H + C_{Hm})A - k_1^- C_{AH} - k_2^- C_{AH} - d_{C_{AH}}.
\end{aligned} \tag{2.2}$$

B cells produce more viral DNA than epithelial cells [4, 25], describing by using a factor of $\eta = 5$ to increase gp42 and gH/gL production in B cells. The half life of HLA-DR, a type of HLA class II that is strongly associated with gp42, was estimated to be approximately 60 min [17]. Interaction with gp42 does not affect the level of HLA-II being expressed on the cell surface [71]. We thus calculate $d_A = 0.0116$ min^{-1}, and let d_{C_A} and $d_{C_{AH}}$ take on the same values. Individuals express different subsets of HLA-II alleles which have different susceptibility to gp42 binding. For example, gp42 binds HLA-DR with strong affinity while it does not bind that well to HLA-DQ [4, 27]. We assume the binding between gp42 and HLA-II, on average, is weaker than

the binding between gp42 and gH/gL. We let the on and off rates of gp42 binding to HLA-II, k_2 and k_2^-, to take on the baseline values that are smaller than the values of k_1 and k_1^-. We will vary the values of k_2 and the production rate of HLA-II, α_A, to study their effects on the levels of gp42 being expressed as a three-part gH/gL/gp42 complexes on the viral envelope, C_H and C_{Hm}. A summary of parameter definition and values using for the model of gp42 interactions in B cells can be found in Tables 2.1 and 2.2.

2.3.3 Results

We use these models (Equations 2.1 and 2.2) to study the effects of intracellular association of gp42 with HLA-II on the level and function of gp42 being produced. Interaction with HLA-II can lead to a decreased ratio of gH/gL/gp42 to gH/gL expressed by virus produced in B cells (Figure 2.2). This decrease is only about 2-fold if we do not distinguish gp42 that have and have not interacted with HLA-II. Because only a small fraction of the three-part complexes include gp42 that has not interacted with HLA-II, the assumption that association with HLA-II can modify gp42 and disrupt its

Table 2.2. Parameter definitions and values for gp42 interactions with HLA-II in B cells (Equation 2.2).

Parameter	Value	Range	Units	Definition
η	5		no unit	Factor of increased viral production in B cells
k_2	$k_1/5$	(0 - $k_1/2$)	$1/(\text{nM} \cdot \text{min})$	Binding rate of gp42 to HLA-II
k_2^-	$k_1^-/5$		1/min	Unbinding rate of gp42 from the complex of gp42 and HLA-II
α_A	4	(0 - 10)	nM/min	Production rate of HLA-II
d_A	0.0116 [17]		1/min	Death rate of HLA-II
d_{C_A}	d_A [71]		1/min	Death rate of gp42/HLA-II
$d_{C_{AH}}$	d_A [71]		1/min	Death rate of gH/gL/gp42/HLA-II

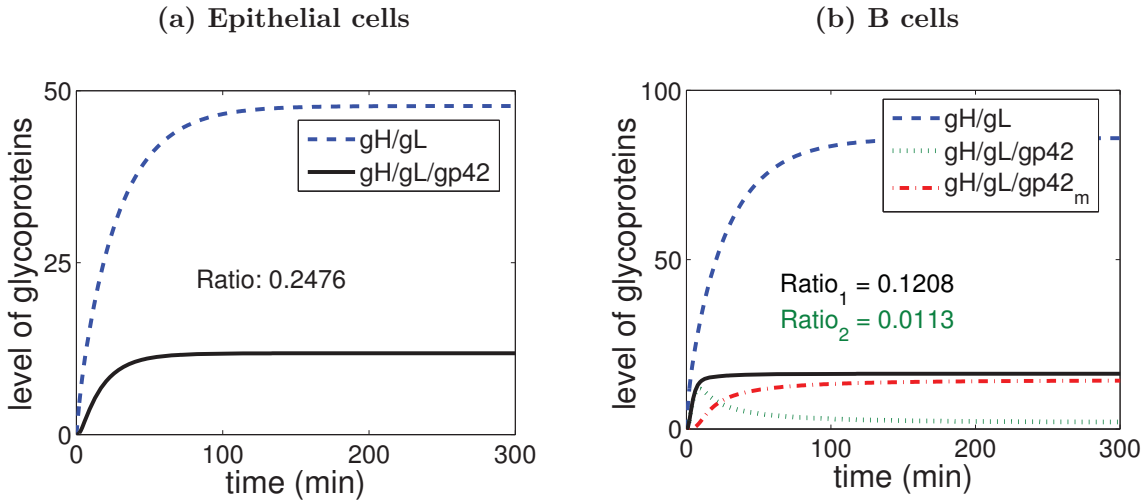

Figure 2.2. Two-part and three-part complexes being produced in epithelial cells (a) and B cells (b). The dashed lines indicate the level of gH/gL (H). The dotted line indicates the level of gH/gL/gp42 (C_H) being produced in B cells with gp42 that has not interacted with HLA-II. The dash-dotted line indicates the level of gH/gL/gp42 (C_{Hm}) being produced in B cells with gp42 that has interacted with HLA-II **(a)** Epithelial cells. **(b)** B cells. Ratio_1 describes the ratio of total number of three-part complexes to two-part complex at equilibrium. Ratio_2 describes the ratio of only three-part complex with gp42 that has not interacted with HLA-II to two-part complexes.

function in fusion can explain the 30- to 100- fold decreased infectivity of B-cell virus compared with epithelial-cell virus.

Variation in the production rate of HLA-II of the infected cells and especially in the binding rate of gp42 to HLA-II molecules can greatly affect the content of functional gp42 on the viral envelope (Figure 2.3). This implies that virus will express high level of functional gp42 if it is derived from B cells that gp42 does not bind well with the cell HLA-II molecules. The virus, hence, will not be efficient at infecting epithelial cells. This is consistent with the observation *in vitro* [4].

2.4 Cooperation of multiple gH/gL/gp42 complexes

In the second hypothesis, we investigate the mechanism of viral entry into a B cell. *In vitro* study of EBV infection of B cells indicates that the first event of viral entry into a B cell is binding of EBV gp350 to the receptor CD21 on the cell [37]. Because gp350 is the most abundant glycoprotein on the viral envelope, we assume this step

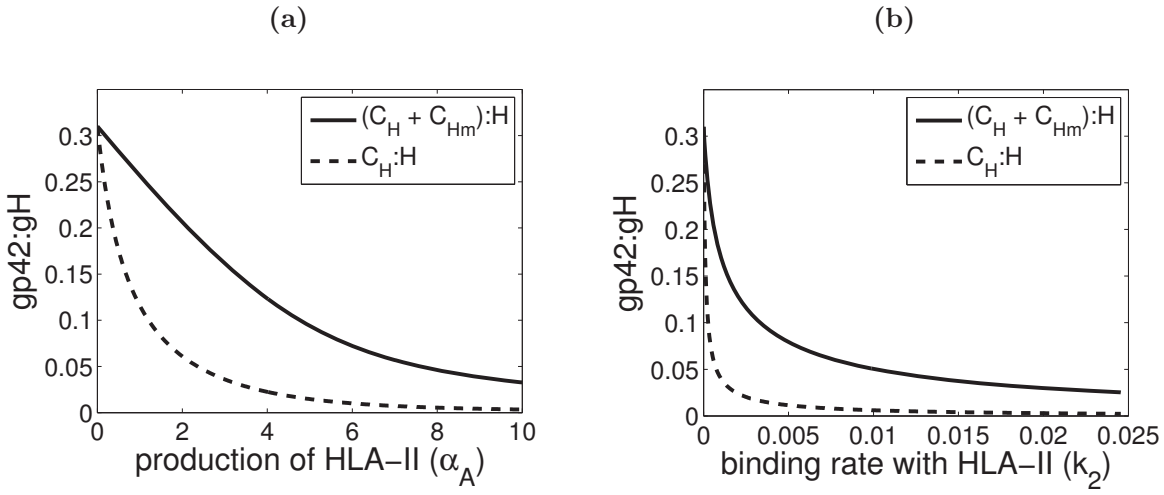

Figure 2.3. Effects of intracellular association of gp42 with HLA-II in B cells on the ratio of three-part to two-part complexes gH/gL/gp42: gH/gL. The solid lines indicate the ratio of total three-part complexes ($C_H + C_{Hm} : H$). The dash lines indicate the ratio of only three-part complexes with gp42 have not interacted with HLA-II ($C_H : H$). **(a)** The ratios as a function of production of HLA-II (α_B). **(b)** The ratios as a function of the binding rate of gp42 with HLA-II (k_2).

is not rate-limiting and begin our model by tracking the complexes of B cells with viruses attached to CD21 (C). Our model describes the kinetics of these complexes of B cells and viruses through different stages of viral entry. We assume no death of B cells during the process of viral entry and hence C remains constant and a B cell is in one of five stages: C_0, C_1, C_2, C_3, or C_f (Figure 2.4). The initial stage with only viral gp350 binding to CD21 is represented by C_0. The next stages in viral entry is for the gH/gL/gp42 (G_4) complexes to bind to HLA-II on the cell (C_1 and C_2). Our key assumption is that two gH/gL/gp42 complexes must bind to HLA-II molecules on a B cell before the involvement of gB (G_B) creates the complex (C_3) that can induce fusion (C_f). We analyze the case where two complexes of gH/gL/gp42 are needed. The model can be extended for any number of gH/gL/gp42 requiring for viral entry.

We let $P_i = C_i/C$ to describe the portion of initial complexes (C) in each stage i, where $i = 0, 1, 2, 3,$ or f, the kinetics of B cells going through different stages of viral entry take the following form

$$\frac{dP_0}{dt} = k_{1G}^{-} P_1 - k_{1G} G_4 P_0$$

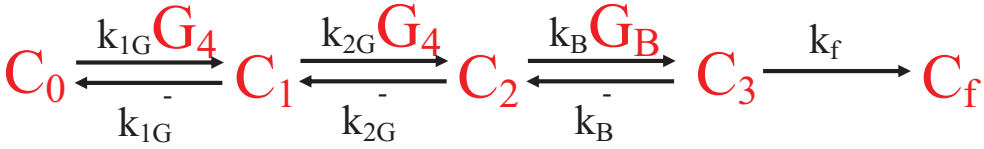

Figure 2.4. Kinetics of B cell going through different stages of viral entry. C_0 is complex of B cell and attached virus with only gp350 binding to CD21. C_1 and C_2 are complexes of B cell and and attached virus with one and two gH/gL/gp42 binding to HLA-II molecules (after binding of gp350 to CD21), respectively. C_3 is complex of B cell and attached virus with gB involvement to trigger fusion. C_f represents virus fusion with B cell (virus successfully enters the cell).

$$\begin{aligned}
\frac{dP_1}{dt} &= k_{1G}G_4P_0 + k_{2G}^-P_2 - k_{1G}^-P_1 - k_{2G}G_4P_1 \\
\frac{dP_2}{dt} &= k_{2G}G_4P_1 + k_B^-P_3 - k_{2G}^-P_2 - k_BG_BP_2 \\
\frac{dP_3}{dt} &= k_BG_BP_2 - k_B^-P_3 - k_fP_3 \\
\frac{dP_f}{dt} &= k_fP_3.
\end{aligned} \tag{2.3}$$

Here, $P_0 + P_1 + P_2 + P_3 + P_f = 1$. We assume that the number of viruses is greater than the number of B cells , where each virus expresses multiple gH/gL/gp42 (G_4) and gB (G_B) complexes.

We can use this system of equation to examine how the amount of three-part gH/gL/gp42 complex (G_4) affects successful fusion to B cells (P_f) at any fixed value of time. The numerical solution of P_f (Equation 2.3) as a function of G_4 is given in Figure 2.5(a). There exists a range of G_4 level (G_4 level is small) such that a small change in this level can greatly affect the level of fusion. A summary of parameter definition can be found in Table 2.3.

The model (Equation 2.3) can be extended to study the case where more than two gH/gL/gp42 complexes are needed. We compare the effects of the amount of three-part gH/gL/gp42 complexes (G_4) on the level of fusion to B cells for the cases $n = 2$ and $n = 3$ (Figure 2.5(b)). When three-part complexes are rare, a small increase (3-fold) can greatly increase virus fusion to B cells (Figure 2.5(c)). This effect is intensified with the increased number of gH/gL/gp42 needed for cooperation (large n). If multiple

Table 2.3. Parameter definitions for the model of viral entry (Equation 2.3).

Parameter	Definition
k_{iG}	Binding rate of the first gH/gL/gp42 to HLA-II [1]
k_{1G}^{-}	Unbinding rate of gH/gL/gp42 from the first gH/gL/gp42/HLA-II complex [2]
k_{2G}	Binding rate of the second gH/gL/gp42 to HLA-II [1]
k_{nG}^{-}	Unbinding rate of gH/gL/gp42 from the second gH/gL/gp42/HLA-II complex [2]
k_B	Binding rate of gB to its receptor on B cell [1]
k_B^{-}	Unbinding rate of gB to its receptor [2]
k_f	Rate of fusion [2]

[1] These parameters have the unit of $\text{min}^{-1}\text{nM}^{-1}$
[2] These parameters have the unit of min^{-1}

three-part gH/gL/gp42 complexes are indeed require for EBV fusion with B cells, the observation of 2 to 5-fold increase in the level of gp42 leading to 30 to 100-fold increase in the infectivity of virus to B cells can be explained better with the case $n = 3$ (Figure 2.5(d)).

2.5 Discussion

The switch of infection between cell types is crucial to viral persistence and maybe diseases, and that it can be explained through intracellular interaction and the kinetic of binding. The 2- to 5-fold increase in gp42 level on the viral envelope inhibits infection of epithelial cells proportional to the level, but increases infection of B cells disproportionally, 30- to 100-fold. In this study, we have used mathematical models to study two different hypotheses on the effect of gp42 level on the infectivity of virus to B cells.

The first hypothesis assumes intracellular association of gp42 with HLA-II not only degrades some gp42, but also modifies gp42 and reduces its function in fusion. This hypothesis can explain the 30- to 100-fold decrease in infectivity of B-cell virus to B cells in comparison with epithelial-cell virus. Indirect support of this hypothesis comes from the observation that changing only a few residue in critical region of gp42

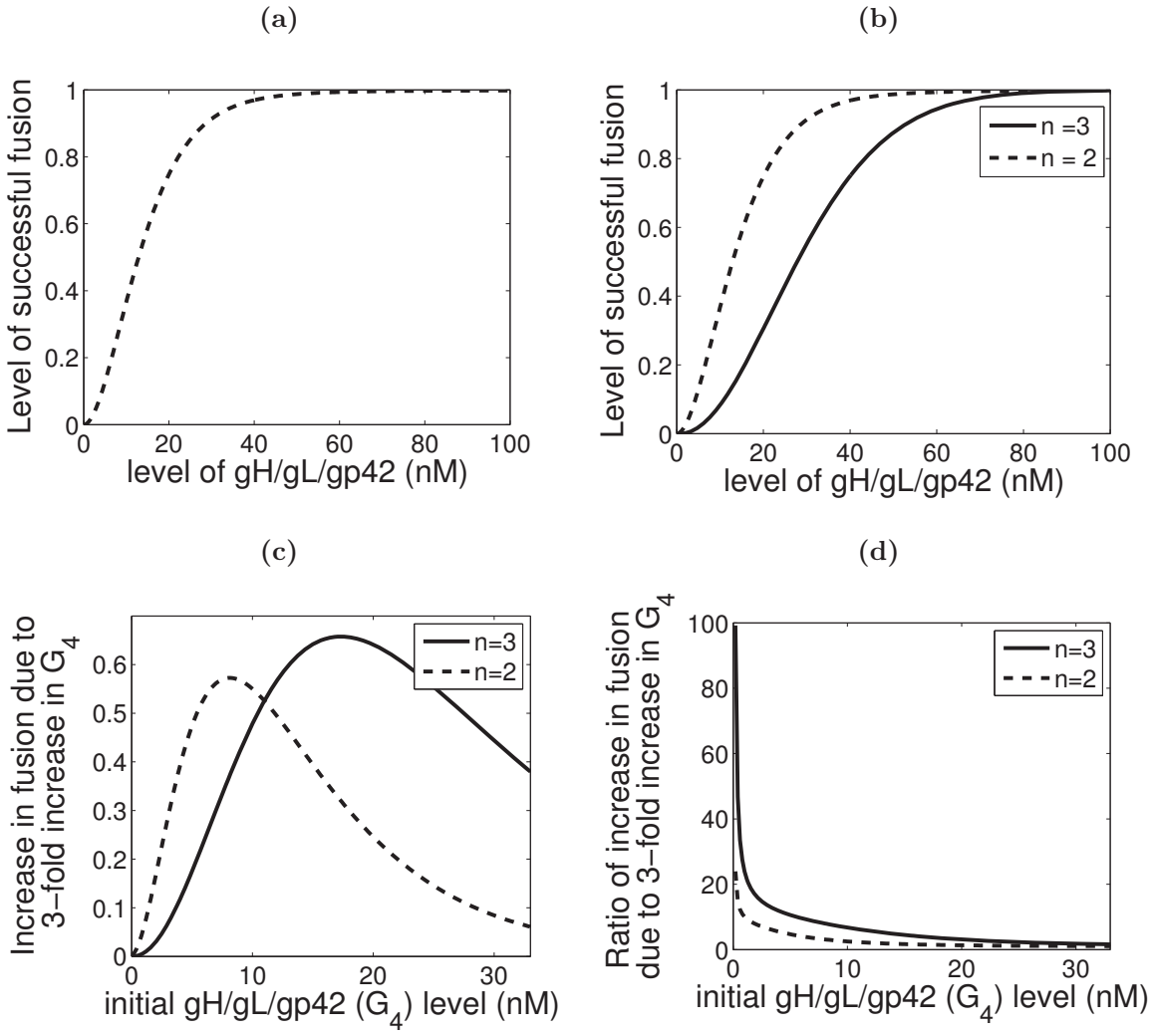

Figure 2.5. Effects of the level of three-part complexes gH/gL/gp42 (G_4) on level of fusion (P_f). The dashed lines are for the case $n = 2$ while the solid lines are for the case $n = 3$. **(a)** Level of successful fusion (P_f) as a function of gH/gL/gp42 (G_4). **(b)** Level of P_f as a function of G_4, comparing the the cases $n = 2$ (dashed line) and $n = 3$ (dotted line). **(c)** The difference of increase in fusion due to 3-fold increase in the level of gH/gL/gp42 as a function of initial level of gH/gL/gp42. **(d)** Ratio of increase in fusion due to 3-fold increase in the level of gH/gL/gp42 as a function of initial level of gH/gL/gp42. Parameter values used for these analyses are $k_{iG} = 0.00098$ nM^{-1}min^{-1}($i = 1,$ or 2), $k_{iG}^{-} = 0.83$ min^{-1}, $k_{nG} = 0.049$ nM^{-1}min^{-1} ($n = 2,$ or 3), $k_{nG}^{-} = 0.042$ min^{-1}, $k_B = 0.0049$ nM^{-1}min^{-1}, $k_B^{-} = 0.0417$ min^{-1}, $k_f = 0.033$ min^{-1}, $t = 300$ min.

protein can disrupt its function in fusion [81]. Our result suggests the value of further studies to investigate functional differences between gp42 expressed on B-cell and on epithelial-cell virus.

Our second hypothesis assumes that multiple three-part complexes gH/gL/gp42 on the viral envelope must bind to HLA-II molecules on B cells in order for viral glycoprotein gB to bind and trigger fusion. We find that multiple gH/gL/gp42 complexes must be needed to explain the 30 to 100-fold increase in viral infectivity. The higher the number of required gH/gL/gp42, the better the increase in the viral infectivity can be explained. The exact number of gH/gL/gp42, however, still relies on further studies of the kinetics of gH/gL/gp42 on the viral envelope binding to HLA-II on B cells with data on different binding affinity of multiple complexes. If this hypothesis holds for the requirement of multiple gH/gL/g42 for fusion, it suggests gp42 might serve as a great potential target for vaccine or therapy in prevention and treatment of EBV infection.

The observation that gp42 serves as a molecular switch of tropism for EBV [4] is of great potential interest for studies of evolution of EBV tropism, the mechanisms of virus entry, and the association of EBV with different types of cancer of B cells and epithelial cells. Obtaining understanding of what can affect the gp42 level being expressed on the viral envelope and how this level affects infectivity and preferred tropism of EBV is critical. If the first hypothesis holds for the effect of the intracellular association of gp42 with HLA-II on the function of gp42, host genetics may play a key role in susceptibility of cell lines to EBV and the course of the long-term infection.

In individuals with HLA-II alleles that interact weakly with gp42, virus derived from B cells would express high level of gp42 and EBV long term infection might focus mainly on B cells. Moreover, the level of infected B cells would be low in this case because gp42 does not bind well to HLA-II. If an individuals carries HLA-II alleles that strongly interact with gp42, EBV can be very effective at switching infection between B cells and epithelial cells. In this case, this individual may be more susceptible to EBV infection and the long-term infection shifts to involve more infection of epithelial cells. Indeed, different studies have linked specific types of HLA-II alleles to EBV associated diseases including infectious mononucleosis, Hodgkin's disease, and nasopharyngeal

carcinoma [2, 31]. Future work can use mathematical models to address how these shifts of tropism affect the dynamics of long-term persistence of EBV infection and association of the infection with cancer of B cells and epithelial cells.

2.6 Acknowledgements

We would like to thank Dr. Thorley-Lawson for the opportunity to come and study the biology of Epstein-Barr virus infection of B cells at his laboratory and Dr. Hutt-Fletcher for insightful discussions on Epstein-Barr virus infection of epithelial cells. Funding for this work was provided by the National Science Foundation (NSF) Research Training Group (RTG) (Award Number DMS0354259).

CHAPTER 3

ALTERNATING HOST CELL TROPISM SHAPES THE PERSISTENCE, EVOLUTION AND COEXISTENCE OF EPSTEIN-BARR VIRUS INFECTIONS IN HUMANS

3.1 Abstract

Epstein-Barr virus (EBV) infects and can persist in a majority of people worldwide. Within an infected host, EBV targets two major cell types, B cells and epithelial cells, and viruses emerging from one cell type preferentially infect the other. We use mathematical models to understand why EBV infects epithelial cells when B cells serve as a stable refuge for the virus and how switching between infecting each cell type affects virus persistence and shedding. We propose a mathematical model to describe the regulation of EBV infection within a host. This model is used to study the effects of parameter values on optimal viral strategies for transmission, persistence, and intrahost competition. Most often, the optimal strategy to maximize transmission is for viruses to infect epithelial cells, but the optimal strategy for maximizing intrahost competition is for viruses to mainly infect B cells. Applying the results of the within-host model, we derive a model of EBV dynamics in a homogeneous population of hosts that includes superinfection. We use this model to study the conditions necessary for invasion and coexistence of various viral strategies at the population level. When the importance of intrahost competition is weak, we show that coexistence of different strategies is

possible.

3.2 Introduction

Epstein-Barr virus (EBV) belongs to the herpesvirus family, infects over 90% of humans worldwide and persists for the lifetime of the person [74]. Most individuals infected with EBV are asymptomatic, but the virus has been associated with many diseases and cancers including infectious mononucleosis (IM), Burkitt's lymphoma, Hodgkin's lymphoma, and nasopharyngeal carcinoma (NPC). EBV is transmitted by intimate contact, mainly through saliva and oropharyngeal secretion [3]. The virus primarily targets two cell types, B cells and epithelial cells. In B cells, EBV can establish a long-term infection. Once successfully entering a naive B cell, EBV can drive an infected B cell through different stages of latent infection where the viral genome remains inside the cell. The virus turns off most of its gene expression when an infected cell differentiates into the memory stage. Within an infected memory B cell, EBV stays quiescent, and remains invisible to the immune response. These infected memory B cells can be activated and become plasma-like B cells within which virions can replicate and burst out (lytic infection) [85]. In epithelial cells, an EBV infection often results in virus replication and production. Latent infection of epithelial cells is rare and has been observed only in the case of NPC.

In vitro, viruses that emerge from one cell type preferentially infect the other [4]. The viral glycoprotein gp42 on EBV's envelope serves as the molecular switch that EBV uses to alternate infections between the two cell types. This viral protein is required for infection of B cells, but inhibits infection of epithelial cells. In B cells, gp42 interacts with HLA class II, human genes that encode antigen presenting proteins on the surface of antigen presenting cells, and becomes a target for degradation. Hence, viruses produced by B cells express low levels of gp42. Epithelial cells do not express HLA class II and hence viruses produced by epithelial cells express high levels of gp42 [4]. As a result, viruses emerging from B cells are approximately five times more efficient at infecting epithelial cells than the viruses emerging from epithelial cells, which are 100 times more efficient in infecting B cells than viruses derived from B cells [36].

The viral infection of B cells and the maintenance of a persistent infection within the host have been intensively studied [75]. The dynamics of EBV infection of B cells and the T cell responses have been investigated using simulations of agent-based models, C-ImmSim and PathSim [9, 78]. The infection of epithelial cells, however, has not been included in these models. Simulations of these models reproduce qualitative features of real infections where the maximum number of infected cells and viruses occur sometimes between one to a few weeks after initial infection, and a persistent infection is established within months. PathSim shows that EBV cannot result in a persistent infection unless it can maintain a latent infection within the memory B cell population. The simulation results of this agent-based model also highlight the sensitivity of the dynamics of infection to variation in the reactivation rate of lytic infection from infected memory B cells. A small increase in this rate causes the number of infected cells to expand quickly and remain at a high level [78]. However, the sensitivity may be due to the lack of T cell expansion and proliferation in this agent-based model.

A mathematical model describing the within-host dynamics of EBV infection has been constructed to study the T cell responses to persistent virus [18]. This model uses ordinary differential equations to track the number of latently and lytically infected cells, viruses, and T cells. However, it does not identify a specific class of target cells, such as B cells or epithelial cells. The model allows newly infected cells to produce viruses without going through latent stages of infection and allows lytically infected cells to become latently infected. The first of these two assumptions only applies for infection of epithelial cells. The second assumption does not reflect the biology of EBV infection of either cell type. Differential equation models have also been developed to study the dynamics of other herpesvirus infections like cytomegalovirus (CMV or HHV-5) [92] and HHV-6 [90]. Both CMV and HHV-6 can infect a wide range of cells in human and share the ability to establish persistent infection within the host cells with other herpesviruses [57, 95].

In this study, we develop and analyze mathematical models describing the within-host and between-host dynamics of infection to explore the effects of switching between host cell types on viral shedding, persistence, and evolution. Within a host, EBV must

infect B cells to establish a long-term infection. However, infection of epithelial cells plays an important role in transmitting the infection. In fact, EBV is transmitted mainly through saliva and most viruses found in the saliva of infected hosts show characteristics of deriving from epithelial cells [44]. We propose a mathematical model to capture the within-host dynamics of virus and host-cell interaction, including the dynamics of epithelial cell infection. Assuming EBV can modify its ability to infect B cells and epithelial cells, we use this model to compute viral strategies that maximize transmission and the total virus population being produced (intrahost competition). We then determine how changes in parameters affect the optimal viral strategy for transmission and for intrahost competition. While infection of epithelial cells plays a key role in transmission, intrahost competition emphasizes the role of infection of B cells. Finally, we apply the results of our within-host model to derive a model of EBV infection at the population level to study the conditions for invasion and coexistence of different viral strategies.

3.3 Model of the within-host dynamics of an EBV infection

3.3.1 Model

Our mathematical model (Figure 3.1 and Equation 3.1) describing the dynamics of EBV infection within an infected host follows two types of target cells (B cells and epithelial cells), two types of viruses (B-cell-derived, V_B, and epithelial-cell-derived, V_E), and two types of cytotoxic T cells or CTLs (attacking latently infected B cells, T_2, and lytically infected cells, T_4, respectively). B cells break into four state variables: naive B cells (B_1), latently infected B cells (B_2), latently infected memory B cells (B_3), and lytically infected B cells or plasma cells (B_4). In B_2, there are still 9 latent genes being expressed and these latently infected cells can be recognized and killed by T cells (T_2). In B_3, the virus genome quietly exists inside the cell and is invisible to T cell responses. Epithelial cells do not ordinarily harbor latent virus and require only two state variables: uninfected epithelial cells (E_1), and lytically infected epithelial cells (E_4). The model consists of a system of 10 ordinary differential equations,

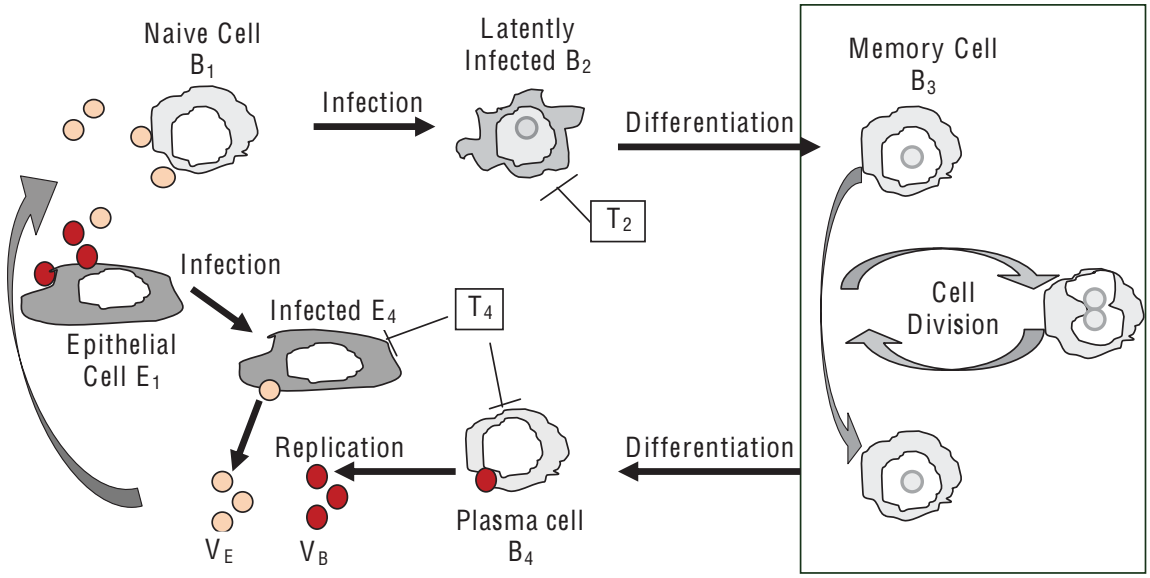

Figure 3.1. Model of EBV infection of B cells and epithelial cells. In this model, we add the infection of epithelial cells to the stages of B-cell infection that have been studied by Thorley-Lawson [85] to describe EBV switching infection between host cell types.

$$
\begin{aligned}
\frac{dB_1}{dt} &= d_1(B_0 - B_1) - \mu_{Eb}V_E B_1 - \mu_{Bb}V_B B_1 \\
\frac{dB_2}{dt} &= \rho(\mu_{Eb}V_E B_1 + \mu_{Bb}V_B B_1) - (d_2 + c)B_2 - k_2 B_2 T_2 \\
\frac{dB_3}{dt} &= cB_2 + rB_3 - srB_3 \\
\frac{dB_4}{dt} &= rB_3 - d_4 B_4 - k_4 B_4 T_4 \\
\frac{dE_1}{dt} &= d_e(E_0 - E_1) - \mu_{Be}V_B E_1 - \mu_{Ee}V_E E_1 \\
\frac{dE_4}{dt} &= \mu_{Be}V_B E_1 + \mu_{Ee}V_E E_1 - (d_e + \gamma)E_4 - k_4 E_4 T_4 \\
\frac{dV_B}{dt} &= nd_4 B_4 - d_v V_B \\
\frac{dV_E}{dt} &= n\gamma E_4 - d_v V_E \\
\frac{dT_2}{dt} &= \phi_2 T_1 w(B_2) + \theta_2 T_2 w(B_2) - \delta T_2 \\
\frac{dT_4}{dt} &= \phi_4 T_1 [w(B_4 + E_4)] + \theta_4 T_4 [w(B_4 + E_4)] - \delta T_4 \,.
\end{aligned}
\tag{3.1}
$$

The dynamics of B cells obey these assumptions:

- Naive B cells begin with an initial population of B_0 and turn over at rate d_1. They can encounter and be infected by the virus populations V_B and V_E with rates $\mu_{Bb}V_B$ and $\mu_{Eb}V_E$, respectively.

- An infection of a naive cell, B_1, gives rise latently infected cells, B_2, by proliferation of these newly infected cells, where ρ is the proliferation factor. These B_2 cells die at a rate d_2, can be recognized and killed by effector T cells at a rate k_2T_2, and can enter the latently infected memory state at rate c, which is driven by EBV gene expression switching off.

- Infected memory cells, B_3, obey homeostatic regulation similar to normal memory B cells. They are invisible to the T cell responses, undergo division with a rate r. On average, one cell becomes lytically infected and one remains in the memory state. The rate sr represents the death of B_3 due to homeostatic regulation of memory cells, where s is the regulation factor. For normal homeostasis, $s = 2$ balances the proliferation rate of $2r$ [54]. The frequent turnover of the memory B cell population helps maintain the supply of plasma B cells that produce antibodies against various types of antigens. EBV takes advantage of this mechanism to activate its lytic cycle.

- Lytically infected B cells, B_4, arise from lytic reactivation of infected memory B cells, B_3, at rate r, die and release viruses at a rate d_4, and can be killed by effector T cells at a rate k_4T_4.

The dynamics of epithelial cells assume the following:

- Uninfected epithelial cells start with initial population E_0, and turn over at a rate d_e. They can encounter and be infected by the virus populations V_B and V_E with rates $\mu_{Be}V_B$ and $\mu_{Ee}V_E$, respectively.

- Lytically infected epithelial cells, E_4, die naturally at a rate d_e, die from virus bursting out at a rate γ, and can be killed by effector T cells at rate k_4T_4.

Free viruses, V_B and V_E, are produced from B cells and epithelial cells at rate nd_4 and $n\gamma$ respectively, where n is the average burst size, and die at rate d_v.

To model the CTL response, we assume that the naive population, T_1, is regulated at a constant level and, upon stimulation by viral antigens, become effector cells against latent or lytic infection with rate ϕ_2 or ϕ_4, respectively. The activated effector cells, T_2 and T_4, can proliferate further with rate θ_2 and θ_4, respectively, upon stimulation by viral antigens from infected cells. Each type of effector cell dies at rate δ. Activation and proliferation of CTLs are saturating function of the available infected cells,

$$w(B_j) = \frac{B_j}{K + B_j}\,, \tag{3.2}$$

where K is the number of infected cells at which activation or proliferation is half maximal. Tables 3.1 and 3.2 present the parameter values used for simulation and analysis of the model.

This system of Equation (3.1) has two equilibria. The infection-free equilibrium is given by

$$B_1^* = B_0\,, \qquad E_1^* = E_0\,,$$

and every other state variable equals zero. If virus replication is sufficiently efficient, there is also a persistent equilibrium, where all state variables take on positive values. The stability of the infection-free equilibrium is determined by the basic reproductive ratio,

$$\begin{aligned} R_0 = {} & \frac{n}{2d_v^2}\left(\frac{\rho\mu_{Bb}B_0c}{(s-1)(d_2+c)} + \frac{\mu_{Ee}E_0\gamma}{d_e+\gamma}\right) \\ & + \frac{n}{2d_v^2}\sqrt{\left(\frac{\rho\mu_{Bb}B_0c}{(s-1)(d_2+c)} - \frac{\mu_{Ee}E_0\gamma}{(d_e+\gamma)}\right)^2 + \frac{4\rho\mu_{Eb}B_0c\mu_{Be}E_0\gamma}{(s-1)(d_2+c)(d_e+\gamma)}}\,, \end{aligned} \tag{3.3}$$

of EBV in a naive host [29] that can be found by the next generation matrix [88]. Infections of both B cells and epithelial cells contribute to the basic reproductive ratio of EBV. If $R_0 < 1$, the infection-free equilibrium is stable and a long term infection cannot establish within a host. If $R_0 > 1$, the infection-free equilibrium is unstable and EBV can establish a persistent infection.

The dynamics of infected cells, viruses, and T cell responses for the case when $R_0 > 1$ are shown in Figure 3.2. The populations of infected cells and viruses peak during the second week of infection and then resolve down to low levels at equilibrium.

Table 3.1. Parameters for the dynamics of B cells (Equation 3.1). We use many parameters from PathSim, where the rates are estimated and given in a unit of per 6 minutes [78], and convert them into the unit of per minute.

Parameter	**Description**	**Value**	**Unit**	Reference
d_1	Turnover rate of naive B cells	$1/6000$	min^{-1}	[78]
μ_{Eb}	B cell infection rate per epithelial-cell virus	3.3×10^{-10}	$\text{min}^{-1}\text{virus}^{-1}$	[78] [1]
μ_{Bb}	B cell infection rate per B-cell virus	$\mu_{Eb}/100$	$\text{min}^{-1}\text{virus}^{-1}$	[36]
ρ	Proliferation factor	2	no unit	[78]
d_2	Death rate of latently infected B cells	$1/11520$	min^{-1}	[78]
c	Rate of latently infected cells going into memory stage	0.001	min^{-1}	[78] [2]
k_2	Rate of latently infected B cells killed by T cells	3.8×10^{-8}	$\text{min}^{-1}\text{cell}^{-1}$	[78] [3]
r	Rate of reactivation of lytic infection from latent infection	8.3×10^{-5}	min^{-1}	[78]
s	Regulation factor of memory B cells	2	no unit	[54]
d_4	Death rate of lytically infected cells due to viruses bursting out	$1/4320$	min^{-1}	[78]
k_4	Rate of lytically infected B cells killed by T cells	7.6×10^{-8}	$\text{min}^{-1}\text{cell}^{-1}$	[78][3]

[1]Probability of virus and cell encounter per minute multiplied by the probability of infection and divided by the number of viruses ($\approx 10^7$)
[2]We take this to be the same rate as the estimation of .1% of lymphocytes leaving the Waldeyer's ring per minute
[3]Probability of lymphocyte encounter per minute multiplied by the probability that T_i kills its target and divided by the number of T_i($\approx 10^4$)

Infection of epithelial cells plays a larger role during the primary infection than during the long-term infection. Simulation of EBV infection using the agent-based model, PathSim, produces clearance of virus and infected-cells in the case of small viral burst size or inability of EBV to enter latency within memory B cells [78]. Furthermore, EBV infection also cannot be established within people with X-linked agammaglobulinemia because they do not have mature B cells. Our model produced similar results; small virus burst size (small value of n), no latency within memory B cells ($c = 0$), or no mature susceptible B cells ($B_0 = 0$) leads to $R_0 < 1$ and virus clearance.

Table 3.2. Parameters for the dynamics of epithelial cells, virus, and T-cell responses (Equation 3.1). We use many parameters from PathSim, where the rates are estimated and given in a unit of per 6 minutes [78], and convert them into the unit of per minute.

Parameter	**Description**	**Value**	**Unit**	Reference
d_e	Turn-over rate of epithelial cells	1/6000	min^{-1}	[1]
μ_{Be}	Epithelial cell infection rate per B-cell virus	3×10^{-11}	$\text{min}^{-1}\text{virus}^{-1}$	[2]
μ_{Ee}	Epithelial cell infection rate per epithelial-cell virus	$\mu_{Be}/5$	$\text{min}^{-1}\text{virus}^{-1}$	[36]
γ	Death rate of infected epithelial cells due to viruses bursting out	1/6000	min^{-1}	[3]
n	Viral burst size	1000	$\text{virus}\cdot\text{cell}^{-1}$	[78]
d_v	Death rate of virus	1/2160	min^{-1}	[78]
ϕ_2	Rate of T cell activation against latent infection	1.95×10^{-5}	min^{-1}	[78][4]
ϕ_4	Rate of T cell activation against lytic infection	4.48×10^{-5}	min^{-1}	[78][4]
θ_2	Rate of T cell proliferation against latent infection	3.25×10^{-5}	min^{-1}	[78][5]
θ_4	Rate of T cell proliferation against lytic infection	3.25×10^{-5}	min^{-1}	[78][5]
K	Number of infected cells when T cell activation is half maximal	10^5	cell	[45]
δ	Death rate of T cells	1/156000	min^{-1}	[78]

[1]Estimated, taken to be the same as d_1
[2]Estimated, taken to be less than μ_{Eb} [87]
[3]Estimated, taken to be less than d_4 [4]
[4]Probability of lymphocyte encounter per minute multiplied by the probability of T_i activation by B_i, where $i = 2$ or 4
[5]Probability of lymphocyte encounter per minute multiplied by the frequency of cell division (every 8-12 hours)

3.3.2 The effects of change in parameter values on transmission, persistent infection and the dynamics of EBV infection

Changes in the parameter values can alter the transmission efficiency, equilibrium viral loads, and short-term dynamics after initial infection. Transmission, as we have seen, depends on the amount of viruses produced by epithelial cells. Most EBV-infected individuals are healthy carriers and can transmit the virus throughout their lifetime. Although the amount of transmissible epithelial cell viruses varies during the course of the infection, over the long term, maximizing transmission is equivalent to maximizing the equilibrium value of epithelial-cell viruses (V_E^*) produced in the long run. A host

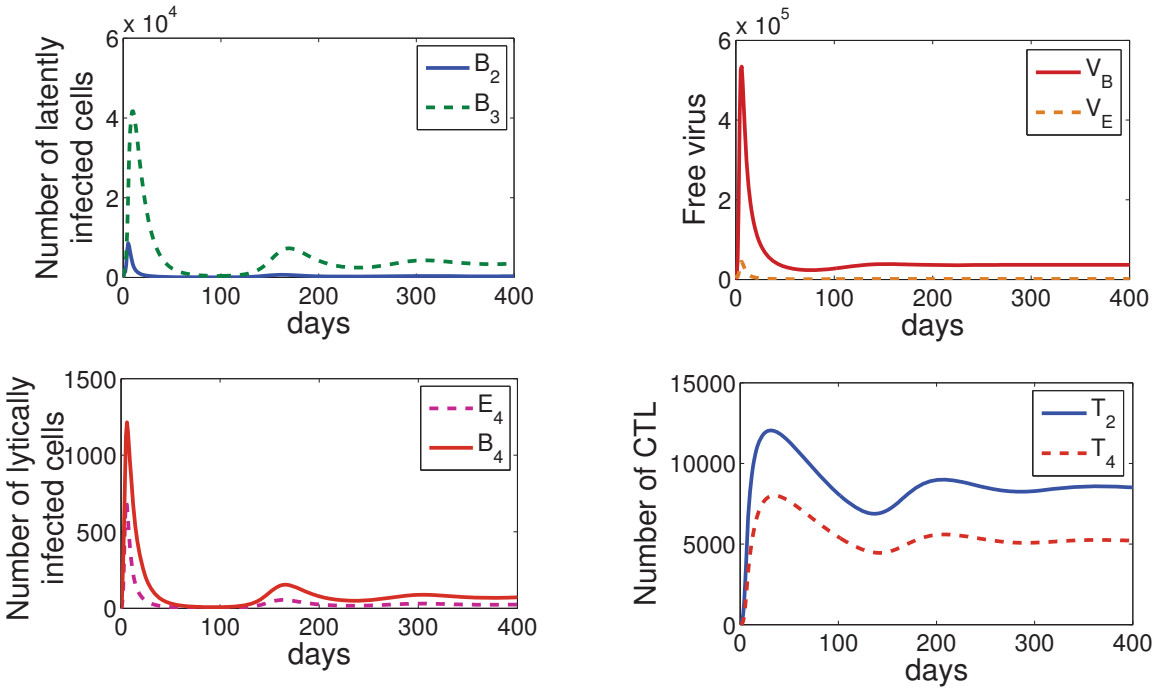

Figure 3.2. Dynamics of infected cells, viruses, and T cell responses using parameter values in Tables 3.1 and 3.2

can be infected by multiple strains of EBV, at least during primary infection [82]. In the case of a perfectly cross-reacting T cell response (i.e., one epitope of T cells responds to all strains of EBV) and a single cell type to infect, the principle of competition exclusion implies that multiple strains cannot coexist within a host [6]. In our model, there are two types of target cells and this principle does not necessarily apply. Numerical solutions of our model, however, do not display equilibrium coexistence in a host. Furthermore, the strain with higher total number of viruses being produced at equilibrium ($V_T^* = V_B^* + V_E^*$) wins out to establish a persistent infection within a host. Assuming EBV can modify its ability to infect B cells and epithelial cells, we investigate the optimal strategy the virus would used to maximize transmission or to maximize viral load in persistent infection.

We first develop a model to describe constraints in viral strategies within a host. We have assume that $\mu_{Eb} > \mu_{Bb}$ and $\mu_{Be} > \mu_{Ee}$ (Tables 3.1 and 3.2) since V_E are more efficient at infecting B cells and V_B are more efficient at infecting epithelial cells

[4]. This same study also found that infection efficiency varies among EBV strains. Assuming EBV can modify its ability to infect B cells and epithelial cells, it can only do so if there is a trade-off between the ability to infect B cells and epithelial cells (Figure 3.3(a)). For example, V_B can improve its ability to infect B cells by increasing its expression of gp42. By doing so, however, it decreases its ability to infect epithelial cells.

To model this tradeoff, we constrain the infection rates to be weighted averages of the pure V_B and V_E strategies, which are represented by $\vec{\mu}_B$ and $\vec{\mu}_E$ respectively. Let $\vec{\eta}_B$ and $\vec{\eta}_E$ be the modified infection rates of V_B and V_E, respectively, given by

$$\begin{pmatrix} \eta_{Bb} \\ \eta_{Be} \end{pmatrix} = \alpha_B \begin{pmatrix} \mu_{Bb} \\ \mu_{Be} \end{pmatrix} + (1-\alpha_B) \begin{pmatrix} \mu_{Eb} \\ \mu_{Ee} \end{pmatrix} \tag{3.4}$$

$$\begin{pmatrix} \eta_{Eb} \\ \eta_{Ee} \end{pmatrix} = \alpha_E \begin{pmatrix} \mu_{Bb} \\ \mu_{Be} \end{pmatrix} + (1-\alpha_E) \begin{pmatrix} \mu_{Eb} \\ \mu_{Ee} \end{pmatrix}. \tag{3.5}$$

The weighted parameters α_B and α_E define strategies of V_B and V_E, respectively. If $\alpha_B = 1$ and $\alpha_E = 0$ (Figure 3.3(b), upper left), the η's take on the same values as the μ's. As α_B decreases, V_B switch from infecting epithelial cells to infecting B cells. As

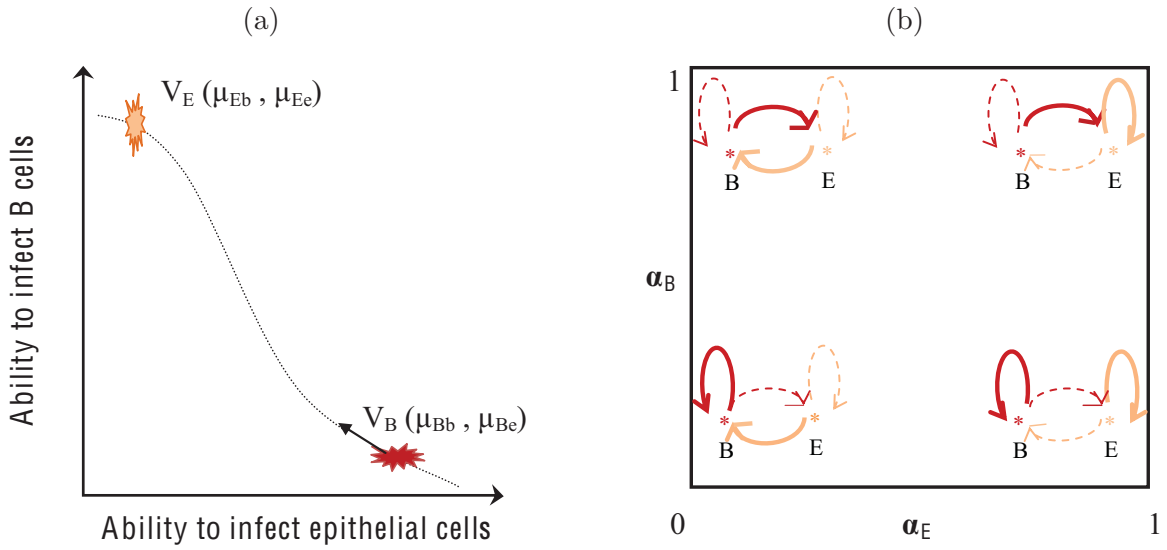

Figure 3.3. Trade-off in the ability to infect B cells and epithelial cells. (a) For a virus, increase in infection of B cells results in decrease in infection of epithelial cells and vice versa. (b) The strategies of V_B and V_E are defined as α_B and α_E, respectively; as these two parameters increase, both types of viruses prefer to infect epithelial cells.

α_E increases, V_E switch from infecting B cells to infecting epithelial cells. When α_B and α_E are small, both V_B and V_E prefer to infect B cells (Figure 3.3(b), bottom left). In contrast, when α_B and α_E are large, both V_B and V_E prefer to infect epithelial cells (Figure 3.3(b), upper right). At the bottom right corner of Figure 3.3(b), where α_B is small and α_E is large, V_B prefer to infect B cells and V_E prefer to infect epithelial cells. Replacing μ by η in the system of Equation (3.1), the equilibrium values $V_E^*(\vec{\alpha_i})$ and $V_T^*(\vec{\alpha_i})$ can be found numerically for any given strategy (α_B, α_E). Our next step is to analyze the effects of parameters on viral strategies that maximize V_E^* and V_T^*.

Natural variation between individuals in the expression of EBV receptors (HLA class II on B cells and CR2 or integrins on epithelial cells) can affect the susceptibility of these cells to EBV infection [26, 37]. The susceptibility of B cells and epithelial cells to virus classes V_B and V_E are described by the parameters μ_{Bb}, μ_{Be}, μ_{Eb}, and μ_{Ee}. We thus focus our sensitivity analysis on these four parameters and the other three parameters that are related to the production of viruses within a host: the rate of virus replication and production from B cells (d_4) and from epithelial cells (γ), and the viral burst size (n). We consider each of these parameters at three different values: the value listed in Tables 3.1 and 3.2 (middle), this value divided by two (small) and multiplied by two (large). For example, the three values for n are 500, 1000, and 2000. We thus have 3^7 (or 2187) parameter combinations to study. We ran the same sensitivity analysis on all other parameters in Table 3.1 and 3.2 but found minimal effects on the optimal strategy for transmission and establishment of a persistent infection.

3.3.2.1 Identifying strategies that maximize transmission

We assume that EBV maximizes transmission to new hosts by maximizing equilibrium amount of virus produced by epithelial cells (V_E^*). We divide the $\alpha_B\alpha_E$-plane in Figure 3.3(b) into 21×21 grid where each of the 441 points on the grid represents a viral strategy. For every parameter set, we find V_E^* numerically for all strategies and locate the strategy where V_E^* is maximized. Figure 3.4 shows the influence of parameter values on the viral strategy that maximizes V_E^*. We focus our presentation of the results at the four corners where V_B and V_E prefer to switch infections between

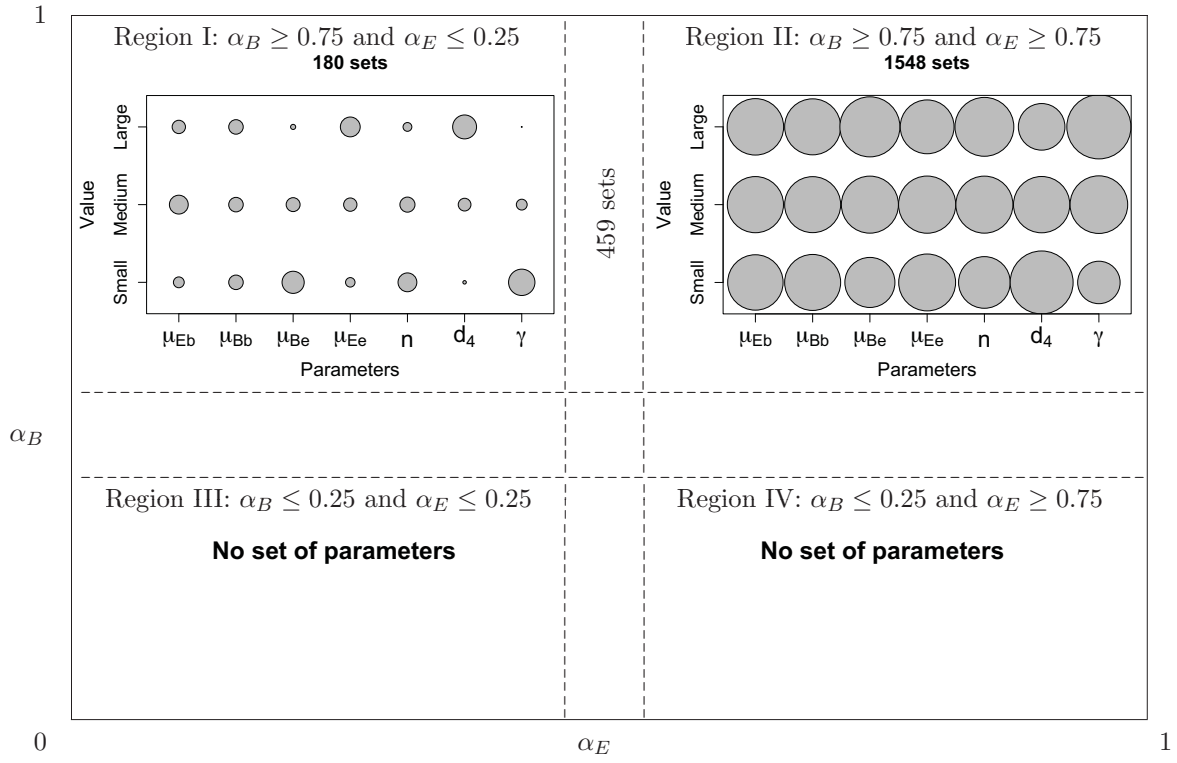

Figure 3.4. Effects of parameter values on optimal transmission (maximizing V_E^*). Each parameter takes on three different values: small, medium, and large. The four panels summarize parameter sets that give optimal V_E^* at the four corners in Figure 3.3(b). Region I: $\alpha_B \geq 0.75$ and $\alpha_E \leq 0.25$; Region II: $\alpha_B \geq 0.75$ and $\alpha_E \geq 0.75$; Region III: $\alpha_B \leq 0.25$ and $\alpha_E \leq 0.25$; Region IV: $\alpha_B \leq 0.25$ and $\alpha_E \geq 0.75$. The dot size represents the number of times the parameters take on particular values.

the two cell types (Region I), to primarily infect epithelial cells (Region II), to mainly target B cells (Region III), and to infect their own producing cells (Region IV).

- A minority of parameters (180 out of 2187 sets) favor a strategy similar to what has been observed *in vitro* where V_B preferentially infect epithelial cells and V_E preferentially infect B cells (Region I) [4]. The parameter sets that maximize V_E^* in this region tend to have μ_{Be}, n, and γ small and μ_{Ee} and d_4 large.

- A large number of parameter sets (1548 out of 2187) favor strategies where both V_B and V_E preferentially infect epithelial cells (Region II).

- The remaining parameter sets (459 out of 2187) favor strategies that lie in a range where α_B is large and α_E is at an intermediate value.

- There are no parameter sets favoring strategies in Region III and IV where α_B is small, implying that B-cell viruses must infect epithelial cells to maximize transmission.

Figure 3.5 shows the time-course dynamics of free viruses and the T cell responses for sample sets of parameters from Region I and Region II in Figure 3.4. The viral load initially elevates, peaks during the second week of infection, and then resolves down to a low equilibrium level. Strategies in Region II of the $\alpha_B\alpha_E$-plane give higher V_E^* at the expense of lower V_B^*.

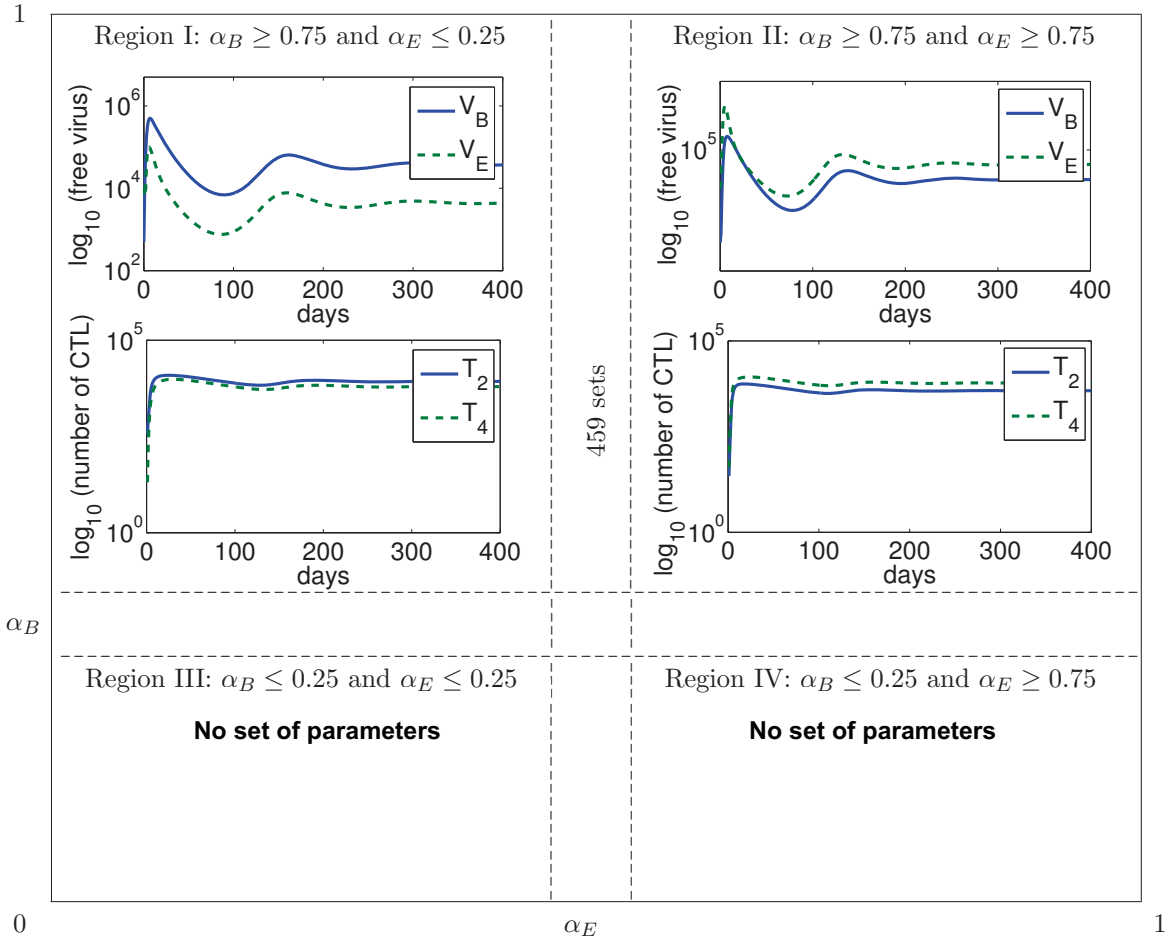

Figure 3.5. Effects of parameter values on dynamics of the model for sample sets of parameters from the two upper corners in Figure 3.4.

3.3.2.2 Identifying strategies that maximize total viral load

We now make the assumption that a host gets infected by two or more EBV strains that differ only in their strategies on the $\alpha_B\alpha_E$-plane. In the case of a perfectly cross-reacting T cell response, our numerical results show that a virus with higher V_T^* would win out to establish a persistent infection with no stable coexistence of multiple strains within a host. We thus assume that the intrahost competition will select the virus that maximizes the total number of virions produced at equilibrium. For each of the 2187 sets of parameters, we found V_T^* numerically and located the strategy where V_T^* is maximized. Figure 3.6 shows the influence of parameter values on viral strategy that maximizes V_T^*. The optimal strategies lie predominantly in Region III (1449 out of

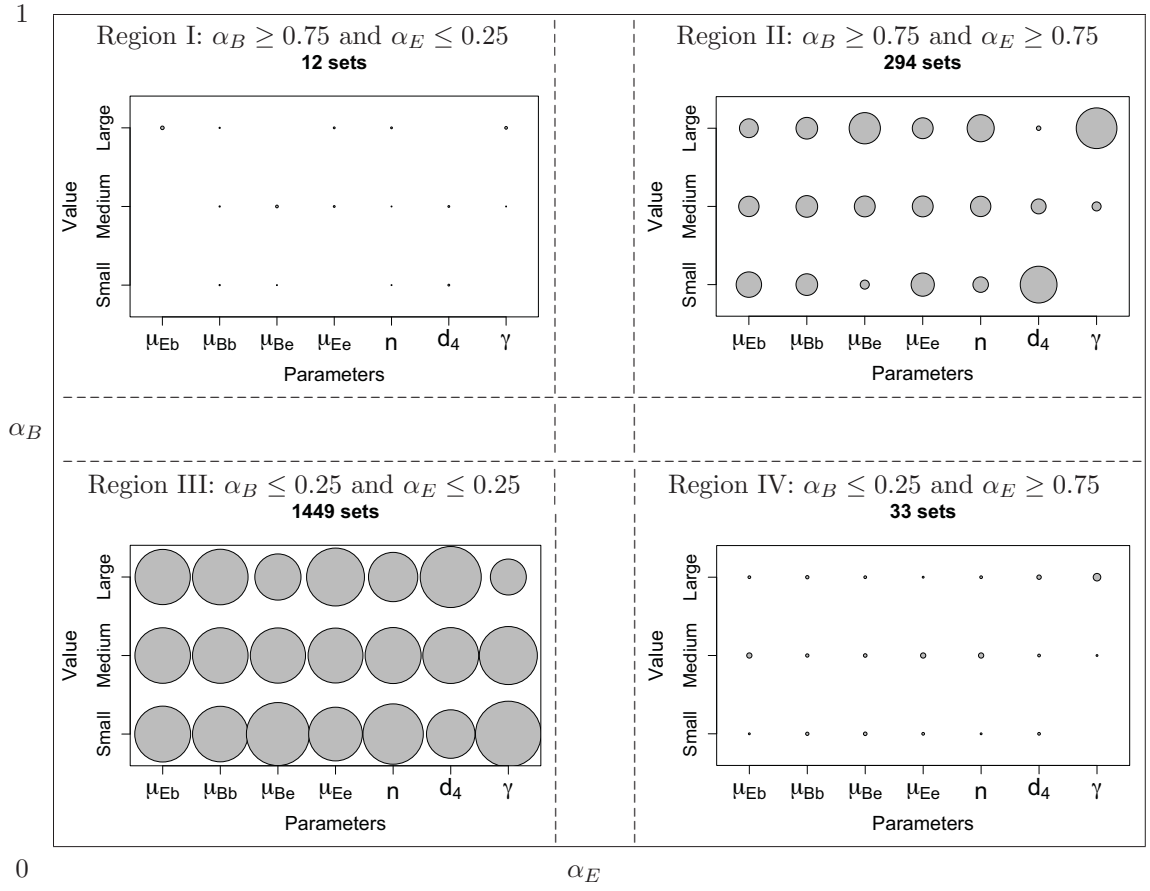

Figure 3.6. Effects of parameter values on a persistent infection (maximizing V_T^*) with similar notation as in Figure 3.4.

2187 sets of parameters), 294 sets in Region II, with only a few conditions favoring a strategy in Region I (12 sets) or Region IV (33 sets). The remaining parameter sets (389) favor strategies in the middle and between the four regions.

- In Region II, both V_B and V_E prefer to infect epithelial cells. The parameters values for which V_T^* is maximized in this region are characterized by a high rate of virus production in epithelial cells (γ) and a low rate of virus production in B cells (d_4).

- The majority of parameter values favor strategies in Region III where both V_B and V_E prefer to infect B cells. This implies that the infection of B cells plays a key role in the intrahost competition and the establishment of a long term infection.

Time-course dynamics of free viruses and the T cell responses for sample sets of parameters from the four Regions I-IV are shown in Figure 3.7. Higher levels of V_E^* often come at the expense of lower V_B^*.

3.4 A model of between-host dynamics

For most sets of parameters, maximizing V_E^* for transmission and maximizing V_T^* for intrahost competition favor different strategies. To predict the outcome of this conflict, we develop an implicit model of EBV dynamics in a homogeneous population of hosts that includes both transmission and superinfection. This model tracks susceptible hosts and hosts infected by one of m strains of viruses. We make the assumption that virus strains do not coexist within a single host. A more competitive virus, with a higher value of V_T^*, can take over a host from one with a lower value of V_T^* although the takeover requires time [1, 58]. We first analyze the model for the case where $m = 2$ and find the conditions for coexistence of different viral strategies within a population. We study the case where $m > 2$ primarily through simulation.

A host population infected with two strains of virus described by $\vec{\alpha}_1$ and $\vec{\alpha}_2$, where $\vec{\alpha}_i = (\alpha_B^i, \alpha_E^i)$, is captured by the following system of equations with three state

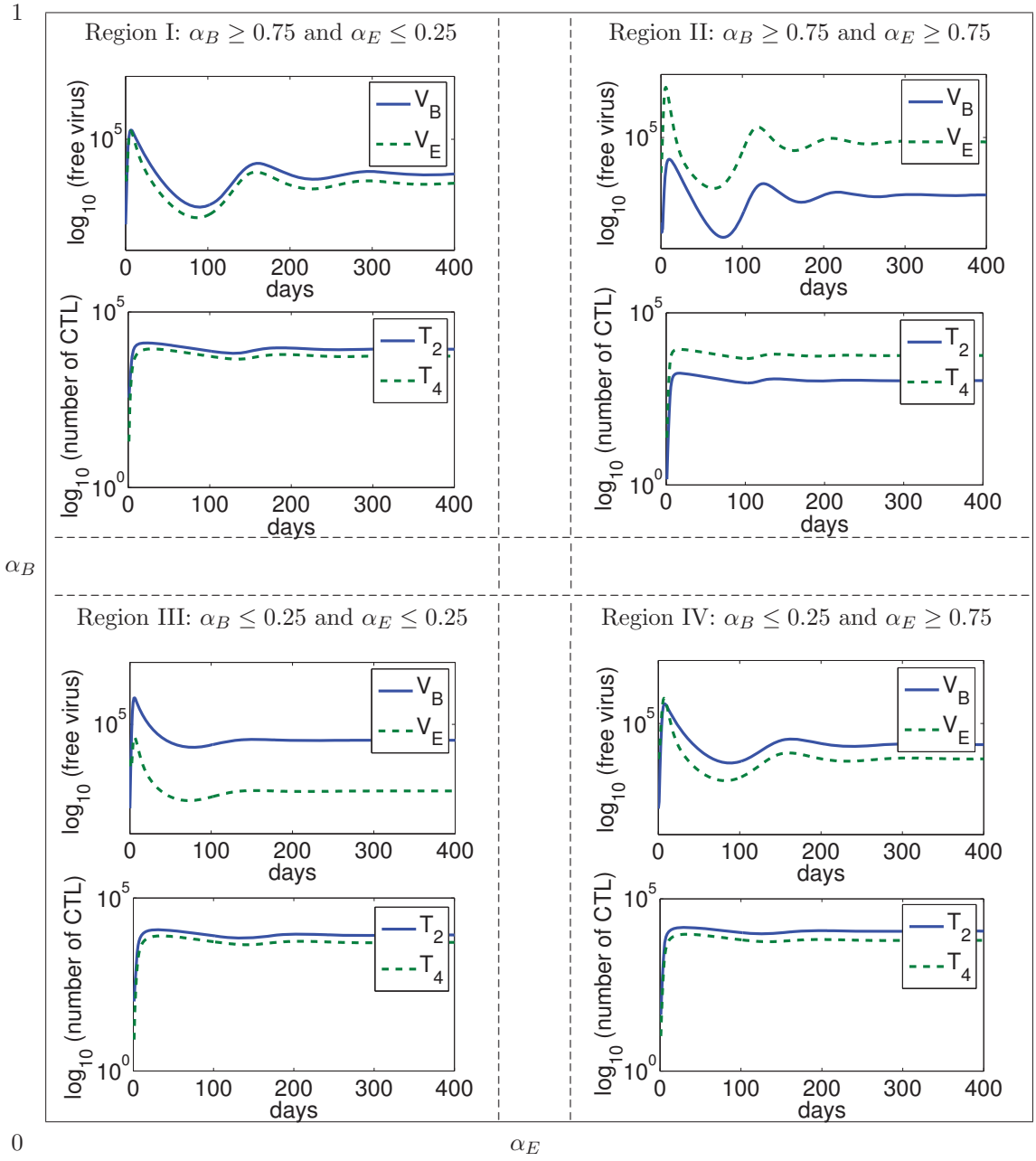

Figure 3.7. Effects of parameter values on dynamics of the model for sample sets of parameters from the four Regions I-IV in Figure 3.6.

variables: susceptible hosts (S), hosts infected by strain 1 (I_1), and hosts infected by strain 2 (I_2).

$$\begin{aligned}
\frac{dS}{dt} &= \sigma N - \mu(\vec{\alpha}_1)\,\frac{I_1}{N}S - \mu(\vec{\alpha}_2)\frac{I_2}{N}\,S - \sigma S \\
\frac{dI_1}{dt} &= \mu(\vec{\alpha}_1)\frac{I_1}{N}\,S - \mu(\vec{\alpha}_2)\nu(\vec{\alpha}_2,\vec{\alpha}_1)\frac{I_2}{N}\,I_1 + \mu(\vec{\alpha}_1)\nu(\vec{\alpha}_1,\vec{\alpha}_2)\frac{I_1}{N}\,I_2 - \sigma I_1 \\
\frac{dI_2}{dt} &= \mu(\vec{\alpha}_2)\frac{I_2}{N}\,S + \mu(\vec{\alpha}_2)\nu(\vec{\alpha}_2,\vec{\alpha}_1)\,I_1\frac{I_2}{N} - \mu(\vec{\alpha}_1)\nu(\vec{\alpha}_1,\vec{\alpha}_2)\frac{I_1}{N}\,I_2 - \sigma I_2\,.
\end{aligned} \tag{3.6}$$

This model assumes that

- There is no infection-induced death because mortality due to EBV infection is very rare even in the case of severe infectious mononucleosis. The total population, $N = S + I_1 + I_2$, is conserved by setting the per capita birth rate equal to the death rate, σ.

- Susceptible individuals are infected by strain i at rate $\mu(\vec{\alpha}_i)I_i/N$, where $\mu(\vec{\alpha}_i) = aV_E^*(\vec{\alpha}_i)$. This implies that the infection rate of strain i is proportional to the number of epithelial-cell viruses of that strain being produced within an infected host.

- Hosts infected by strain i can be superinfected, or taken over, by virus strain j at rate $\mu(\vec{\alpha}_j)\nu(\vec{\alpha}_j,\vec{\alpha}_i)I_j/N$. Because intrahost competition is determined by V_T^*, we assume that

  $$\nu(\vec{\alpha}_j,\vec{\alpha}_i) = g(V_T^*(\vec{\alpha}_j) - V_T^*(\vec{\alpha}_i))$$

  where g is an increasing function with $g(0) = 0$ and $g(-x) = -g(x)$. We set

  $$g(x) = \frac{2}{\pi}\arctan(x/A), \tag{3.7}$$

  which is scaled so that $g'(0) = 1/A$ and $\lim_{x\to\infty} g(x) = 1$.

- For all i, the transmission rate is larger than the birth and death rates ($\mu_i > \sigma$).

Equation (3.6) can be rewritten as

$$\begin{aligned}\frac{dI_1}{dt} &= \mu(\vec{\alpha}_1)\frac{I_1}{N}\left(N - I_1 - I_2\right) - f_{21}\frac{I_2}{N}\,I_1 - \sigma I_1\\ \frac{dI_2}{dt} &= \mu(\vec{\alpha}_2)\frac{I_2}{N}\left(N - I_1 - I_2\right) + f_{21}\frac{I_1}{N}\,I_2 - \sigma I_2\,,\end{aligned} \tag{3.8}$$

where

$$f_{21} = \mu(\vec{\alpha}_2)g(V_T^*(\vec{\alpha}_2) - V_T^*(\vec{\alpha}_1)) - \mu(\vec{\alpha}_1)g(V_T^*(\vec{\alpha}_1) - V_T^*(\vec{\alpha}_2))$$

summarizes the competitive ability of strain 2 relative to strain 1.

If $V_E^*(\vec{\alpha}_1) > V_E^*(\vec{\alpha}_2)$ and $V_T^*(\vec{\alpha}_1) > V_T^*(\vec{\alpha}_2)$, strain 1 is better at both transmission and intrahost competition and will thus always win. If $V_E^*(\vec{\alpha}_1) > V_E^*(\vec{\alpha}_2)$ and $V_T^*(\vec{\alpha}_1) < V_T^*(\vec{\alpha}_2)$, strain 1 is better at transmission while strain 2 is better at intrahost competition. Then $\mu_1 = \mu(\vec{\alpha}_1) > \mu_2 = \mu(\vec{\alpha}_2)$ and $f_{21} > 0$.

Equation (3.8) has four equilibria:

$$\begin{aligned}P_0 &= (0,0),\\ P_1 &= \left(N(1-\frac{\sigma}{\mu_1}),0\right),\\ P_2 &= \left(0, N(1-\frac{\sigma}{\mu_2})\right), \text{ and}\\ P_{12} &= \left(\frac{(\mu_1-\sigma)N - (\mu_1+f_{21})I_2^*}{\mu_1}, I_2^* = \frac{\mu_1 N}{\mu_1-\mu_2+f_{21}} - \frac{\sigma N}{f_{21}}\right).\end{aligned} \tag{3.9}$$

Linear stability analysis implies that:

- The disease-free equilibrium, P_0, is unstable if $\mu_i > \sigma$.
- The strain 1 equilibrium, P_1, is positive and stable if $f_{21} < \frac{\sigma(\mu_1-\mu_2)}{(\mu_1-\sigma)}$.
- The coexistence equilibrium, P_{12}, is positive and stable if $\frac{\sigma(\mu_1-\mu_2)}{(\mu_1-\sigma)} < f_{21} < \frac{\sigma(\mu_1-\mu_2)}{(\mu_2-\sigma)}$.
- The strain 2 equilibrium, P_2, is positive and stable if $f_{21} > \frac{\sigma(\mu_1-\mu_2)}{(\mu_2-\sigma)}$.

If f_{21} is small, the force of superinfection is weak and strain 1 wins since it has a higher transmission rate. As f_{21} increases, strain 2 can coexist, and will eventually outcompete strain 1 for larger values of f_{21}.

The model with $m > 2$ strains of viruses can be written as

$$\begin{aligned}\frac{dS}{dt} &= \sigma N - \sum_{i=1}^{m} \mu_i \frac{I_i}{N} S - \sigma S \\ \frac{dI_i}{dt} &= \mu_i \frac{I_i}{N} S + \sum_{j=1}^{m} f_{ij} \frac{I_i}{N} I_j - \sigma I_i \,. \end{aligned} \tag{3.10}$$

Let

$$F_i = \sum_{j=1}^{m} f_{ij} \frac{I_j}{N} \,,$$

where $f_{ij} = 0$ when $i = j$. Using the assumption of constant population size, Equation (3.10) can be reduced to

$$\dot{I}_i = \mu_i \frac{I_i}{N} \left(N - \sum_{j=1}^{m} I_j \right) + F_i I_i - \sigma I_i \,. \tag{3.11}$$

We can think of F_i as the total force of strain i taking over other strains. If $V_T^*(\vec{\alpha}_i)$ is small, f_{ij} can be negative and, hence, F_i can have a negative value. If $V_T^*(\vec{\alpha}_i)$ is large, f_{ij} is more likely to be positive and so is F_i. At equilibrium, we have

$$I_i^* = 0 \qquad \text{or} \qquad I_i^* = \frac{N \left(\mu_i \left(1 - \sum_{j \neq i}^{m} I_j^*/N \right) + F_i^* - \sigma \right)}{\mu_i} \,.$$

Strain i thus can exist at equilibrium if

$$F_i^* + \mu_i \left(1 - \sum_{j \neq i}^{m} I_j^*/N \right) > \sigma \,. \tag{3.12}$$

The condition for invasion can be expressed in terms of Equation (3.12). Let G be a set of strains ($\mathrm{G} \subset \{1, 2, ..., k\}$) that can exist in the equilibrium state. Strain i, which is not in G, can invade the equilibrium if Equation (3.12) is satisfied. This implies that if strain i is not intrahost competitive (low $V_T^*(\vec{\alpha}_i)$ and hence F_i^* is negative), then it can only invade the equilibrium if it has a high transmission rate (high $V_E^*(\vec{\alpha}_i)$ and hence μ_i).

The force of infection, F_i^*, depends on the scaling factor A (Equation 3.7). When A is small, $|f_{ij}|$ is large and the force of superinfection is strong making it easier for a

strain with a higher V_T^* to win via intrahost competition (Figure 3.8: row 1, col. 1). When A is large, the force of superinfection is weaker. It is more difficult for a strain with higher V_T^* to take over a host from a strain with lower V_T^*. Instead, strains with lower V_T^* but higher V_E^* (higher transmission) can invade and exist in the equilibrium (Figure 3.8).

The pressure of intrahost competition thus favors strains with small α_B and small α_E to maximize V_T^*. The pressure of transmission, however, supports strains with large α_B and large α_E such that V_E^* is maximized. When the importance of intrahost competition is weak, strategies of higher transmission become dominant and coexistence of multiple strains is possible at the population level.

3.5 Discussion

We have developed models of the within-host and the between-host dynamics of EBV infection to study the effects of switching host cell tropism on transmission, persistence, and viral evolution. The model of the within-host dynamics tracks B cells, epithelial cells, T cells, and viruses. Although our model does not explicitly include spatial dynamics, the numerical solution of the dynamics of B cell infection (Figure 3.2) are consistent with simulations of the agent-based model, PathSim, such that small virus burst size or exclusion of a memory stage produces clearance [78]. This result supports the key role of virus latency within memory B cells in the establishment of a persistent EBV infection within a host. The agent-based models, however, did not address the importance of epithelial cell infection.

Viruses derived from B cells (V_B) preferentially infect epithelial cells and viruses derived from epithelial cells (V_E) preferentially infect B cells [4]. Viruses derived from epithelial cells are the main type that is shed in saliva, and play a key role in transmission [44]. Assuming EBV can modify its ability to infect B cells and epithelial cells, we compute viral strategies that maximize transmission and persistent infection. Maximizing transmission is assumed to be equivalent to maximizing the equilibrium amount of virus produced from epithelial cells. Maximizing intrahost competitive ability, in contrast, favors strains that produce the highest total number of

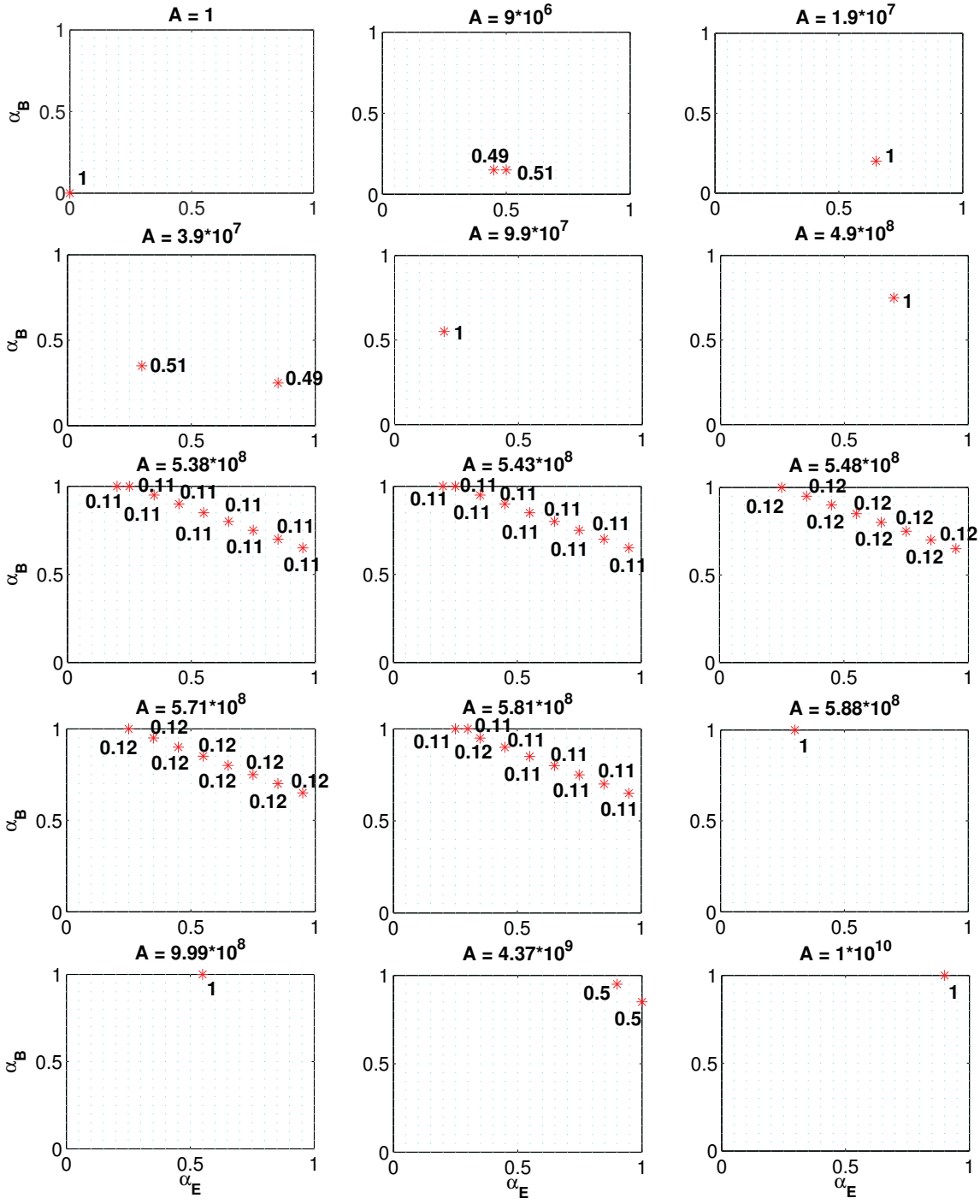

Figure 3.8. Snapshots of winning and coexisting strains with the corresponding density of infected hosts at equilibrium (red '*') as A increases ($|f_{ij}|$ decreases) for a sample set of parameter from Region III in Figure 3.6. We consider 441 strains (blue '*') representing different viral strategies on the $\alpha_B\alpha_E$ plane.

viruses at equilibrium. Under most conditions, the optimal strategy for transmission is having both types of viruses (V_B and V_E) to preferentially infect epithelial cells. Under conditions when the rate of virus replication and production from B cells is high and production from epithelial cells is low, maximizing transmission favors viral strains that have viruses produced by one cell type infecting the other, in accord with observations of viral behavior *in vitro* [4]. In contrast, the optimal strategy for establishing and maintaining a persistent infection (intrahost competition) is for both types of viruses to mainly infect B cells, an observation consistent with reports that, at least in healthy carriers, EBV primarily targets and maintains its persistent infection within the population of B cells [33].

For the majority of parameter combinations we studied, maximizing V_E^* for transmission and maximizing V_T^* for intrahost competition favor different strategies. No stable coexistence of multiple strategies is observed within a host. This may be due to the assumption of perfect cross-reactivity of T cells in our model. To further understand the conflict of strategies, we combine these results of the within-host model with a model at the population level and show that coexistence is possible. This between-host model includes both transmission and superinfection. In this case, when the force of superinfection is strong, viruses that preferentially infect B cells survive within and between hosts. When the importance of intrahost competition is weak, strategies of higher transmission become dominant and coexistence of multiple strains is possible at the population level.

Multiple strains of EBV, indeed, have been detected within healthy carriers for periods of more than 300 days [82]. There are at least two possible explanations for this. If multiple strains coexist at the host population level, as in our model, but within-host takeovers are slow, individuals could have transient multiple infections. Alternatively, coexistence of multiple strains within a host could result from either partial or no cross-reactivity of T cell responses. Our model can be modified to allow for either of these complications.

The existence of multiple strains, T cell responses, and the switching of infection between cell types may not only play important roles in the evolution of EBV but

also in the pathology of EBV-associated diseases like infectious mononucleosis and nasopharyngeal carcinoma. Infectious mononucleosis (IM) is thought to be caused by primary infection of EBV in teenagers and young adults with symptoms including fever, fatigue, and sore throat. The overwhelming number of T cells, especially against viral lytic proteins cause these symptoms [33]. With the existence of multiple strains, it is possible that IM may be caused by a secondary infection with a strain that is particularly efficient at lytic replication and production of new viruses. For example, an infection with a strain that is highly efficient at infecting epithelial cells may generate an extreme T cell response against EBV lytic proteins and cause symptoms of IM.

Nasopharyngeal carcinoma is a cancer of epithelial cells in the nose and pharynx. EBV infection of epithelial cells normally results in lytic infection. In NPC patients, however, EBV can maintain latency within epithelial cells. Expression of virus latent proteins within these cells contributes to cell proliferation, cell survival, and inefficient T cell responses, all of which can accelerate tumor development. The shift of tropism from B cell to epithelial cell disease may be induced by immunoglobulin A (IgA) [83], which can enhance the viral entry into epithelial cells while interfering with the infection of B cells. Ongoing research extends the basic model of within-host dynamics (Equation 3.1) to study the association of EBV infection with these two important pathologies, IM and NPC.

3.6 Acknowledgements

We would like to thank Dr. Thorley-Lawson and other members of his laboratory for the opportunity to visit their lab and study the biology of Epstein-Barr virus infection of B cells, and Dr. Hutt-Fletcher for insightful discussions on Epstein-Barr virus infection of epithelial cells. Funding for this work was provided by the National Science Foundation (NSF) Research Training Group (RTG) (Award Number DMS0354259).

CHAPTER 4

MATHEMATICAL MODELING THE AGE DEPENDENCE OF EPSTEIN-BARR VIRUS ASSOCIATED INFECTIOUS MONONUCLEOSIS

4.1 Abstract

Most people get Epstein-Barr virus (EBV) infection at young age and are asymptomatic. Primary EBV infection in adolescents and young adults however, often leads to infectious mononucleosis (IM) with symptoms including fever, fatigue, and sore throat that can persist for months. Expansion in the number of $CD8^+$ T cells, especially against EBV lytic proteins, are the main cause of these symptoms. We propose a mathematical model for the regulation of EBV infection within a host to address the dependence of IM on age. This model tracks the number of virus, infected B cell and epithelial cell, and $CD8^+$ T-cell responses to the infection. We use this model to investigate three hypotheses for the high incidence of IM in teenagers and young adults: saliva and antibody effects that increase with age, high cross-reactive T-cell responses, and a high initial viral load. The model supports the first two of these hypotheses, and suggests that variation in host antibody responses and the complexity of the pre-existing cross-reactive T cell repertoire, both of which depend on age, may play important roles in the etiology of IM.

4.2 Introduction

EBV is transmitted by intimate contact, mainly through saliva and oropharyngeal secretion [3]. Within a host, the virus primarily targets two cell types, B cells and epithelial cells. Host saliva and antibodies, like IgA and IgG, to viral glycoproteins can decrease the infection of B cells but enhance the infection of epithelial cells [83, 87].

Most people get EBV infection at young age and are asymptomatic. Adolescents and young adults infected with EBV develop infectious mononucleosis in up to 50% of cases, with symptoms including fever, fatigue, and sore throat that can persist for months [3, 15]. These symptoms are caused mainly by expansion in the number of $CD8^+$ T cells, especially against EBV lytic proteins expressed during lytic replication and production of virions [33].

In the previous chapter (Chapter 3), we developed a mathematical model of the within-host dynamics to study EBV long term infection and viral evolution. In this chapter, we extend the within-host model to include features of immune system thought to be important in IM: the role of antibodies in shifting infections between the two cell types and the effect of specific and cross-reactive T-cell responses. The model tracks the number of viruses, infected B cells and epithelial cells, specific $CD8^+$ T cells, and cross-reactive $CD8^+$ T cells responding to the infection.

We use this model to investigate the following three hypotheses.

- **Saliva and antibody effects**

  Host saliva and antibodies to EBV proteins promote infection of epithelial cells which, in turn, can induce an elevated $CD8^+$ T-cell response against lytic infection. This hypothesis comes from observations that some unknown factor in host saliva and antibodies to viral proteins have been observed to enhance epithelial cell infection, and that salivary IgA level increases with age [42, 83, 87, 91].

- **Cross-reactive T-cell responses**

  The complexity of the pre-existing memory T-cell repertoire may change with age. Adolescents infected with EBV may recruit large numbers of cross-reactive memory T cells previously created in response to other viral infections. These cross-reactive T-cell responses may be more quickly activated, but less efficient in controlling the infection than primary responses from naive T cells [14, 73].

- **The initial viral load**

  High viral challenges in adolescents, often acquired via kissing, may induce aggressive CD8+ T-cell response [33].

4.3 Model

Addressing the three hypotheses for the causes of IM requires consideration of antibody effects and state variables representing cross-reactive T-cell responses to latent and lytic infection. Our mathematical model (Figure 4.1 and Equation 4.1) tracks two types of target cells, B cells and epithelial cells, both B-cell derived (V_B) and epithelial-cell derived (V_E) viruses, two types of specific cytotoxic T cells (CTLs) attacking latently infected B cells (T_2) and lytically infected cells (T_4), respectively, and two types of cross-reacting CTLs against latently (T_{2c}) and lytically (T_{4c}) infected cells. B cells is classified further into four state variables: naive B cells (B_1), latently infected B cells (B_2), latently infected memory B cells (B_3), and lytically infected B cells or plasma cells (B_4). Epithelial cells do not ordinarily harbor latent infection and require only two state variables: uninfected epithelial cells (E_1), and lytically infected

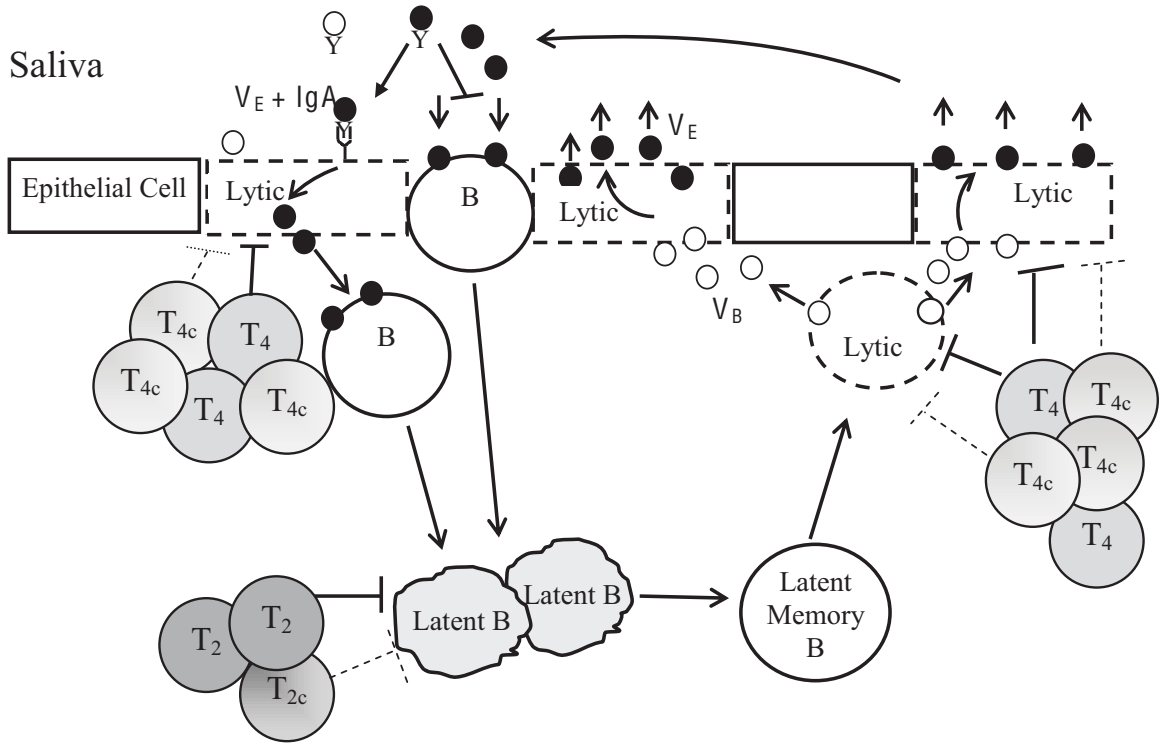

Figure 4.1. Model of EBV infection of B cells and epithelial cells. Antibodies like IgA can shift the viral target from B cells to epithelial cells. Activation of cross-reactive memory T cells (T_C) that are not efficient in killing infected cells may contribute to the pathology of IM.

epithelial cells (E_4). The model consists of a system of twelve ordinary differential equations:

$$\begin{aligned}
\frac{dB_1}{dt} &= d_1(B_0 - B_1) - f(a)\mu_{Eb}V_E B_1 - f(a)\mu_{Bb}V_B B_1 \\
\frac{dB_2}{dt} &= \rho(f(a)\mu_{Eb}V_E B_1 + f(a)\mu_{Bb}V_B B_1) - (d_2 + c)B_2 - k_2 B_2 T_2 - \chi_2 k_2 B_2 T_{2c} \\
\frac{dB_3}{dt} &= cB_2 + rB_3 - srB_3 \\
\frac{dB_4}{dt} &= rB_3 - d_4 B_4 - k_4 B_4 T_4 - \chi_4 k_4 B_4 T_{4c} \\
\frac{dE_1}{dt} &= d_e(E_0 - E_1) - h(a)\mu_{Be}V_B E_1 - h(a)\mu_{Ee}V_E E_1 \\
\frac{dE_4}{dt} &= h(a)\mu_{Be}V_B E_1 + h(a)\mu_{Ee}V_E E_1 - (d_e + \gamma)E_4 - k_4 E_4 T_4 - \chi_4 k_4 E_4 T_{4c} \qquad (4.1) \\
\frac{dV_B}{dt} &= nd_4 B_4 - d_v V_B \\
\frac{dV_E}{dt} &= n\gamma E_4 - d_v V_E \\
\frac{dT_2}{dt} &= (1 - \sigma_2)\phi_2 T_N w(B_2) + \theta_2 T_2 w(B_2) - \delta T_2 \\
\frac{dT_{2c}}{dt} &= \sigma_2 m\phi_2 T_M w(B_2) + m\theta_2 T_{2c} w(B_2) - m\delta T_{2c} \\
\frac{dT_4}{dt} &= (1 - \sigma_4)\phi_4 T_N[w(B_4 + E_4)] + \theta_4 T_4[w(B_4 + E_4)] - \delta T_4 \\
\frac{dT_{4c}}{dt} &= \sigma_4 m\phi_4 T_M[w(B_4 + E_4)] + m\theta_4 T_{4c}[w(B_4 + E_4)] - m\delta T_{4c}\,.
\end{aligned}$$

The dynamics of B cells obey these assumptions:

- Naive B cells have an initial population size of B_0 and turnover rate d_1. They encounter and are infected by V_B and V_E with rates $f(a)V_B\mu_{Bb}$ and $f(a)V_E\mu_{Eb}$, respectively, where $f(a)$ represents the inhibiting effect of host saliva and antibody responses on infection of B cells (Equation 4.3).

- An infection of a naive cell, B_1, may give rise to one or more latently infected cells, B_2, due to the limited proliferation of these newly infected cells, where ρ is the proliferation factor. These B_2 cells die at rate d_2, and are recognized and killed by specific or cross-reactive effector T cells at rate k_2 or $\chi_2 k_2$, respectively. They can also enter the latently infected memory state, driven by EBV turning off its gene expression, at rate c.

- Infected memory cells, B_3, obey homeostatic regulation similar to normal memory B cells. They are invisible to the immune system, and undergo cell division with rate r, where one cell goes into lytic infection and one stays in the memory state. The rate sr represents the death of B_3 due to homeostasic regulation of memory cells, where s is the regulation factor. For a normal homeostasis, $s = 2$ balances the proliferation rate of $2r$ [54].

- Lytically infected B cells, B_4, arise from lytic reactivation of memory infected B cells at rate r, die and release viruses at rate d_4, and can be killed by specific or cross-reactive effector T cells at rate k_4 or $\chi_4 k_4$, respectively.

Here, χ_j ($j = 2$ or 4), with $0 \leq \chi_j \leq 1$, characterizes the efficiency of cross-reactive T cells in killing infected cells, compared to specific T cells. The smaller χ_j is, the more inefficient cross-reactive T cells are in killing infected cells.

The dynamics of epithelial cells assume the following:

- Uninfected epithelial cells have initial population size of E_0 with turnover rate d_e. They encounter and are infected by V_B and V_E with rates $h(a)V_B\mu_{Be}$ and $h(a)V_E\mu_{Ee}$, respectively. Here, $h(a)$ represents the enhancement effect of host saliva and antibody responses on infection of epithelial cells (Equation 4.4).

- Lytically infected epithelial cells, E_4, die at natural rate d_e, die due to virus bursting out at rate γ, and can be killed by specific or cross-reactive effector T cells at rate k_4 or $\chi_4 k_4$, respectively.

The effects of host saliva and antibody responses on the infection of the two cell types are represented by the functions f and h, and included as parameters in the cell-specific infection terms. This is based on the observation that host saliva and antibodies to viral glycoproteins interfere with infection of B cells and enhance infection of epithelial cells [87]. From limited data in this *in vitro* study, we obtain the linear relationship between f and h that can be described in the following equation:

$$h = 1 + \lambda - \lambda f\,, \tag{4.2}$$

where $\lambda \approx 32$. The functions f and h carry no units. Without the antibody effect, $f = 1$ and $h = 1$. With antibody effects, f decreases to represent decreased efficiency in infection of B cells and h increases to represent increased efficiency in infection of epithelial cells. To model the dependence of f and h on antibody response, we assume that the two functions take on the forms

$$f(a) = 1 - \frac{a^2}{A^2 + a^2}\,, \tag{4.3}$$

$$h(a) = 1 + \frac{\lambda a^2}{A^2 + a^2}, \tag{4.4}$$

where a represents the strength of saliva and antibody effects. We will refer to a as the antibody effect from now on because the factor(s) in saliva that can enhance infection of epithelial cells remain unknown. The functions $f(a)$ and $h(a)$ take the form of Hill functions, where λ is the maximum level of the antibody effect on the infection of epithelial cells and A is the level of a where the effect on the infection of B cells and epithelial cells is half maximal. As a increases, $f(a)$ decreases while $h(a)$ increases before saturating. This saturating form assumes that a certain level of antibody response is required to have strong effects on the infection of both cell types.

Free viruses, V_B and V_E, are produced from B cells and epithelial cells at rates nd_4 and $n\gamma$, respectively, where n is the average burst size. These viruses die at rate d_v. To model the CTL response, we separate the specific responses against latent (T_2) and lytic (T_4) infection coming from naive T cells and the cross-reactive responses (T_{2c} and T_{4c}) coming from the memory T cells specific to other encountered pathogens.

We assume that the naive and memory populations, T_N and T_M, are fixed at constant levels. Upon stimulation by viral antigens, T_N become effector cells against latent or lytic infection at rate $(1 - \sigma_2)\phi_2$ or $(1 - \sigma_4)\phi_4$, respectively, where σ_j is the fraction of cross-reactive T-cell response. With further stimulation by viral antigens from infected cells, the activated effector cells, T_2 and T_4, can proliferate with rates θ_2 and θ_4, respectively. Each type of effector cell dies at a similar rate δ. Activation and proliferation of CTLs saturate as a function of the available infected cells

$$w(B_j) = \frac{B_j}{K + B_j}\,, \tag{4.5}$$

where K is the number of infected cells at which activation or proliferation is half maximal and is assumed to be the same for both responses.

Cross-reactive responses, T_{2c} and T_{4c}, are activated from the memory population at rate $\sigma_j m \phi_j$, where $m \geq 1$ is a measurement of how much faster a response can be activated from memory T cells compared to activation from naive T cells. These cross-reactive memory cells are assumed to have faster dynamics than specific T cells. Although they may be activated quickly and proliferate rapidly, they die faster (by a factor m). This comes from observations that memory cells respond with fast kinetics [46], but are also more susceptible to death [10]. Furthermore, T cells obtained from acute IM patients have been shown to have high expression of programmed-death-1 [33].

The system Equation (4.1) has two equilibria: an infection-free equilibrium and a persistent equilibrium. The infection-free equilibrium is given by

$$B_1^* = B_0\,, \qquad E_1^* = E_0\,,$$

with other state variables equal zero. The stability of the infection-free equilibrium is determined by the basic reproductive ratio, of EBV in a naive host [29]:

$$\begin{aligned} R_0 = {} & \frac{n}{2d_v^2}\left(\frac{\rho f(a)\mu_{Bb}B_0 c}{(s-1)(d_2+c)} + \frac{h(a)\mu_{Ee}E_0\gamma}{d_e+\gamma}\right) \\ & + \frac{n}{2d_v^2}\sqrt{\left(\frac{\rho f(a)\mu_{Bb}B_0 c}{(s-1)(d_2+c)} - \frac{h(a)\mu_{Ee}E_0\gamma}{(d_e+\gamma)}\right)^2 + \frac{4\rho f(a)\mu_{Eb}B_0 c h(a)\mu_{Be}E_0\gamma}{(s-1)(d_2+c)(d_e+\gamma)}}. \end{aligned} \tag{4.6}$$

Infections of both B cells and epithelial cells contribute to the basic reproductive ratio of EBV. The antibody effects, $f(a)$ and $h(a)$, shift the weight of R_0 contribution from B cells to epithelial cells. If $R_0 < 1$, the infection-free equilibrium is stable and the infection cannot establish within a host. If $R_0 > 1$, the infection-free equilibrium is unstable and EBV can establish a persistent infection, where all state variables take on positive values. Tables 4.1 and 4.2 present the parameter values used for simulations and analysis of the model.

Assuming no cross-reactive responses ($\sigma_2, \sigma_4 = 0$), the dynamics of viruses and T cells for the cases without antibody effect ($a = 0$) and with antibody effect ($a = 10$) are

Table 4.1. Parameters for the dynamics of B cells and antibody effect used in the model simulations (Equation 4.1). We use many parameters from PathSim, where the rates are estimated and given in a unit of per 6 minutes [78], and convert them into the unit of per minute.

Parameter	**Description**	**Value**	**Value**	**Reference**
d_1	Turnover rate of naive B cells	1/6000	min^{-1}	[78]
μ_{Eb}	B cell infection rate per epithelial-cell virus	3.3×10^{-10}	$\text{min}^{-1}\text{virus}^{-1}$	[78] [1]
μ_{Bb}	B cell infection rate per B-cell virus	$\mu_{Eb}/100$	$\text{min}^{-1}\text{virus}^{-1}$	[36]
ρ	Proliferation factor	2	no unit	[78]
d_2	Death rate of latently infected B cells	1/11520	min^{-1}	[78]
c	Rate of latently infected cells going into memory stage	0.001	min^{-1}	[78] [2]
k_2	Rate of latently infected B cells killed by T cells	3.8×10^{-8}	$\text{min}^{-1}\text{cell}^{-1}$	[78] [3]
r	Rate of reactivation of lytic infection from latent infection	8.3×10^{-5}	min^{-1}	[78]
s	Regulation factor of memory B cells	2	no unit	[54]
d_4	Death rate of lytically infected cells due to viruses bursting out	1/4320	min^{-1}	[78]
k_4	Rate of lytically infected B cells killed by T cells	7.6×10^{-8}	$\text{min}^{-1}\text{cell}^{-1}$	[78][3]
a	The strength of antibody effect	variable (0-40)	no unit	
A	Level of a where antibody effect is half maximal	10	no unit	
λ	Maximal level of antibody effect on epithelial cell infection	32	no unit	[87][4]

[1]Probability of virus and cell encounter per minute multiplied by probability of infection and divided by the number of viruses ($\approx 10^7$)
[2]We take this to be the same rate as the estimation of .1% of lymphocytes leaving the Waldeyer's ring per minute
[3]Probability of lymphocyte encounter per minute multiplied by the probability that T_i kills its target and divided by the number of $T_i(\approx 10^4)$
[4]Estimated from limited data given in an *in vitro* study [4]

Table 4.2. Parameters for the dynamics of epithelial cells, virus, and T-cell responses used in the model simulations (Equation 4.1).

Parameter	**Description**	**Value**	**Unit**	Reference
d_e	Turn-over rate of epithelial cells	1/6000	min^{-1}	[1]
μ_{Be}	Epithelial cell infection rate per B-cell virus	3×10^{-11}	$\text{min}^{-1}\text{virus}^{-1}$	[2]
μ_{Ee}	Epithelial cell infection rate per epithelial-cell virus	$\mu_{Be}/5$	$\text{min}^{-1}\text{virus}^{-1}$	[36]
γ	Death rate of infected epithelial cells due to viruses bursting out	1/6000	min^{-1}	[3]
n	Viral burst size	1000	$\text{virus}\cdot\text{cell}^{-1}$	[78]
d_v	Death rate of virus	1/2160	min^{-1}	[78]
σ_j	Fraction of effector cells activated from cross-reactive memory T cells	variable (0-1)	no unit	
m	Factor of faster response from memory T cells	5	no unit	[46]
ϕ_2	Rate of T cell activation against latent infection	1.95×10^{-5}	min^{-1}	[78][4]
ϕ_4	Rate of T cell activation against lytic infection	4.48×10^{-5}	min^{-1}	[78][4]
θ_2	Rate of T cell proliferation against latent infection	3.25×10^{-5}	min^{-1}	[78][5]
θ_4	Rate of T cell proliferation against lytic infection	3.25×10^{-5}	min^{-1}	[78][5]
K	Number of infected cells when T cell activation is half maximal	10^5	cell	[45]
δ	Death rate of T cells	1/156000	min^{-1}	[78]

[1]Estimated, taken to be the same as d_1
[2]Estimated, taken to be less than μ_{Eb} [87]
[3]Estimated, taken to be less than d_4 [4]
[4]Probability of lymphocyte encounter per minute multiplied by the probability of T_i activation by B_i, where $i = 2$ or 4
[5]Probability of lymphocyte encounter per minute multiplied by the frequency of cell division (every 8-12 hours)

shown in Figure 4.2(i) and 4.2(ii), respectively. The antibody effect greatly increases the number of viruses being produced, with most of this increase coming from epithelial-cell viruses. Elevated number of T cells against viral lytic proteins are induced during primary infection.

4.4 Application to infectious mononucleosis

EBV infection in children of young age is usually asymptomatic. Adolescents and young adults infected with EBV may develop flu-like symptoms, referred to as infectious mononucleosis (IM). These symptoms result from a massive T-cell response to EBV a few weeks after the initial viral infection that can last from a few weeks to several months [15]. The T-cell responses against viral latent proteins are generally

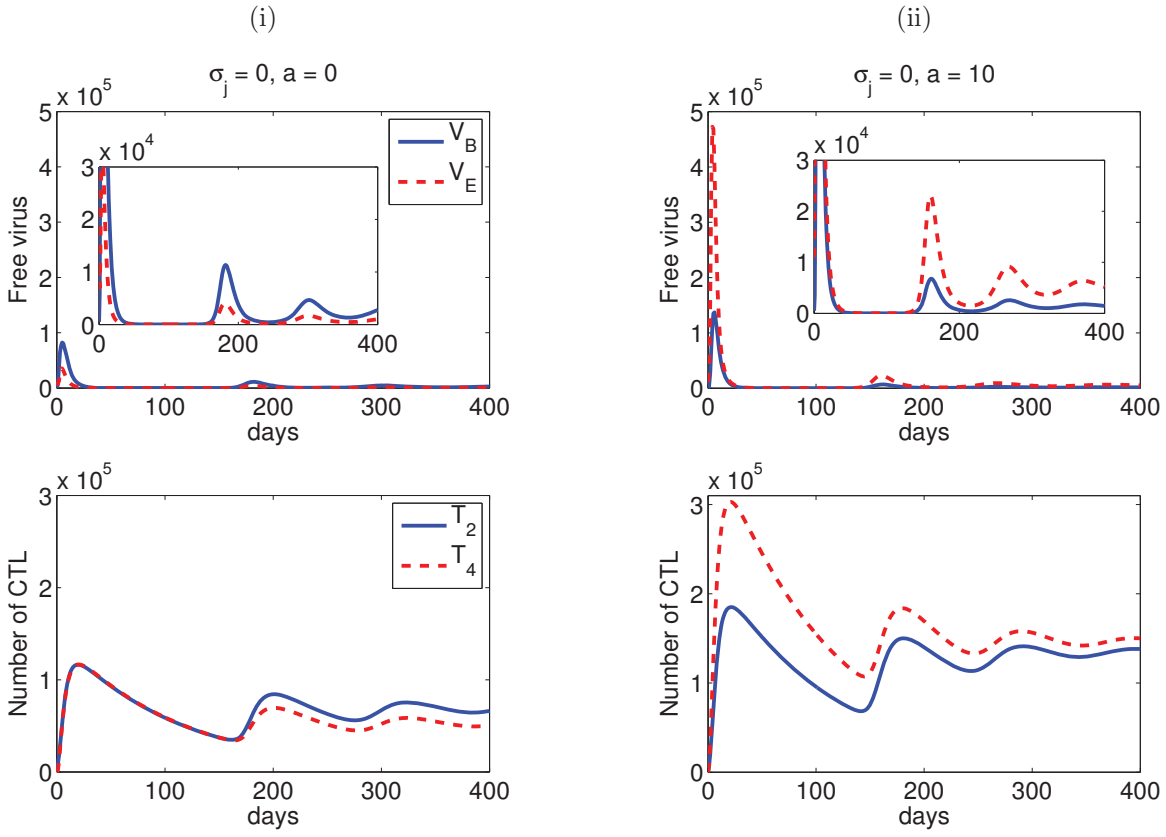

Figure 4.2. Dynamics of viruses and T cells in the case of no cross-reactive T-cell responses ($\sigma_j = 0$). **(i)** Without antibody effect ($a = 0$). **(ii)** With antibody effect ($a = 10$). The insets show the level of persistent virus for the two cases. Parameter values used are shown in Tables 4.1 and 4.2.

smaller in magnitude than the T-cell responses against viral lytic proteins during the acute phase of IM. The acute phase is followed by convalescence and eventually a virus carrier state where the CD8+ population resolves to a level comparable to that in asymptomatic carriers [33].

We use numerical solutions of our model to investigate the three hypotheses for the high prevalence of IM in teenagers and young adults: saliva and antibody effects, cross-reactive T-cell responses, and the initial viral load. The total number of T cells (both specific and cross-reactive ones) and the lytic T cell ratio at the peak of infection are used as the two key measurements of IM. The lytic T cell ratio is the ratio between effector T cells responding against lytic infection and effector T cells responding against latent infection, $(T_4+T_{4C})/(T_2+T_{2C})$. A wide range of values of these two measurements has been observed in IM patients. Individual epitope responses against latent and lytic infections can account for 0.1%-5% and 1%-40% of the total $CD8^+$ T cell population, respectively [33].

4.4.1 Antibody effects

Race, sex, and age are at least in part responsible for individual differences in antibody responses [7, 13, 42], which may influence the outcomes of EBV infection. Titers of antibody responses specific to EBV viral capsid antigen, IgA and IgG, have been observed to increase with age and IgA attains its highest level during the onset of disease within IM patients [21, 67]. Furthermore, individuals are exposed to more pathogens as they age. EBV infection in young adults may activate antibody responses that are specific to other viruses, but cross-reactive to EBV. As IgG and IgA responses to EBV glycoproteins can enhance the lytic infection of epithelial cells, the probability of getting IM may increase with age.

To examine this hypothesis with our model, we vary the strength of the antibody effect (a) and study its influence on the total number of T cells and the lytic T cell ratio (Figure 4.3) measured at the peak of infection. The total number of T cells increases with the level of a, but then decreases when a is large. At high levels of antibody response, infection of B cells is strongly suppressed while the effect on enhancement of lytic infection of epithelial cells saturates, leading to a decreased total number of T

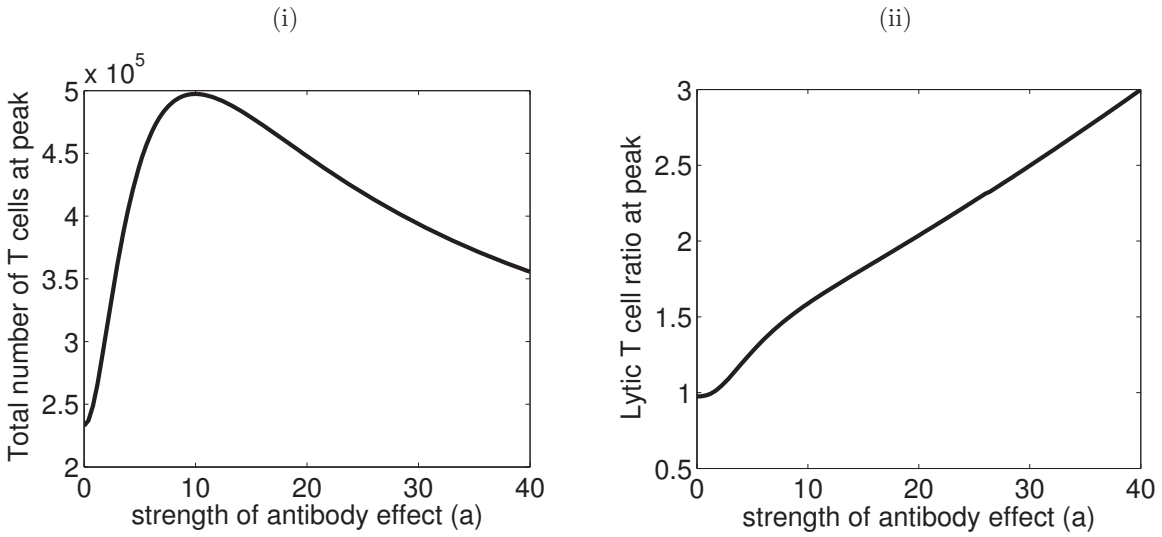

Figure 4.3. Antibody effects on the total number of T cells ($T_2 + T_{2c} + T_4 + T_{4c}$) and the lytic T cell ratio ($(T_4 + T_{4c})/(T_2 + T_{2c})$) in the absence of cross-reactive T cells ($\sigma_j = 0$). **(i)** Total number of CD8$^+$ T cells at the peak of infection. **(ii)** The lytic T cell ratio at peak: ratio between the number of T cells against lytic infection (T_4) and the number of T cells against latent infection (T_2), evaluated at the peak of infection. Parameter values are shown in Tables 4.1, and 4.2.

cells (Figure 4.3(i)) and increased lytic T cell ratio (Figure 4.3(ii)).

4.4.2 Cross-reactive T-cell responses

Massive expansion of CD8$^+$ T cells responding to EBV causes the symptoms of IM [80]. It has been proposed that the high susceptibility of teenagers and young adults to IM may be due to a more complex memory CD8 repertoire than in young children. As individuals age, the memory CD8 repertoire gets more complex due to exposure to different pathogens. Adolescents infected with EBV may recruit a large number of cross-reactive memory T cells previously created in response to other viral infections [73]. In fact, it has been shown that memory CD8$^+$ T cells specific to influenza virus can be activated and respond to stimulation by EBV lytic proteins [14]. Both the magnitude and the efficiency of cross-reactive T cells in killing infected cells may contribute to the etiology of IM. The level of cross-reactive memory T cell can increase with age. These memory cells may be faster at activation and proliferation compared to naive T cells [89], but less efficient in controlling the infection [85].

A large fraction of $CD8^+$ T cells created during the course of IM respond to lytic infection (5-50%, compared to 1-3% for T cells responding to latent infection) [8, 32]. Since EBV has many more lytic genes than latent genes [75], it is likely that there are more cross-reactive T cells to EBV lytic infection than to latent infection. We first assume cross-reaction of only T-cell responses against lytic infection. To address this assumption with our model, we set $\sigma_2 = 0$ and consider five different values of σ_4, 0, 0.3, 0.6, 0.8, and 1. As σ_4 increases, the fraction of lytic T-cell response coming from cross-reactive memory T cells increases. At $\sigma_4 = 1$, there is no specific lytic T-cell response; all lytic T cells are cross-reactive.

To facilitate comparison with the antibody effect (Figure 4.3), we present the effects of cross-reactive T cells on the development of IM using similar plots, with five curves in each representing different values of the level of cross-reactive lytic T cells (σ_4) (Figure 4.4). This figure also illustrates the impact of χ_4, the efficiency of cross-reactive T cells in killing lytically infected cells, on the two measurements of IM. Across all levels of antibody effects (a), the increase in σ_4 greatly elevates the total number of T cells and the lytic T cell ratio. This effect, however, diminishes as χ_4 increases. At $\chi_4 = 1$, cross-reactive lytic T cells are as efficient as specific T cells in killing infected cells. In fact, due to their faster response, cross-reactive T cells reduce the overall T-cell responses and the probability of IM.

We now add the possibility of cross-reactive T-cell responses against latent infection. Figure 4.5 shows the effects of this addition on the two measurements of IM. For each level of σ_4, we set $\sigma_2 = 0.2\sigma_4$, to assume lower levels of cross-reactive T cells against latent infection, compared to lytic infection. We analyzed and observed only minimal impacts of variation in the efficiency of cross-reactive T cells in killing latently infected cells (χ_2), on the results. We thus, fix $\chi_2 = 0.5$ for this analysis. In comparison to the results presented in Figure 4.4(i), addition of cross-reactive T cells to latent infection does not induce visible effect on the total number of T cells while the lytic T cell ratios are significantly reduced. This implies that cross-reactive T-cell responses to latent infection do not induce the high lytic ratio observed in IM patients.

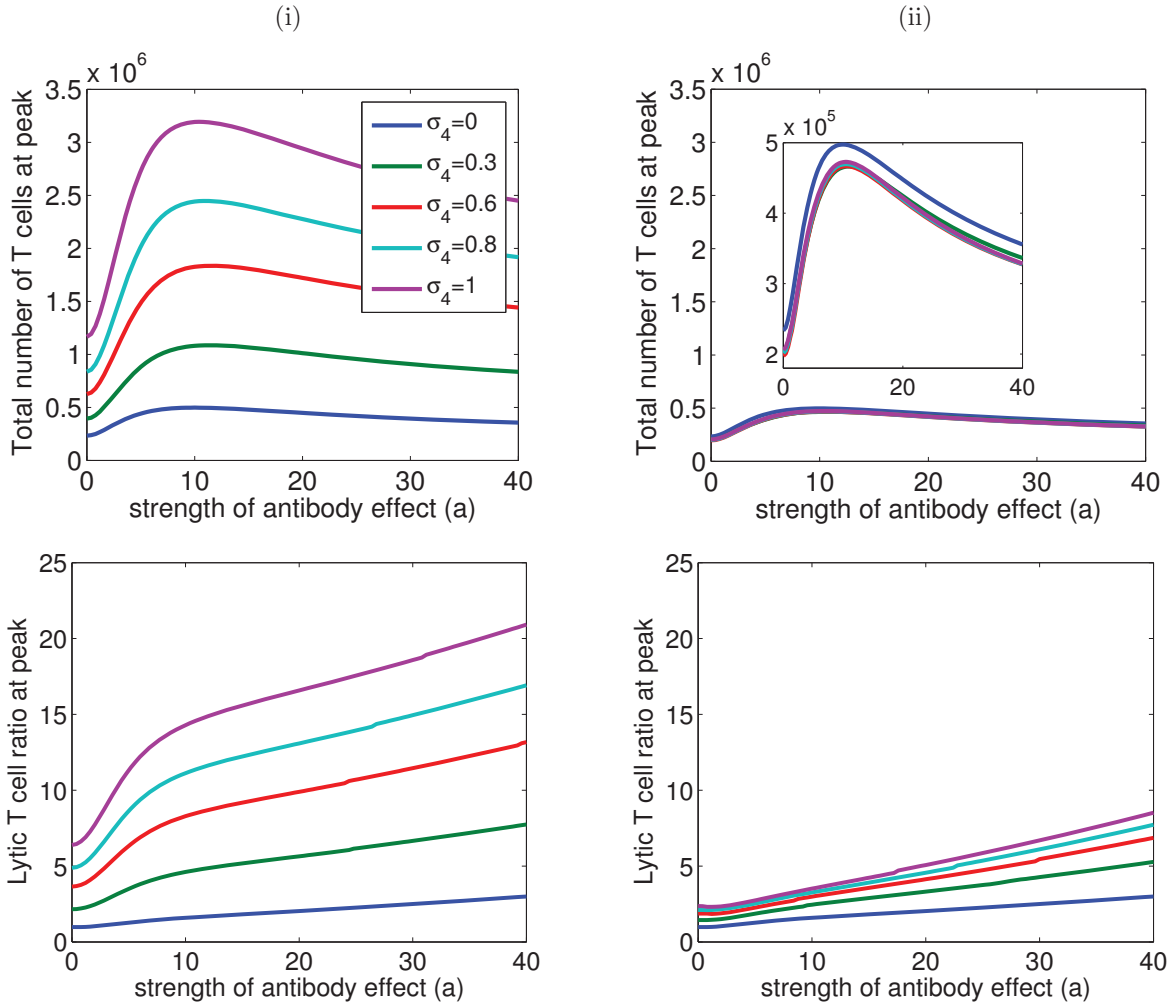

Figure 4.4. The effects of cross reactive T-cell responses to viral lytic proteins ($\sigma_4 > 0$) on the total number of T cells and the lytic T cell ratio during primary infection as a function of the strength of the antibody effect (a). The five different degrees of cross-reactive responses are shown in each plot. **(i)** Left column: low efficiency of cross-reactive lytic T cells in killing infected cells ($\chi_4 = 0.1$). **(ii)** Right column: cross-reactive T cells are as efficient as specific T cells in killing infected cells ($\chi_4 = 1$). Other parameter values are shown in Tables 4.1, and 4.2.

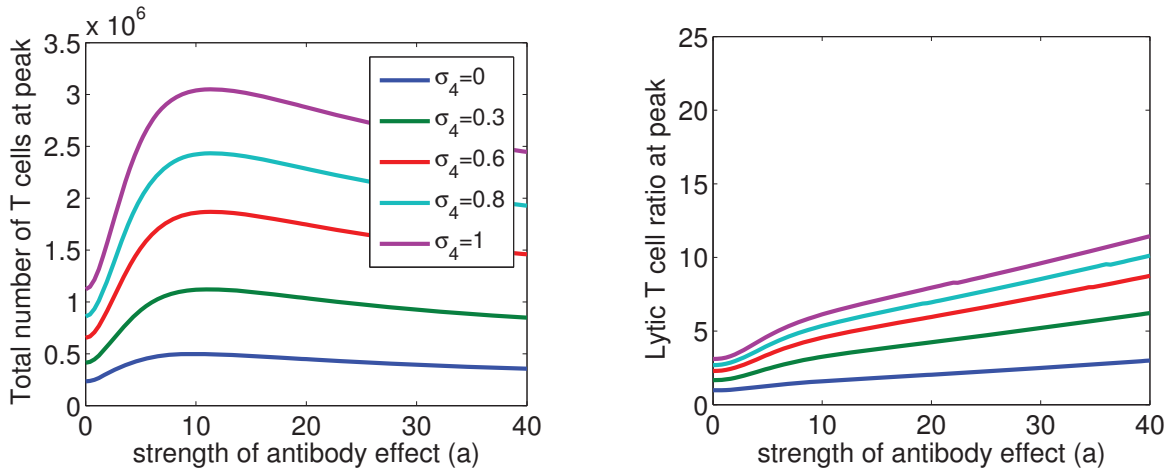

Figure 4.5. The effects of both latent and lytic cross reactive T cells ($\sigma_j > 0$) on the total number of T cells and the lytic T cell ratio during primary infection as a function of the strength of the antibody effect (a). The five different degrees of cross-reactive responses are shown in the plots. For each level of σ_4, $\sigma_2 = 0.2\sigma_4$. We set $\chi_2 = 0.5$ and $\chi_4 = 0.1$. Other parameter values are shown in Tables 4.1, and 4.2.

4.4.3 High initial viral load

A third hypothesis suggests that transmission often occurs through kissing in adolescents which may transmit a large number of viruses and hence lead to aggressive CD8+ T-cell responses. To analyze this hypothesis, we numerically solve Equation (4.1) with five different levels of the initial viral load, V_0. In comparison to antibody and cross-reactive T-cell effects, the initial viral load has very little effect on either the total number of T cells or the lytic T cell ratio (Figure 4.6).

4.4.4 Combined effects of antibody and cross-reactive T-cell responses

So far, our model supports the roles of antibody effects and the cross-reactive T cells in the development of IM. To summarize our analysis of the two hypotheses, we define two new ratios. The relative lytic T cell ratio gives the lytic T cell ratio for given value of σ_j and a compared with a baseline at $\sigma_j = 0$ and $a = 0$,

$$\left(\frac{T_4 + T_{4C}}{T_2 + T_{2C}}\right) \Big/ \left(\frac{T_4 + T_{4C}}{T_2 + T_{2C}}\right)_{\sigma_j=0, a=0}.$$

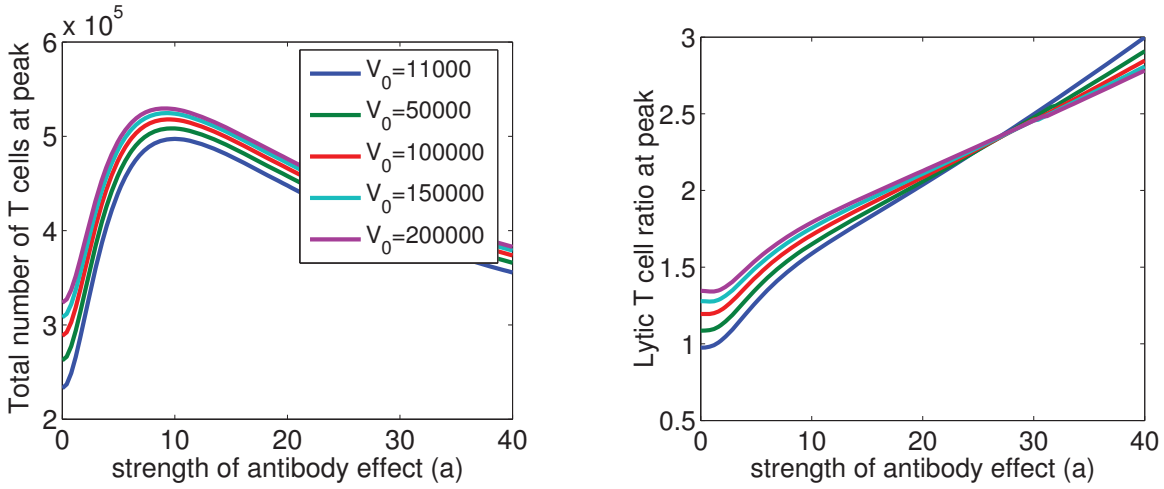

Figure 4.6. The effect of initial viral load (V_0) on the total number of T cells and the lytic T cell ratio during primary infection as a function of the strength of the antibody effect (a). We set $\sigma_j = 0$, which represents no cross-reactive T cell response. Other parameter values are shown in Tables 4.1, and 4.2.

The relative total T cell number gives the ratio between the total number of T cells given values of σ_j and a and the one with a baseline $\sigma_j = 0$ and $a = 0$,

$$\frac{(T_2 + T_4 + T_{2C} + T_{4C})}{(T_2 + T_4 + T_{2C} + T_{4C})_{\sigma_j=0,a=0}}.$$

We examine five different levels of cross-reactive T cells to lytic infection (σ_4), four different levels of cross-reactive T cell against latent infection (σ_2), five different levels of the efficiency of lytic T cells in killing infected cells (χ_4), and fix $\chi_2 = 0.5$ (Figure 4.7).

Infectious mononucleosis (IM) is assumed to be possible when both ratios, the relative total T cell number and the relative lytic T cell ratio are large (≥ 5). Studies give a wide range for these ratios [8, 32, 80], so these threshold levels of ≥ 5 are not to be conclusive. In the absence of antibody effects ($a = 0$), IM can only be explained with very high levels of cross-reactive lytic T cells together with a low efficiency of these cells in killing infected cells. In the absence of cross-reactive T cells ($\sigma_j = 0$, $a > 0$), antibody effects induce increases in the total number of T cells and the lytic T cell ratio. However, these increases are not as significant as those induced by the combined effects of antibodies with cross-reactive T cells. Thus, IM is characterized by

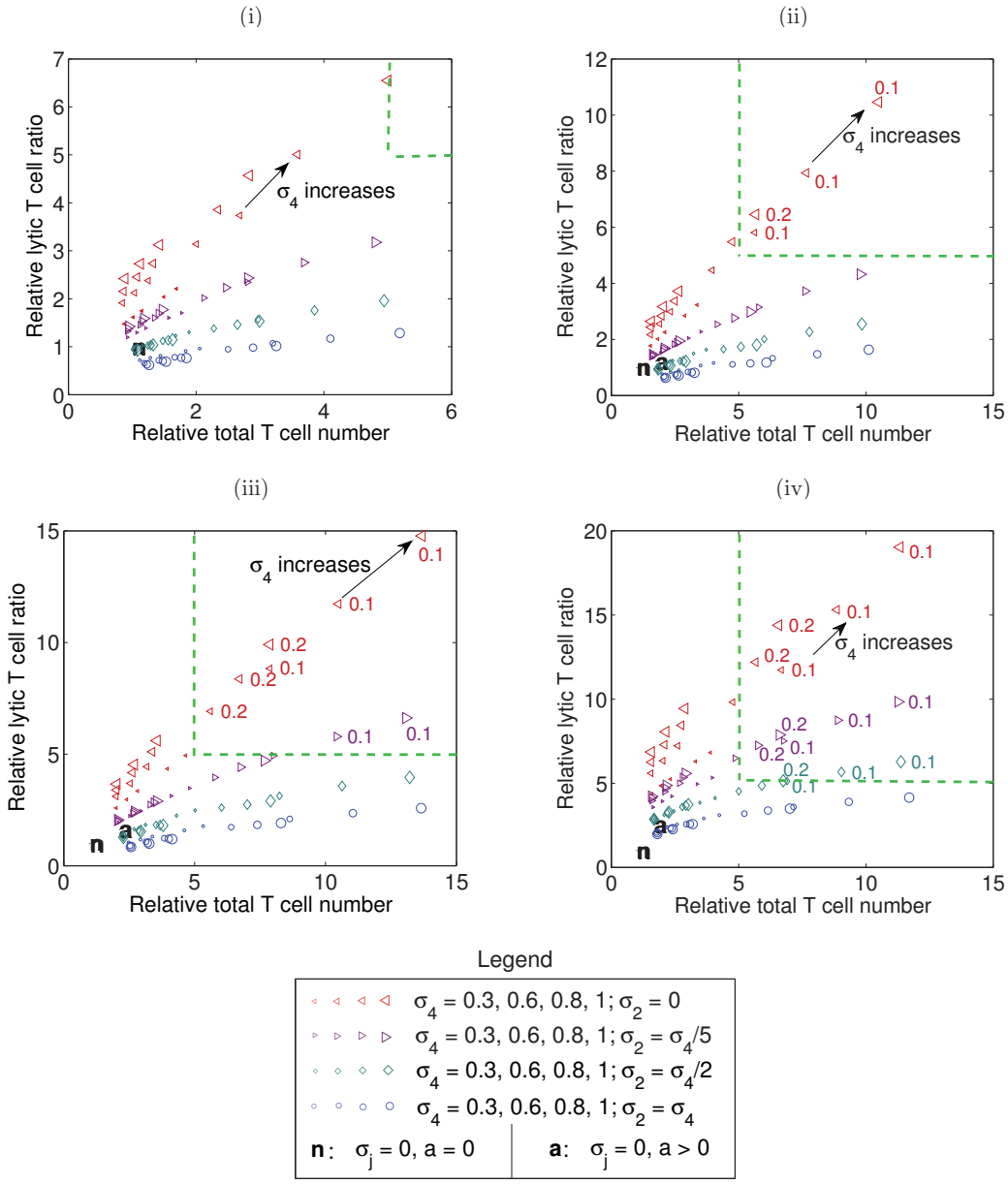

Figure 4.7. Combined effects of antibodies with cross-reactive T cells on the relative T cell number and the relative lytic T cell ratio. (i) $a = 0$. (ii) $a = 4$. (iii) $a = 10$. (iv) $a = 30$. The green lines show the area of possible IM cases with high levels of the relative total T cell number and the relative lytic T cell ratio (≥ 5). Four different colors (symbols) represents different levels of cross-reactive latent T cells (σ_2). Symbol size represents different levels of cross-reactive lytic T cells ($\sigma_4 = 0.3, 0.6, 0.8, 1$). The label numbers next to the symbol represent the efficiency of lytic T cells in killing infected cells (χ_4). We examine five different levels of χ_4 $(0.1, 0.2, 0.5, 0.7, 1)$ and only label the points of possible IM cases. The characters **n** and **a** represent the normal condition ($\sigma_j = 0$, $a = 0$) and the conditions with only antibody effects ($\sigma_j = 0$, $a > 0$), respectively.

high level of antibody effects, high level of cross-reactive T cells to lytic infection, and low efficiency of cross-reactive T cell in killing infected cells. As individuals age, the levels of antibody effects and the cross-reactive T cells increase; hence, the probability of IM increases if the cross-reactive T cells do not efficiently kill infected cells.

4.5 Discussion

Infectious mononucleosis (IM) is characterized by a large T-cell response, primarily to the lytic phase of the infection and thus can result from two broad changes in the course of acute infection. First, the virus could be biased towards creating a large fraction of lytically infected cells. EBV alternates between infecting B cells (its primary target), with either latent or lytic infection, and epithelial cells (important in viral persistence and shedding), as lytic infection only. Any factor that biasses infection toward epithelial cells can increase the importance of lytic infection and potentially increase the probability of IM. Switching between B-cell and epithelial-cell virus is modulated by antibody responses and unknown constituents in the saliva [87]. Hosts with increased IgA antibodies may be prone to large expansions of T cell against viral lytic proteins. Second, a host could have a less efficient T-cell response against the virus. EBV infection can activate cross-reactive memory T cells that are specific to other pathogens [14]. If these cells are activated in large number, but recognize and kill target cells inefficiently, IM may result. The high initial viral load hypothesis cannot produce large expansions of T cells and thus cannot be used to explain the age dependence of IM.

In economically developed countries, IM has highest incidence in the 15- to 25-year-old age group. In developing countries like Brazil, the age distribution of IM is shifted downward with mean age of IM around 13 years [62]. If people in developing countries are exposed to more diseases at an earlier age, they could have both higher antibody level and a larger pre-existing memory CD8 repertoire compared to age matched counterparts from developed countries. Together, these effects may explain the difference in age distribution of IM.

We built the component of antibody effects in our model based on an in vitro study

of the host saliva and antibody effects on the infections of B cells and epithelial cells with limited data from saliva samples of infected and uninfected individuals [87]. The goal of our study was not to predict the exact level of antibodies that induces large expansion of T cells and symptoms of IM, but to identify the potential risks in their effects. Our model highlights a need for further studies on the constituents of the saliva influencing infection of the two cell types, and studies to compare the levels of antibodies, especially IgA, to EBV viral capsid antigens and glycoproteins during the acute phase of infection between asymptomatic and symptomatic patients. These studies would help to identify the existence of thresholds of antibody levels or other factors in the host saliva that direct the course of infection.

We have used our model to show that both the magnitude and the quality of T cells in killing the infected cells are critical determinants of the outcomes of the infection. Indeed, our result suggests that large expansion of $CD8^+$ T cells occur only when they are inefficient at killing. A study on mice shown that infection with lymphocytic choriomeningitis virus (LCMV), Pichinde virus (PV), or vaccinia virus (VV) can activate cross-reactive T cells that are specific to one of these viruses [77]. These cross-reactive responses are fast, functionally efficient, and hence help to clear the secondary virus infection. Study of T-cell responses to dengue virus has shown that different cross-reactive T cell clones can have very different efficiencies in recognizing and killing the infected cells [40]. *In vitro* study has shown that EBV antigen can activate cross-reactive T cells that are specific to influenza-A virus, but the killing efficiency of these cells has not yet been determined [14]. As the pre-existing memory CD8 repertoire evolves with age, we do not know how the functional efficiency of these memory cells changes. Further studies to compare the recognizing and killing efficiency of effector T cells during primary infection of EBV between different age groups, and between healthy and IM patients, are needed to address this question and to validate the results of our model.

Studies have also suggested that genetic factors can contribute to differences in efficiency of T-cell responses to EBV, which implies difference in susceptibility to IM between individuals [56]. Individuals with certain HLA class I alleles are linked to

higher risk of IM. HLA class I plays a key role in the process of antigen presentation by infected cells to T cells [23]. Hence, a difference in HLA alleles can induce different rates at which T cells can be activated, proliferate, recognize, and kill infected cells. Similar to the way we model the cross-reactive T-cell responses, we can utilize our model to address this hypothesis on the genetic predisposition to IM.

Even though infectious mononucleosis is rarely lethal, it may induce long-term effects on the population of T cells [76, 33]. Infectious mononucleosis is strongly correlated with increased risk of EBV-positive Hodgkin's lymphoma in the years after infection [34]. Understanding risk factors for IM may help to investigate the long-term effects of the disease and its association with more serious disease like cancers.

4.6 Acknowledgements

We would like to thank Dr. Thorley-Lawson for the opportunity to come and study the biology of Epstein-Barr virus infection of B cells at his laboratory and Dr. Hutt-Fletcher for insightful discussions on Epstein-Barr virus infection of epithelial cells. Funding for this work was provided by the National Science Foundation (NSF) Research Training Group (RTG) (Award Number DMS0354259).

CHAPTER 5

MODELING THE ASSOCIATION OF EPSTEIN-BARR VIRUS INFECTION WITH THE DEVELOPMENT OF NASOPHARYNGEAL CARCINOMA

5.1 Abstract

Nasopharyngeal carcinoma (NPC) is a cancer of epithelial cells in the nose and pharynx that has distinct patterns of incidence in different populations and geographic locations. The highest incidence is found in the populations of southern China, South-east Asia, and Mediterranean Africa, and in Eskimos of the Arctic region, while it is much lower in the populations of North America and Europe. The undifferentiated type III is most common and strongly linked with Epstein-Barr virus (EBV) infection where all tumor samples contain EBV DNA. Latent EBV infection within epithelial cells in the pharynx, genetic factors, and diet play key roles in the pathogenesis of NPC. Tumors are found to represent the clonal expansion of an EBV latently infected epithelial cell. We use mathematical models to examine the interaction between latent EBV infection and effector T cells in the development of NPC. Our model predicts a threshold of the number of effector T cells below which a bifurcation leads to an increase in the number of latently infected cells. If the probability of developing NPC is proportional to the number of these EBV latently infected epithelial cells, our model supports the hypothesis that genetics and diet drive the differences observed between the NPC incidence in high risk and low risk populations.

5.2 Introduction

Persistent infection with the Epstein-Barr virus (EBV) has been associated with many diseases including different types of B cell and epithelial cell cancers such as Burkitt's lymphoma, Hodgkin's lymphoma, and nasopharyngeal carcinoma (NPC) [96]. Within a host, EBV infects two major cell types, B cells and epithelial cells, and can maintain a latent infection in B cells, within which its genome remains as an episome. EBV infection of epithelial cells normally results in a lytic infection where viral particles are released and the cell lyses. Latent infection of epithelial cells, however, occurs in cases of nasopharyngeal carcinoma (NPC) [70]. NPC is a cancer of epithelial cells that originates in the pharynx and is classified into three subtypes (I-III), which refer to the differentiation status of the tumor cells. The undifferentiated type III NPC is the most common and is strongly associated with EBV infection, where all samples have EBV DNA present.

In latently infected type-III tumor cells, the EBV genome is retained as an episome in the cell nucleus, not integrated into the host chromosomes [70]. It has been suggested that genetic changes and consumption of certain carcinogenic foods, such as salted fish and preserved foods, predispose epithelial cells to an EBV latent infection [11, 70]. These factors, together with a high prevalence of EBV infection in the populations of Southeast Asia, southern China, and Mediterranean Africa and in Eskimos of the Arctic region, are thought to explain the high frequency of NPC in these populations [5, 70]. NPC incidence rates in these high risk populations can reach up to 40 per 100,000 persons per year for the age group of 45 years old or above, at least 20 times higher than NPC incidence in a low risk population of North America or Europe [5].

Although these predisposed epithelial cells are susceptible to EBV latent infection, *in vitro* studies have shown that EBV remains inefficient at infecting these cells [53]. Intriguingly, immunoglobulin A (IgA) to the EBV viral capsid antigen (VCA), particularly to the viral glycoprotein 350 (gp350), can enhance EBV infection of cells that are predisposed [53, 83]. Furthermore, elevated levels of IgA to EBV VCA and gp350 can be observed a few years before the diagnosis of NPC, and have been used as an early predictor of the onset of this disease [43, 70, 94]. Infection of the predisposed

epithelial cells gives rise to a pool of latently infected epithelial cells. Expression of EBV latent genes in these infected cells contribute to increased cell proliferation, cell survival, and accumulation of regulatory T cells [50, 86], all of which can accelerate tumor development.

The roles of EBV latent gene expression in NPC have been confirmed[70, 86]. However, most people are infected with EBV at early age and remain healthy carriers of the virus without symptoms. Immune responses, especially specific T cells to EBV, play a key role in the regulation and control of EBV infection in healthy carriers [33]. EBV infection in immunosuppressed patients, like transplant and HIV infected individuals, can lead to different types of life threatening lymphomas with uncontrolled proliferation of EBV infected cells [96]. Although T cells can recognize and kill the EBV latently infected tumor cells [51], genetic factors, like certain human leukocyte antigen (HLA) types and alteration of EBV latent genes, may affect the ability of T cells to recognize and kill latently infected epithelial cells [70]. Furthermore, regulatory T cells (T_{reg}), which can suppress the activation and proliferation of $CD8^+$ T cells [69, 93], have also been shown to circulate in the blood and infiltrate tumors in NPC patients [50]. These cells accumulate with age and EBV latent gene expression [19, 86]. Within the framework of multistage cancer development, it has been suggested that genetic alteration and diet contribute to the first step while EBV latent infection of epithelial cells in the pharynx is the second step of the pathogenesis of NPC [5]. Our aim is to use mathematical models to investigate the dynamics of EBV latently infected epithelial cells to understand the timing of cancer onset.

Mathematical models have been used to study the dynamics of other viruses that have a latent stage and have strong associations with cancers, including HPV (cervical cancer), HBV and HCV (liver cancer), and Kaposi's sarcoma-associated herpesvirus (Kaposi's sarcoma) [20, 61, 64, 65, 68]. The dynamics of EBV infection and the T cell responses have been investigated using simulations of agent-based models, C-ImmSim and PathSim [9, 78]. We have developed mathematical models to study the dynamics of EBV, infected cells, T cell responses, and EBV associated infectious mononucleosis [38, 39]. However, modeling the mechanisms of virus induced cancers remains an open

field. There are as yet no published mathematical models of the association of EBV infection with cancers.

In this study, we develop a mathematical model that describes the dynamics of EBV latently infected epithelial cells through the initial two steps of NPC pathogenesis. This is an adaptation of a model that has been built to describe the dynamics of tumors being attacked by effector $CD8^+$ T cells [30]. We determine the critical parameters that affect the dynamics of infected cells and the delay time to tumor development in NPC patients assuming the risk of developing NPC is proportional to the number of the latently infected epithelial cells.

5.3 Model

5.3.1 The dynamics of latently infected epithelial cells

Most people infected with EBV are healthy carriers with low, persistent levels of latent and lytic infections of B cells and epithelial cells [28, 33, 38]. In this study, we assume the levels of these infections are constant and focus on the dynamics of latently infected epithelial cells locally in the pharynx. Only predisposed epithelial cells that may have been genetically altered (E_M) can be latently infected by EBV. These latently infected cells proliferate and die naturally or die from being killed by effector T cells (Figure 5.1) according to the equation,

$$\frac{dE_{La}}{dt} = \text{infection} + \text{proliferation} - \text{death by T cell killing} - \text{natural death}. \quad (5.1)$$

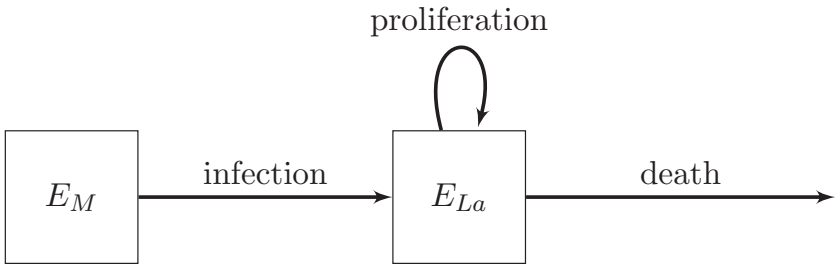

Figure 5.1. Model of latently infected epithelial cells (E_{La}), arriving from EBV infection of genetically altered epithelial cells (E_M).

Creation of new latently infected cells depends on existence of E_M, the amount of virus present, and the levels of antibodies to EBV VCA and glycoproteins local to the pharynx. We assume the existence of a low and constant level of E_M that is due to diet or to genetic alterations. Free virus (V) and antibodies (A) are also at constant levels because of the presence of a low and persistent infection of normal B cells and epithelial cells. New latent infection of epithelial cells is described by

$$\text{infection} = g(A, V)E_M, \tag{5.2}$$

where $g(A, V)$ is the per cell rate at which E_M are latently infected and is an increasing function of the levels of virus and antibodies. For example, we can set

$$g(A, V) = \mu_{La} V \left(1 + \frac{\eta A^n}{A^n + \alpha^n}\right),$$

where μ_{La} is the rate at which EBV successfully establishes a latent infection within E_M, η is the maximal effect of antibodies on the infection efficiency of EBV, and α is the level of antibodies at which the antibody effect is half maximum.

The expression of EBV latent genes promotes cell proliferation. We adapt a model of tumors being attacked by T cells [30] to build the terms for proliferation and death by T cell killing in Equation (5.1). We assume a carrying capacity (K_E) to the number of epithelial cells that can be contained in the limited space of the pharynx. Proliferation is described by

$$\text{proliferation } = \rho E_{La} \left(1 - \frac{E_{La}}{K_E}\right), \tag{5.3}$$

where ρ is the rate of replication of the latently infected epithelial cells.

EBV latent proteins within infected epithelial cells can be recognized by circulating effector T cells (T_{La}) during the response to a persistent, latent infection in B cells. We assume that the total number of T_{La} remains constant locally at the site of the pharynx and these cells are in one of two states: free (T_f) or bind to and in the process of killing an infected cell (T_b). The efficiency of the effector T cell response to latently infected epithelial cells depends on the rates at which T_f recognize and T_b kill the infected cells, k_1 and k_2, respectively (Figure 5.2).

$$E_{La} \quad + \quad T_f \xrightarrow{k_1} T_b \xrightarrow{k_2} T_f \quad + \quad E_D$$

Figure 5.2. The kinetics of effector T cells interacting with EBV latently infected epithelial cells.

The kinetics of effector T cells in recognizing and killing EBV latently infected epithelial cells are described by,

$$\frac{dT_f}{dt} = k_2 T_b - k_1 E_{La} T_f \tag{5.4}$$

$$\frac{dT_b}{dt} = k_1 E_{La} T_f - k_2 T_b. \tag{5.5}$$

The key assumptions here are $T_f + T_b = T_{La}$ remains constant and the process of recognizing an infected cell is much faster than the process of killing one ($k_1 E_{La} >> k_2$). These conditions allow us to further assume the quasi-steady state equilibrium for T_b^* and derive the equation for the death rate of latently infected epithelial cells that is due to T cells killing,

$$\text{death by T cell killing} = \frac{dE_D}{dt} \quad = k_2 T_b^* = \frac{k_2 k_1 T_{La} E_{La}}{k_1 E_{La} + k_2}. \tag{5.6}$$

Putting the Equations (5.2), (5.3), and (5.6) into Equation (5.1), together with a constant natural death rate (δ_E) for E_{La}, gives a single differential equation for the dynamics of latently infected epithelial cells,

$$\frac{dE_{La}}{dt} = g(A,V)E_M + \rho E_{La}\left(1 - \frac{E_{La}}{K_E}\right) - \frac{k_2 k_1 T_{La} E_{La}}{k_1 E_{La} + k_2} - \delta_E E_{La}. \tag{5.7}$$

The dynamics of latently infected cells are generally slower than the dynamics of normal latent and lytic infection. This occurs because of a low efficiency of EBV to establish a latent infection within a genetically altered epithelial cell ($g(A,V)$), a low replication rate (ρ), a low efficiency of effector T cell killing (k_2), and a low natural death rate (δ_E) are all low. A summary of parameter definitions can be found in Table 5.1.

Table 5.1. Parameter definitions for the dynamics of latently infected epithelial cells (Equation 5.7).

Parameter	**Units**	**Definition**
$g(A,V)$	1/day	Rate at which EBV successfully establishes a latent infection within a predisposed epithelial cell
E_M	cells	Number of genetically altered epithelial cells
ρ	1/day	Replication rate of latently infected epithelial cells
K_E	cells	Carrying capacity of latently infected epithelial cells
k_1	1/(cells $\cdot$ day)	Rate at which effector T cells recognize an infected epithelial cell
k_2	1/day	Rate at which effector T cells kill an infected epithelial cell
δ_E	1/day	Death rate of latently infected epithelial cells

The equilibrium solutions for Equation (5.7) are the roots of the following polynomial,

$$\vartheta(E_{La}) = -\frac{k_1\rho}{K_E}E_{La}^3 + \zeta E_{La}^2 + \beta E_{La} + k_2 g(A,V)E_M, \tag{5.8}$$

where

$$\zeta = \left(k_1 - \frac{k_2}{K_E}\right)\rho - k_1\delta_E, \text{ and} \tag{5.9}$$

$$\beta = k_1 g(A,V)E_M + k_2(\rho - \delta_E) - k_1 k_2 T_{La}. \tag{5.10}$$

The number of positive equilibria and their stability depends on the values of E_M, and the composite parameters ζ and β. This polynomial has a positive root if E_M is positive, and constant consumption of carcinogenic foods can increase the value of E_M. Increased cell replication and survival that may be promoted by expression of

EBV latent genes within the infected cells can lead to an increased value of ρ and a decreased value of δ_E, respectively. Selection of EBV strains, with change in their latent proteins, that reduces the efficiency of T cell recognition and killing (immune escape) [70] can lead to decreased values of k_1 and k_2. An increase in antibodies to the viral capsid antigen and glycoproteins will increase $g(A, V)$. Immunosuppression from an increase in the number of regulatory T cells with age will decrease the value of T_{La}. All of these effects lead to increased values of ζ and β.

Treatments that activate latently infected cells to go into lytic replication of virus within the cells will increase the value of δ_E. Cell therapy or treatments to improve the number and functionality of effector T cells responding to EBV latent genes [52, 84, 16] will increase the value of T_{La}, k_1, and k_2. These changes will lead to decreases in the values of ζ and β.

When $\zeta < 0$, the model has only one stable positive equilibrium. Using Equation (5.9), the condition $\zeta < 0$ implies

$$\rho\left(1 - \frac{k_2}{K_E k_1}\right) < \delta_E, \tag{5.11}$$

Since $k_1 K_E >> k_2$, the inequality above is satisfied if the replication rate (ρ) is small or natural death rate (δ_E) is large. In this case, there is a low number of latently infected epithelial cells (Figure 5.3(a)). This number increases with β and only attains a high value when β is large, which can happen in the case of immunosuppression that decreases the number of T_{La}.

When $\zeta > 0$, there are critical values of β, β_1 and β_2, such that multiple solutions exist for $\beta_1 < \beta < \beta_2$ (Figure 5.3(b)). If $\beta < \beta_1$, there is only one stable equilibrium solution of a low level of latently infected cells. For $\beta > \beta_1$, there exists another stable equilibrium solution of a high level of latently infected cells. This high number of latently infected cells increases with β and becomes the only stable solution when $\beta > \beta_2$. As we have seen, several parameters, including the number of effector T cells change in the value of β (Figure 5.3(c)).

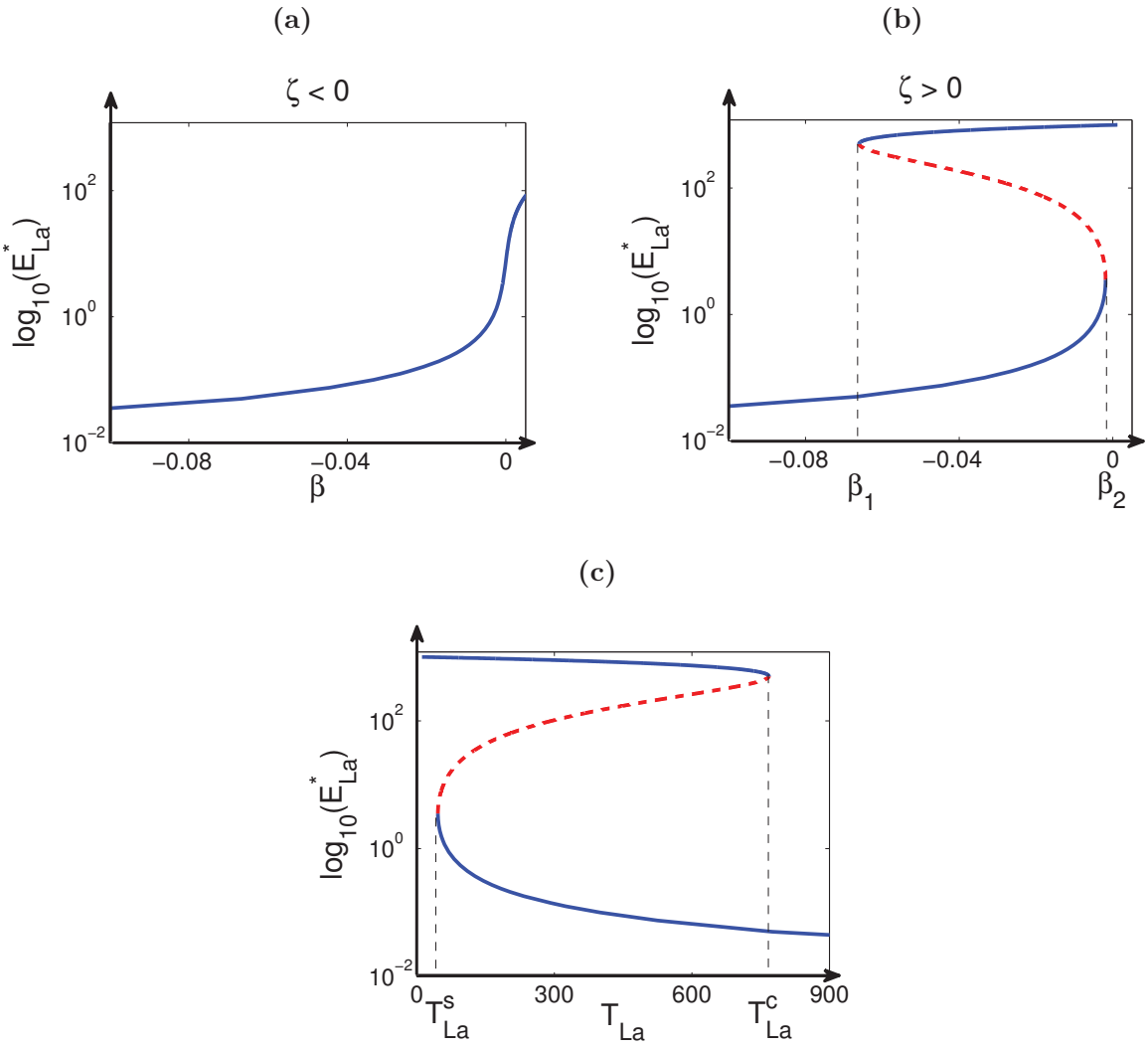

Figure 5.3. Bifurcation diagrams for the model of latently infected epithelial cells (Equation 5.7). The solid lines indicate stable solutions and dashed lines indicate unstable solutions. **(a)** Logarithmic scale of the number of latently infected epithelial cells at equilibrium ($\log_{10}(E^*_{La})$) as a function of β when $\zeta < 0$. **(b)** Logarithmic scale of the number of latently infected epithelial cells at equilibrium ($\log_{10}(E^*_{La})$) as a function of β when $\zeta > 0$. **(c)** Logarithmic scale of the number of latently infected epithelial cells at equilibrium ($\log_{10}(E^*_{La})$) as a function of T_{La} when $\zeta > 0$. Parameter values used to compute the bifurcation diagrams: $k_1 = 0.007$ cells^{-1}day^{-1}, $k_2 = 0.007$ day^{-1}, $E_M = 500$ cells, $g(A,V) = 0.0005$ day^{-1}, $K_E = 1000$ cells. (a) $\rho = 0.001$ day^{-1}, $\delta_E = 0.01$ day^{-1}. (b) $\rho = 0.0033$ day^{-1}, $\delta_E = 0.0001$ day^{-1}.

If the number of effector T cells is small as in the case of immunosuppression ($T_{La} < T^s_{La}$), the latently infected cells can proliferate with little regulation and hence persist at a high level. If the number of effector cells is large ($T_{La} > T^c_{La}$), these effector cells can control and maintain a population of latently infected, proliferating epithelial cells at a low level.

5.3.2 Quasi-steady state approximation of effector T cells

We assume that the effector T cells, which have a short lifespan, have faster dynamics than the latently infected cells. In our model, we also fix the level of naive T cells (T_N) at constant level. Upon stimulation by latently infected B cells and epithelial cells, these naive T cells become effector cells (T_{La}) at rate ϕ. These effector cells can proliferate with further stimulation by infected cells with rate θ and die with rate d_T, where $d_T > \theta$. The dependence of T cell activation and proliferation on the available infected cells takes the saturating functional form,

$$w(B + E_{La}) = \frac{B + E_{La}}{K + B + E_{La}}, \tag{5.12}$$

where K is the number of infected cells at which activation or proliferation is half maximal, and B is the constant number of latently infected cells that are close to the infection site in the pharynx. The dynamics of T cells obey the differential equation

$$\frac{dT_{La}}{dt} = \phi w(B + E_{La})T_N + \theta w(B + E_{La})T_{La} - d_T T_{La}. \tag{5.13}$$

A summary of parameter definition used in the dynamics of effector T cells can be found in Table 5.2.

By assuming that the dynamics of effector T cells are fast, we can calculate its quasi-steady state equilibrium,

$$T^*_{La} = \frac{\phi w(B + E_{La})T_N}{d_T - \theta w(B + E_{La})}. \tag{5.14}$$

The value of effector T cells can be affected by the number of regulatory T cells (T_{reg}), which may increase with age, and the level of EBV latent genes being expressed within the infected cells [19, 86]. Increase in the level of T_{reg} can suppress activation and proliferation of effector T cells [69, 93], which decreases the values of ϕ and θ. By

Table 5.2. Parameter definitions for the dynamics of effector T cells (Equation 5.13).

Parameter	Units	Definition
ϕ	1/day	Rate of effector T cell activation in response to a latent infection
θ	1/day	Rate of effector T cell proliferation
d_T	1/day	Death rate of effector T cells
B	cells	Number of latently infected B cells local to the pharynx
K	cells	Number of infected cells at which T cell activation and proliferation is half maximal
T_N	cells	Number of naive T cells at the site of the pharynx

substituting Equation (5.14) into Equation (5.7), we obtain the equation describing the population of latently infected epithelial cells,

$$\frac{dE_{La}}{dt} = g(A,V)E_M + \rho E_{La}\left(1 - \frac{E_{La}}{K_E}\right) - \frac{k_2 k_1 E_{La}}{(k_1 E_{La} + k_2)} \frac{\phi w (B + E_{La}) T_N}{(d_T - \theta w (B + E_{La}))} - \delta_E E_{La}. \tag{5.15}$$

5.3.3 Numerical results

We solve Equation (5.15) numerically to investigate the effects of parameters controlling the infection ($g(A,V)$ or E_M), proliferation (ρ), T cell activation (ϕ), and T cell recognition of infected cells for killing (k_1) on the dynamics of latently infected epithelial cells (E_{La}). The number of latently infected cells is maintained at a low level when there are few predisposed epithelial cells (E_M), a low EBV infection or replication rate, or an efficient T cell response (ϕ and k_1 are high) (Figure 5.4). Variation in these parameters leads to changes in the dynamics of latently infected cells. For a substantial range of each parameter, its effects on the dynamics occur only after a long delay, with the number of latently infected cells remains at a low level for many years before increasing quickly and approaching a much higher level.

The dynamics of latently infected cells is especially sensitive to variation in the rate of T cell activation (ϕ) (Figure 5.4(c)). Immunosuppression can decrease this activation rate and, hence, the number of effector T cells responding to the latently infected cells (Equation 5.14). A small decrease in the value of ϕ changes changes equilibrium number of latently infected cells from a very low to a high level.

5.4 Application to the rate of cancer development

The existence of genetically altered or predisposed epithelial cells and EBV infection of these cells creates the pool of latently infected epithelial cells. Clonal expansion of one of these cells gives rise to type-III NPC tumors [70]. We assume that the rate of tumor development ($r(t)$) is proportional to the number of latently infected epithelial cells (E_{La}) within an EBV infected host. This tumor development rate can differ between individuals or groups of people because of differences in genetics, diet, and circulating virus strains. The incidence rates of NPC (the number of new NPC cases per year per 10^5 persons) is high in Southern China and Southeast Asia (high risk) and low in North America and Europe (low risk) [5]. In our model, the rate of tumor development takes on the form

$$r(t,p) = \sigma E_{La}(t,p), \tag{5.16}$$

where σ is the probability rate of developing NPC, and p is a parameter of the model that can be different between individuals.

Genetics and diet are the key features have been hypothesized to drive the differences in the incidence rates between the high risk and the low risk groups by generating the predisposed epithelial cells that are susceptible to EBV latent infection. We let $p = g(A,V)E_M$, which describes the rate of EBV infection of predisposed epithelial cells to study and compare the rates of getting NPC between groups or population. If $f(p)$ is the probability density function for p with $p_{min} < p < p_{max}$, the incidence of NPC will obey

$$R = s\int_{p_{min}}^{p_{max}} \sigma E_{La}(t,p)f(p)dp, \tag{5.17}$$

with s is a scale factor such that $s\displaystyle\int_{p_{min}}^{p_{max}} f(p)dp = 1$.

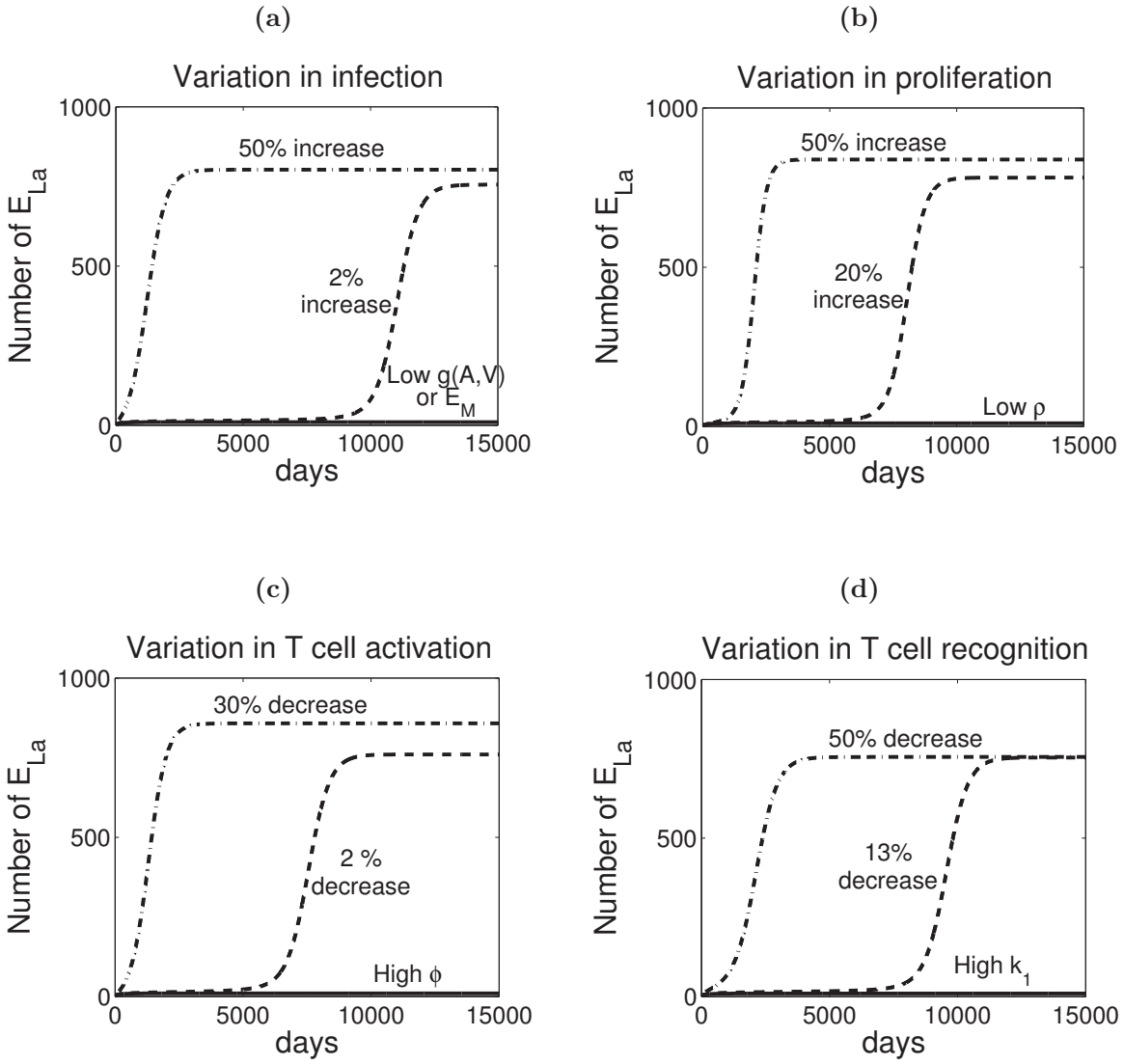

Figure 5.4. Effects of the parameters on the dynamics of latently infected epithelial cells (E_{La}). The solid lines show the dynamics of E_{La} for baseline parameter values while the dashed lines and dash-dotted lines show the dynamics of E_{La} for altered values of the indicated parameters. **(a)** Variation in the infection rate ($g(A,V)$) or the number of predisposed epithelial cells (E_M). **(b)** Variation in replication rate (ρ). **(c)** Variation in the T cell activation rate (ϕ). **(d)** Variation in the replication rate at which effector T cells recognize infected cells for killing (k_1). The baseline parameter values used for the simulations are $k_1 = 0.007$ cells^{-1}day$^{-1}, k_2 = 0.007$ day$^{-1}, E_M = 500$ cells, $g(A,V) = 0.0005$ day^{-1}, $\rho = 0.0033$ day$^{-1}, K_E = 1000$ day$^{-1}, \delta_E = 0.0001$ day$^{-1}, \phi = 0.0281$ day^{-1}, $\theta = 0.0468$ day$^{-1}, d_T = 0.125$ day$^{-1}, B = 500$ cells, $K = 30000$ cells, $T_N = 10000$ cells.

Assuming $p = g(A, V)E_M$ has the Weibull distribution, then the probability distribution function for p has the form

$$f(p) = \frac{k}{\lambda}\left(\frac{p}{\lambda}\right)^{(k-1)} e^{-(p/\lambda)^k}, \tag{5.18}$$

where k is the shape parameter and λ is the scale parameter. We let the mean ($E(p)$) of the parameter ($p = g(A, V)E_M$) equal its baseline value, $E(p) = \lambda\Gamma(1+1/k) = 0.0005 \cdot 500$, and analyze the effect of variation in the shape of the probability distribution function on the incidence of NPC (Figure 5.5).

When k is large (i.e., $k = 50$), the parameter $p = g(A, V)E_M$ has little variation around its baseline value. Most people in the group or population have low susceptibility of epithelial cells to EBV latent infection (Figure 5.5(a)). The rate of developing NPC remains low in this group and only increases modestly with time or age (Figure 5.5(b)), consistent with the appearance of the age-incidence curves of NPC observed for the low risk groups [5]. When k is small (i.e., $k = 1$), the probability distribution function for p is more spread out. In this case, a greater number of individuals in the group have a high number of predisposed epithelial cells and higher

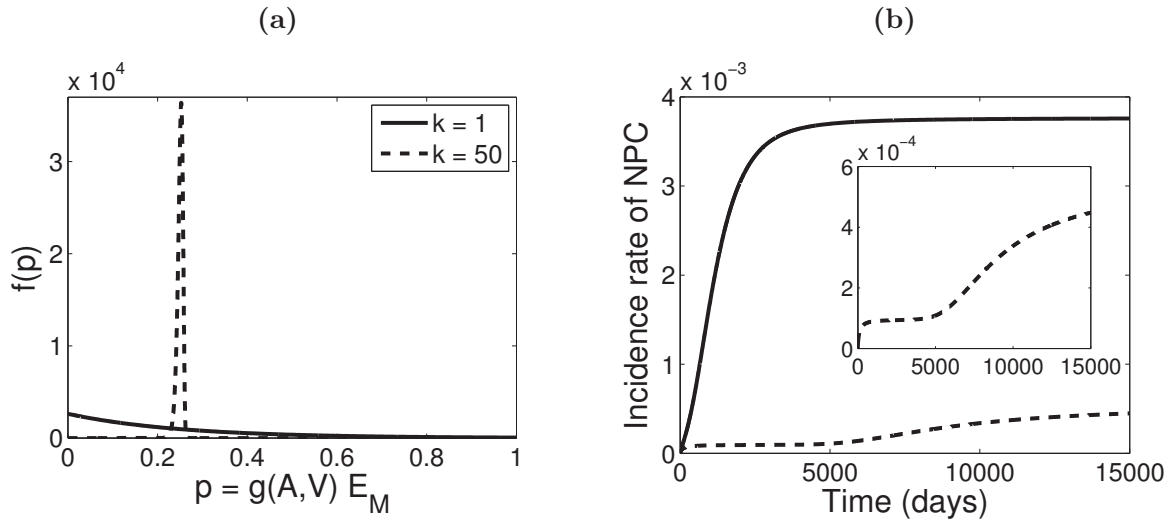

Figure 5.5. Effects of the shape of the probability distribution function on the rate of developing NPC. **(a)** The probability distribution function for $k = 1$ (solid line) and $k = 50$ (dashed line). **(b)** The NPC incidence rate as a function of time, with $k = 1$ (solid line) and $k = 50$ (dashed line). Parameter values used: $\lambda = 0.25\,(k = 1), \lambda = 0.253\,(k = 50), p_{min} = 0, p_{max} = 0.25 \times 4, \sigma = 1 \times 10^{-5}$.

susceptibility of epithelial cells to EBV latent infection (Figure 5.5(a)). The rate of developing NPC in this group increases steadily and saturates at a high level over time (Figure 5.5(b)).

5.5 Discussion

We have presented a model describing the dynamics of EBV latently infected epithelial cells in the pharynx to explore the role of EBV infection in the pathogenesis of NPC. We show that genetically predisposed epithelial cells that are susceptible to latent EBV infection produce at least a low level of such infected cells. Genetic alterations in cells, consumption of carcinogenic foods, and increased levels of IgA antibodies to EBV antigens can increase the susceptibility of epithelial cells to EBV latent infection, which is essential to the progression toward NPC.

The expression of EBV latent genes can increase cell proliferation, cell survival, and accumulation of regulatory T cells [50, 86]. Our model predicts the thresholds of these effects above which the number of latently infected epithelial cells jumps from a low to a high level. Type-III NPC tumors have been shown to develop from clonal expansion of a latently infected epithelial cell [70]. Our model supports a key role for the expression of EBV latent genes in the pathogenesis of NPC such that these genes can greatly elevate the number of infected cells and, hence, the risk of developing NPC.

We have adapted a model that describes the dynamics of tumors being attacked by effector T cells [30]. Our model is simple, keeping track of only one state variable, but includes regulation of the dynamics of infected cells through infection, proliferation, T cell response, and cell death. This simple model can capture the long delay between the initial EBV latent infection of epithelial cells and the time at which the number of infected cells quickly elevates to a high level (Figure 5.4). Furthermore, with the additional assumption that the rate of getting NPC is proportional to the number of latently infected epithelial cell, the model reproduces the measured age-incidence curves for NPC similar to the appearance of the age-incidence curves of NPC that have been observed in both low risk and high risk populations.

Numerical results are especially sensitive to variation in the level of effector T cell

responses. If these model results reflect a similar sensitivity to the *in vivo* dynamics of infected epithelial cells, treatment that increases effector T cell responses to EBV latent genes might effectively eliminate tumor cells. However, the accumulation of regulatory T cells within patients might make the treatment ineffective. Also, any factor that induces immunosuppression in a patient can greatly increase the risk of NPC.

Although our model predicts the threshold value of parameters supporting high population of latently infected epithelial cells, the quantitative values of these thresholds are not yet conclusive because many other parameters can only be estimated [38]. The main goal of this study was not to predict the exact values, but rather to develop a model that includes all the mechanisms of regulation that these parameters describe. Further studies and analysis of data on latent infection of epithelial cells in the pharynx, the replication rate of these latently infected cells, and efficiency of effector T cell response are needed to validate both the assumptions and the predictions of the model.

In vitro studies show IgA to EBV VCA and gp350 can enhance an EBV infection of epithelial cells [53, 83]. Intriguingly, the levels of IgA greatly increase up to a few years before the onset of NPC [43]. This elevation of IgA could be induced by EBV. Positive feedback could be a key to accelerate the development of NPC. Future work addressing the possibility of positive feedback between the dynamics of IgA and the latently infected epithelial cells will give insight into the role of elevated IgA levels in the pathogenesis of NPC.

Our model can also be extended to include a more detailed mechanism of how cell growth is regulated. A submodel of molecular pathways involved in the expression of EBV latent genes and how these genes affect the regulation of cell proliferation and survival could be included to establish a connection between the effects of genetic alternation at the molecular level and the dynamics of the cell population. EBV infection is not only associated with NPC, but also other cancers of B cells including Burkitt's and Hodgkin's lymphomas. Understanding the mechanisms of how EBV latent genes affect the regulation of cell cycles will provide insight into the study of EBV associated B cell cancers.

5.6 Acknowledgements

We would like to thank Dr. Hutt-Fletcher for insightful discussions on Epstein-Barr virus infection of epithelial cells. Funding for this work was provided by the National Science Foundation (NSF) Research Training Group (RTG) (Award Number DMS0354259).

REFERENCES

[1] F.R. Adler and J. Mosquera, *Is space necessary? Interference competition and limits to biodiversity*, Ecology **81** (2000), no. 11, 3226–3232.

[2] F.E. Alexander, R.F. Jarrett, R.A. Cartwright, A.A. Armstrong, D.A. Gokhale, E. Kane, D. Gray, D.J. Lawrence, and G.M. Taylor, *Epstein-Barr virus and HLA-DPB1-*0301 in young adult Hodgkin's disease*, Cancer Epidemiol. Biomarkers Prev. **10** (2001), no. 6, 705–709.

[3] W.A. Andiman, *Epidemiology of primary Epstein-Barr virus infection and infectious mononucleosis*, Epstein-Barr Virus (A. Tselis and H.B. Jenson, eds.), vol. 1, Taylor & Francis Group, New York, NY, 1st ed., 2006, pp. 39–57.

[4] C.M. Borza and L.M. Hutt-Fletcher, *Alternate replication in B cells and epithelial cells switches tropism of Epstein-Barr virus*, Nat. Med. **8** (2002), no. 6, 594–599.

[5] F. Bray, M. Haugen, T. Moger, S. Tretli, O.O. Aalen, and T. Grotmol, *Age-incidence curves of nasopharyngeal carcinoma worldwide: bimodality in low-risk populations and aetiologic implication*, Cancer Epidemiol. Biomarkers Prev. **17** (2008), no. 9, 2356–2365.

[6] H.J. Bremermann and H.R. Thieme, *A competitive exclusion principle for pathogen virulence*, J. Math. Biol. **27** (1989), no. 2, 179–190.

[7] C.E. Buckley and F.C. Dorsey, *Serum immunoglobulin levels throughout the life-span of healthy man*, Ann. Intern. Med. **75** (1971), no. 5, 673–682.

[8] M.F.C Callan, L. Tan, and N. Annels, *Direct visualization of antigen-specific CD8+ T cells during the primary immune response to Epstein-Barr virus in vivo*, J. Exp. Med. **187** (1998), no. 9, 1395–1402.

[9] F. Castiglione, K. Duca, A. Jarrah, R. Laubenbacher, D. Hochberg, and D.A. Thorley-Lawson, *Simulating Epstein-Barr virus infection with C-ImmSim*, Bioinformatics **23** (2007), no. 11, 1371–1377.

[10] A. Cerwenka, T.M. Morgan, and R.W. Dutton, *Naive, effector, and memory CD8 T cells in protection against pulmonary influenza virus infection: homing properties rather than initial frequencies are crucial*, J. Immunol. **163** (1999), no. 10, 5535–5543.

[11] E.T. Chang and H.O. Adami, *The enigmatic epidemiology of nasopharyngeal carcinoma*, Cancer Epidemiol. Biomarkers Prev. **15** (2006), no. 10, 1765–1777.

[12] L.S. Chesnokova, S.L. Nishimura, and L.M. Hutt-Fletcher, *Fusion of epithelial cells by Epstein–Barr virus proteins is triggered by binding of viral glycoproteins gHgL to integrins v6 or v8*, Proc. Natl. Acad. Sci. **106** (2009), no. 48, 20464–20469.

[13] N.K. Childers, C. Greeleaf, F. Li, A.P. Dasanayake, W.D. Powell, and S.M. Michalek, *Effect of age on immunoglobulin A subclass distribution in human parotid saliva*, Oral Micr. Immunol. **18** (2003), no. 5, 298–301.

[14] S.C. Clute, L.B. Watkin, M. Cornberg, Y.N. Naumov, J.L. Sullivan, K. Luzuriaga, R.M. Welsh, and L.K. Selin, *Cross-reactive influenza virus-specific CD8+ T cells contribute to lymphoproliferation in Epstein-Barr virus-associated infectious mononucleosis*, J. Clin. Invest. **115** (2005), no. 12, 3602–3612.

[15] J.I. Cohen, *Clinical aspects of Epstein-Barr virus infection*, Epstein-Barr Virus (E.S. Robertson, ed.), vol. 1, Caister Academic Press, Norfolk, England, 1st ed., 2005, pp. 35–54.

[16] P. Comoli, P. Pedrazzoli, R. Maccario, S. Basso, O. Carminati, M. Labirio, R. Schiavo, S. Secondino, C. Frasson, C. Perotti, M. Moroni, F. Locatelli, and S. Siena, *Cell therapy of stage IV nasopharyngeal carcinoma waith autologous Epstein-Barr virus targeted cytotoxic T lymphocytes*, J. Clin. Oncol. **23** (2005), no. 35, 8942–8949.

[17] T. Cotner and Pious D., *HLA-DR beta chains enter into an aggregated complex containing GRP-78/BiP prior to their degradation by the pre-Golgi degradative pathway*, J. Biol. Chem. **270** (1995), no. 5, 2379–2386.

[18] M. Davenport, C. Fazou, A.J. McMichael, and M.F.C. Callan, *Clonal selection, clonal senescence, and clonal succession: the evolution of the T cell response to infection with a persistent virus*, J. Immunol. **168** (2002), no. 7, 3309–3317.

[19] C. Dejaco, C. Dufner, and M. Schirmer, *Are regulatory T-cells linked with aging?*, Exp. Gerontol. **41** (2006), no. 4, 339–345.

[20] G.M. Depler, H.K. Nguyen, J. Webster-Cyriaque, and H.T. Banks, *A dynamic model for induced reactivation of latent virus*, J. Theor. Biol. **244** (2007), no. 3, 451–462.

[21] J.M.B. Edwards and M. Woodroof, *EB virus-specific IgA in serum of patients with infectious mononucleosis and of healthy people of different ages*, J. Clin. Pathol. **32** (1979), no. 10, 1036–1040.

[22] M.A. Epstein, *The origins of EBV research: discovery and characterization of the virus*, Epstein-Barr Virus (E.S. Robertson, ed.), vol. 1, Gaister Academic Press, Norfolk, England, 1st ed., 2005, pp. 1–14.

[23] P.J. Farrell, *Role for HLA in susceptibility to infectious mononucleosis*, J. Clin. Invest. **117** (2007), no. 10, 2756–2758.

[24] E.B. Griffin and R. Rochford, *Endemic Burkitt's lymphoma*, Epstein-Barr Virus (Robertson E.S., ed.), vol. 1, Caister Academic Press, Norfolk, England, 1st ed., 2005, pp. 113–137.

[25] A.O. Guerreiro-Cacais, L. Li, D. Donati, M.T. Bejarano, A. Morgan, M.G. Masucci, L.M. Hutt-Fletcher, and V. Levitsky, *Capacity of Epstein-Barr virus to infect monocytes and inhibit their development into dendritic cells is affected by the cell type supporting virus replication*, J. Gen. Virol. **85** (2004), no. 10, 2767–2778.

[26] K.M. Haan, W.W. Kwok, R. Longnecker, and P. Speck, *Epstein-Barr virus entry utilizing HLA-DP or HLA-DQ as a coreceptor*, J. Virol. **74** (2000), no. 5, 2451–2454.

[27] K.M. Haan and R. Longnecker, *Coreceptor restriction within the HLA-DQ locus for Epstein-Barr virus infection*, PNAS **97** (2000), no. 16, 9252–9257.

[28] V. Hadinoto, M. Shapiro, C.C. Sun, and D.A. Thorley-Lawson, *The dynamics of EBV shedding implicate a central role for epithelial cells in amplifying viral output*, PLos Pathogens **5** (2009), no. 7, 1–15.

[29] J.M. Heffernan, R.J. Smith, and L.M. Wahl, *Perspectives on the basic reproductive ratio*, J.R. Soc. Interface **2** (2005), no. 4, 281–293.

[30] J.R. Hiernaux and R. Lefever, *Population dynamics of tumors attacked by immunocompetent killer cells*, Theoretical immunology II (A.S. Perelson, ed.), vol. 2, Addison Wesley, New York, 1st ed., 1988, pp. 19–35.

[31] A. Hildesheim, R.J. Apple, C.J. Chen, S.S¿ Wang, Y.J. Cheng, W. Klitz, S.J. Mack, I.H. Chen, M.M. Hsu, C.S. Yang, L.A. Brinton, P.H. Levine, and H.A. Erlich, *Association of HLA class I and II alleles and extended haplotypes with nasopharyngeal carcinoma in Taiwan*, J. Natl. Cancer Inst. **94** (2002), no. 23, 1780–1789.

[32] A.D. Hislop, N.E. Annels, N.H. Gudgeon, A.M. Leese, and A.B. Rickinson, *Epitope-specific evolution of human CD8+ T cell responses from primary to persistent phases of Epstein-Barr virus infection*, J. Exp. Med. **195** (2002), no. 7, 893–905.

[33] A.D. Hislop, G.S. Taylor, D. Sauce, and A.B. Rickinson, *Cellular responses to viral infection in humans: lessons from Epstein-Barr virus*, Annu. Rev. Immunol. **25** (2007), no. 1, 587–617.

[34] H. Hjalgrim, J. Asking, K. Rostgaard, S. Hamilton-Dutoit, F.R.C. Path, M. Frisch, J. Zhang, M. Madsen, N. Rosdahl, H.B. Konradsen, H.H. Storm, and M. Melbye, *Characteristics of Hodgkin's lymphoma after infectious mononucleosis*, N. Engl. J. Med. **349** (2003), no. 14, 1324–1332.

[35] D. Hochberg, T. Souza, M. Catalina, J.L. Sullivan, K. Luzuriaga, and D.A. Thorley-Lawson, *Acute infection with Epstein-Barr virus targets and overwhelms the peripheral memory B-cell compartment with resting, latently infected cells*, J. Virol. **78** (2004), no. 10, 5194–5204.

[36] L.M. Hutt-Fletcher, *EBV entry and epithelial infection*, Epstein-Barr Virus (Robertson E.S., ed.), vol. 1, Caister Academic Press, Norfolk, England, 1st ed., 2005, pp. 359–378.

[37] L.M. Hutt-Fletcher, *Epstein-Barr virus entry*, J. Virol. **81** (2007), no. 15, 7825–7832.

[38] G.T. Huynh and F.R. Adler, *Alternating host cell tropism shapes the persistence, evolution and coexistence of Epstein-Barr virus infections in human*, B. Math. Biol. In-press, (2010).

[39] G.T. Huynh and F.R. Adler, *Mathematical modeling the age dependence of Epstein-Barr virus associated infectious mononucleosis. Manuscript submitted for publication*, (2010).

[40] A. Imrie, J. Meeks, A. Gurary, M. Sukhbataar, P. Kitsutani, P. Effler, and Z. Zhao, *Differential functional avidity of dengue virus-specific T-cell clones for variant peptides represeting heterologous and previously encountered serotypes*, J. Virol. **81** (2007), no. 18, 10081–10091.

[41] B.F. Israel and S.C. Kenney, *EBV lytic infection*, Epstein-Barr Virus (Robertson E.S., ed.), vol. 1, Caister Academic Press, Norfolk, England, 1st ed., 2005, pp. 571–612.

[42] A. Jafarzadeh, A. Mostafaie, M. Sadeghi, M. Nemati, M.T. Rezayati, and G. Hassanshahi, *Age-dependent changes of salivary IgA and IgE levels in healthy subjects*, Dent. Res. J. **5** (2008), no. 2, 89–93.

[43] M.F. Ji, D.K. Wang, Y.L. Yu, Y.Q. Guo, J.S. LIang, W.M. Cheng, Y.S. Zong, K.H. Chan, S.P. Ng, W.I. Wei, D.T.T. Chua, J.S.T. Sham, and M.H. Ng, *Sustained elevation of Epstein-Barr virus antibody level preceding clinical onset of nasopharyngeal carcinoma*, Br. J. Cancer **96** (2007), no. 4, 623–630.

[44] R. Jiang, R.S. Scott, and L.M. Hutt-Fletcher, *Epstein-Barr virus shed in saliva is high in B-cell-tropic gp42*, J. Virol. **80** (2006), no. 14, 7281–7283.

[45] L. Jones and A. Perelson, *Opportunistic infection as a cause of transient viremia in chronically infected HIV patients under treatment with HAART*, B. Math. Biol. **67** (2005), no. 6, 1227–1251.

[46] R.M. Kedl and M.F. Mescher, *Qualitative differences between naive and memory T cells make a major contribution to the more rapid and efficient memory CD8+ T cell response*, J. Immunol. **161** (1998), no. 2, 674–683.

[47] A.N. Kirschner, A.S. Lowrey, R. Longnecker, and T.S. Jardetzky, *Binding-site interactions between Epstein-Barr virus fusion proteins gp42 and gH/gL reveal a peptide that inhibits both epithelial and B-cell membrane fusion*, J. Virol. **81** (2007), no. 17, 9216–9229.

[48] A.N. Kirschner, J. Sorem, R. Longnecker, and T.S. Jardetzky, *Structure of Epstein-Barr virus glycoprotein 42 suggests a mechanism for triggering receptor-activated virus entry*, Cell Press **17** (2009), no. 2, 223–233.

[49] L.L. Laichaalk, D. Hochberg, G.J. Babcock, R.B. Freeman, and D.A. Thorley-Lawson, *The dispersal of mucosal memory B cells: evidence from persistent EBV infection*, Immunity **16** (2002), no. 5, 745–754.

[50] K.M. Lau, S.H. Cheng, S.A. Lo, J.K. Woo, and C.A. Van Hasselt, *Increase in circulating $Foxp3^{+}CD4^{+}CD25^{high}$ regulatory T cells in nasopharyngeal carcinoma patients*, Br. J. Cancer **96** (2007), no. 4, 617–622.

[51] S.P. Lee, A.T.C. Chan, S. Cheung, W.A. Thomas, D. CroomCarter, C.W. Dawson, C. Tsai, S. Leung, P.J. Johnson, and D.P. Huang, *CTL control of EBV in nasopharyngeal carcinoma (NPC): EBV-specific CTL responses in the blood and tumors of NPC patients and the antigen-processing function of the tumor cells*, J. Immunol. **36** (2000), no. 1, 573–582.

[52] C. Lin, W. Lo, T. Lee, Y. Ren, S. Hwang, Y. Cheng, C. Chen, Y. Chang, S.P. Lee, A.B. Rickinson, and P.K.H. Tam, *Immunization with Epstein-Barr virus (EBV) peptide-pused dendritic cells induces functional CD8+ T cell immunity and may lead to tumor regression in patients with EBV-positive nasopharyngeal carcinoma*, Cancer Res. **62** (2002), no. 23, 6952–6958.

[53] J. Liu, L. Cassar, A. Pinto, and H. Li, *Mechanisims of cell immortalization mediated by EB viral activation of telomerase in nasopharyngeal carcinoma*, Cell Research **16** (2006), no. 10, 809–817.

[54] D.C. Macallan, D.L. Wallace, Y. Zhang, H. Ghattas, B. Asquith, C. Lara, A. Worth, G. Panayiotakopoulos, G.E. Griffin, D.F. Tough, and P.C. Beverley, *B-cell kinetics in humans: rapid turnover of peripheral blood memory cells*, Blood **105** (2005), no. 9, 3633–3640.

[55] M.G. Masucci, *Epstein-Barr virus oncogenesis and the ubiquitin-proteasome system*, Oncogene **23** (2004), no. 11, 2107–2115.

[56] K.A. McAulay, C.D. Higgins, K.F. Macsween, A. Lake, R.F. Jarrett, F.L. Robertson, H. Williams, and D.H. Crawford, *HLA class I polymorphisms are associatd with development of infectious mononucleosis upon primary EBV infection*, J. Clin. Invest. **117** (2007), no. 10, 3042–3048.

[57] E.S. Mocarski, T. Shenk, and R.F. Pass, *Cytomegaloviruses*, Field's Virol (D.M. Knipe and Howley P.M, eds.), vol. 2, Lippincott Williams and Wilkins, Philadelphia, PA, 5th ed., 2007, pp. 2701–2772.

[58] J. Mosquera and F.R. Adler, *Evolution of virulence: a unified framework for coinfection and superinfection*, J.Theor.Biol **195** (1998), no. 3, 293–313.

[59] M.M. Mullen, K.M. Haan, R. Longnecker, and T.S. Jardetzky, *Structure of Epstein-Barr virus gp42 protein bound to the MHC class II receptor HLA-DR1*, **9** (2002), no. 2, 375–385.

[60] C. Munz, *Immune response and evasion in the host-EBV interaction*, Epstein-Barr Virus (Robertson E.S., ed.), vol. 1, Caister Academic Press, Norfolk, England, 1st ed., 2005, pp. 197–231.

[61] A.U. Neumann, N.P. Lam, H. Dahari, D.R. Gretch, T.E. Wiley, T.J. Layden, and A.S. Perelson, *Hepatitis C viral dynamics in vivo and the antiviral efficacy of interferon-alpha therapy*, Science **282** (1998), no. 5386, 103–107.

[62] J.C. Niederman and A.S. Evans, *Epstein-Barr Virus*, Infections of humans: epidemiology and control (A.S. Evans and R.A. Kaslow, eds.), vol. 1, Plenum Medical Book Co., New York, 4th ed., 1997, pp. 253–282.

[63] S. Nikiforow, K. Bottomly, and G. Miller, *CD4+ T-cell effectors inhibit Epstein-Barr virus-induced B-cell proliferation*, J. Virol. **75** (2001), no. 8, 3740–3752.

[64] M.A. Nowak and C.R. Bangham, *Population dynamics of immune responses to persistent viruses*, Science **272** (1996), no. 5258, 74–79.

[65] M.A. Nowak, S. Bonhoeffer, A.M. Hill, R. Boehme, H.C. Thomas, and H. McDade, *Viral dynamics in hepatitis B virus infection*, Proc. Natl. Acad. Sci. **93** (1996), no. 9, 4398–4402.

[66] M.A. Nowak and R.M. May, *Virus dynamics: Mathematical principles of immunology and virology*, 1st ed., Oxford, New York, USA, 2000.

[67] H. Oberender, E. Straube, M. Kunkel, L. Gartner, and I. Morfiadakis, *Epstein-Barr virus-specific immunoglobulin A in patients with infectious mononucleosis, an age-dependent factor*, Eur. J. Clin. Microbiol. Infect. Dis. **5** (1986), no. 2, 173–174.

[68] A.S. Perelson, *Modeling viral and immune system dynamics*, Nat. Reviews Immunol. **2** (2002), no. 1, 28–36.

[69] C.A. Piccirillo and E.M. Shevach, *Cutting edge: control of CD8+ T cell activation by CD4+CD25+ immunoregulatory cells*, J. Immunol. **167** (2001), no. 3, 1137–1140.

[70] N. Raab-Traub, *Epstein-Barr virus in the pathogenesis of NPC*, Epstein-Barr Virus (E.S. Robertson, ed.), vol. 1, Caister Academic Press, Norfolk, England, 1st ed., 2005, pp. 71–92.

[71] M.E. Ressing, D. van Leeuwen, F.A.W. Verreck, S. Keating, R. Gomez, K.L.M.C. Franken, T.H.M. Ottenhoff, M. Spriggs, T.N. Schumacher, L.M. Hutt-Fletcher, M. Rowe, and E.J.H.J. Wiertz, *Epstein-Barr virus gp42 is posttranslationally*

modified to produce soluble gp42 that mediates HLA class II immune evasion, J. Virol. **79** (2005), no. 2, 841–852.

[72] A. Rickinson, *Epstein-Barr virus: Summary, conclusion and forward look*, vol. 1, Caister Academic Press, Norfolk, England, 2005, pp. 711–753.

[73] A. Rickinson and E. Kieff, *Epstein-Barr virus*, Field's Virol (B.N. Fields, D.M. Knipe, and Howley P.M, eds.), vol. 2, Lippincott-Raven, Philadelphia, PA, 3rd ed., 1996, pp. 2397–2446.

[74] A. Rickinson and E. Kieff, *Epstein-Barr Virus*, Field's Virol (D.M. Knipe and Howley P.M, eds.), vol. 2, Lippincott Williams and Wilkins, Philadelphia, PA, 4th ed., 2001, pp. 2575–2627.

[75] E.S. Robertson (ed.), *Epstein-Barr virus*, 1st ed., vol. 1, Caister Academic Press, Norfolk, England, 2005.

[76] D. Sauce, M. Larsen, S.J. Curnow, A.M. Leese, and P.A. Moss, *EBV-associated mononucleosis leads to long-term global deficit in T cell responsiveness to IL-15*, Blood **108** (2006), no. 1, 11–18.

[77] L.K. Selin, S.M. Varga, I.C. Wong, and R.M. Welsh, *Protective heterologous antiviral immunity and enhanced immunopathogenesis mediated by memory T cell populations*, J. Exp. Med. **188** (1998), no. 9, 1705–1715.

[78] M. Shapiro, K.A. Duca, K. Lee, E. Delgado-Eckert, J. Hawlins, A.S. Jarrah, R. Laubenbacher, R. Laubenbacher, N.F. Polys, V. Hadinoto, and D.A. Thorley-Lawson, *A virtual look at Epstein-Barr virus infection: Simulation mechanism*, J. Theor. Biol. **252** (2008), no. 4, 633–648.

[79] P.L. Shaw, A.N. Kirschner, T.S. Jardetzky, and R. Longnecker, *Characteristics of Epstein-Barr virus envelope protein gp42*, Virus Genes **40** (2010), no. 3, 307–319.

[80] S.L. Silins, M.A. Sherritt, J.M. Silleri, S.M. Cross, S.L. Elliott, M. Bharadwaj, T.T. Le, L.E. morrison, R. Khanna, D.J. Moss, A. Suhrbier, and I.S. Misko, *Asymptomatic primary Epstein-Barr virus infection occurs in the absence of blood T-cell repertoire perturbations despite high levels of systemic viral load*, Blood **98** (2001), no. 13, 3739–3744.

[81] A.L. Silva, J. Omerovic, T.S. Jardetzky, and R. Longnecker, *Mutational analyses of Epstein-Barr virus glycoprotein 42 reveal functional domains not involved in receptor binding but required for membrane fusion*, J. Virol. **78** (2004), no. 11, 5946–5956.

[82] D. Sitki-Green, M. Covington, and N. Raab-Traubb, *Compartmentalization and transmission of multiple Epstein-Barr virus strains in asymptomatic carriers* , J. Virol. **77** (2003), no. 3, 1840–1847.

[83] J.W. Sixbey and Q.Y. Yao, *Immunoglobulin A-induced shift of Epstein-Barr virus tissue tropism*, Science **255** (1992), no. 5051, 1578–1580.

[84] K.C.M. Straathof, C.M. Boolard, U. Popat, M.H. Huls, T. Lopez, M.C. Morriss, M.V. Gresik, A.P. Gee, H.V. Russell, M.K. Brenner, C.M. Rooney, and H.E. Heslop, *Treatment of nasopharyngeal carcinoma with Epstein-Barr virus-spcific T lymphocytes*, Blood **105** (2005), no. 5, 1898–1904.

[85] D.A. Thorley-Lawson, *EBV persistence and latent infection in vivo*, Epstein-Barr Virus (Robertson E.S., ed.), vol. 1, Caister Academic Press, Norfolk, England, 1st ed., 2005, pp. 309–349.

[86] S.W. Tsao, K.W. Lo, and D.P. Huang, *Nasopharyngeal carcinoma*, Epstein-Barr Virus (A. Tselis and H.B. Jenson, eds.), vol. 1, Taylor and Francis Group, New York, 1st ed., 2006, pp. 273–295.

[87] S.M. Turk, R. Jiang, L.S. Chesnokova, and L.M. Hutt-Fletcher, *Antibodies to gp350/220 enhance the ability of Epstein-Barr virus to infect epithelial cells*, J. Virol. **80** (2006), no. 19, 9628–9633.

[88] P. van den Driessche and J. Watmough, *Reproduction numbers and sub-threshold endemic equilibria for compartmental models of disease transmission*, Math. Biosci. **180** (2002), no. 1-2, 29–48.

[89] H. Veiga-Fernandes, U. Walter, C. Bourgeois, A. McLean, and B. Rocha, *Response of naive and memory CD8+ T cells to antigen stimulation in vivo*, Nature Immunol. **1** (2000), no. 1, 47–53.

[90] G. Wang, G.R.F. Krueger, and L.M. Buje, *Mathematical model to simulate the cellular dynamics of infection with human herpesvirus-6 in EBV-negative infectious mononucleosis*, J. Med. Virol. **71** (2003), no. 4, 569–577.

[91] D. Weber-Mzell, P. Kotanko, A.C. Hauer, U. Goriup, J. Haas, N. Lanner, W. Erwa, I.A. Ahmaida, S. Haitchi-Petnehazy, M. Stenzel, G. Lanzer, and J. Deutsch, *Gender, age and seasonal effects on IgA deficiency: a study of 7293 Caucasians*, Euro. J. Clin. Invest. **34** (2004), no. 3, 224–228.

[92] D. Wodarz, S. Sierro, and P. Klenerman, *Dynamics of killer T cell inflation in viral infections*, J.R.S. Interface **4** (2007), no. 14, 533–543.

[93] E.Y. Woo, H. Yeh, C.S. Chu, K. Schlienger, R.G. Carroll, J.L. Riley, L.R. Kaiser, and C.H. June, *Cutting edge: regulatory T cells from lung cancer patients directly inhibit autologous T cell proliferation*, J. Immunol. **168** (2002), no. 9, 4272–4276.

[94] J.W. Xu, A. Ahmad, and J. Menezes, *Clinical relevance of serum immunoglobulin A antibodies to Epstein-Barr virus envelope glycoprotein gp350 in nasopharyngeal carcinoma patients*, J. Clin. Microbiol. **36** (1998), no. 12.

[95] K. Yamanishi, Y. Mori, and P.E. Pellett, *Human herpesviruses 6 and 7*, Field's Virol (D.M. Knipe and Howley P.M, eds.), vol. 2, Lippincott Williams and Wilkins, Philadelphia, PA, 5th ed., 2007, pp. 2701–2772.

[96] L.S. Young and A.B. Rickinson, *Epstein-Barr virus: 40 years on*, Nat. Rev. Cancer **4** (2004), no. 10, 757–768.